Arctic Biology Field Course

Qeqertarsuaq 2022

Arctic Biology Field Course

Qeqertarsuaq 2022

For information about the Arctic Station visit: www.arktiskstation.ku.

Table of Contents

Publication information and how to cite this report

Title: Arctic Biology Field Course, Qeqertarsuaq 2022

Published by: Arctic Station
University of Copenhagen
3953 Qeqertarsuaq
Greenland

Marine Biological Section
Department of Biology
University of Copenhagen
Universitetsparken 4
2100 Copenhagen Ø
Denmark

Publishing year: 2022

Edited by: Niels Daugbjerg and Per Juel Hansen, Department of Biology, University of Copenhagen, Denmark

ISBN: 978-87-89143-32-3

Cover page photo: Niels Daugbjerg

Citation: The report can be cited in full:
Arctic Biology Field Course 2022, Qeqertarsuaq 2025. Hansen, P.J. and Daugbjerg, N. (Eds.). Arctic Station, University of Copenhagen, p. 1-129.

or in part:

Author(s), 2025. Title of paper. In: Arctic Biology Field Course, Qeqertarsuaq 2025. Hansen, P.J. and Daugbjerg, N. (Eds.). Arctic Station, University of Copenhagen, p. 1-129.

Preface

The detailed planning of this field course, in fact, started almost 2 years before we started our travel toward the Arctic Station on the 21 July. The reason being that the course planned for 2021 was cancelled due to Covid-19 travel and quarantine restrictions. This resulted in massive disappointment and disillusioned students and responsible teachers. However, 6 of the original course participants managed to reorganize their study plans and therefore took the course in 2022, and six new students were appointed through a new application round. We thank Kirsten Christoffersen for supporting our wish to organize a “new” Arctic marine field course in the summer 2022.

In total four group projects were conducted; each project had three participants. All groups worked with samples collected in the Disko Bay area and the topics covered were (1) diversity and size distribution of phytoplankton, (2) the impact of iron on the growth of phytoplankton size groups, (3) the effects of acidification on the planktonic food web and (4) the response of protistan grazer community to the addition of prey. Hence, all projects included a combination of work in the field and in the lab using equipment either present at Arctic Station or brought by us. We had no problems filling up the available space in lab building, the cooler, and the garage next to the main building.

The course went very well, and everyone worked hard and invested countless hours in their own project. However, we also found (a little) time for a few hikes to Østerlien and Kuanit either as the hole group or in smaller groups. During our stay we also found time one late afternoon to play the traditional football match against one of the two clubs at Qeqertarsuaq. This was as always great fun and afterwards we completely forgot about the score.

It is our pleasure to thank the staff at the Arctic Station for giving project groups the logistical support needed both on land and on sea. We thank Morten Rauch (Scientific leader) for taking us all on a geological hike, where he shared some of his enormous knowledge of the local area. Emilie Henningsen (Assisting scientific leader) is thanked for her help with the CTD at sea and for always being prepared to help with practical matters. The captain Jørgen-Peter Lund and crew (Erik Wille and Eli) on board Porsild are thanked for help with CTD profiles and collection water samples from numerous depths. Finally. we thank the Station manager, Kjeld (Akaaraq) Mølgaard and Antoinette for keeping a tidy station.

The Department of Biology at the Faculty of Science and the Board of the Arctic Station covered the main expenses. We are indeed grateful for this support.

It is always great to see how students quickly adapt to working in the Arctic, where resources and possibilities of course differ compared to what they are used to. Yet, the complete renovation of the Arctic Station, which opened just weeks before our arrival, allowed laboratory work under modern conditions. In all respects our 10-day stay at the Arctic Station was a pleasure.

Per Juel Hansen and Niels Daugbjerg (course responsible), August 2022

KØBENHAVNS UNIVERSITET
FACULTY OF SCIENCE

Possible effects of acidification on the planktonic food web during summer in Disko Bay, West Greenland

Arctic Biology Field Course 2022

Emmeli Agerskov Claré, Caroline Brügger & Katrine Skovsen

Supervisors: Per Juel Hansen & Niels Daugbjerg

Table of contents

Abstract

Rising CO2 in the atmosphere caused by the burning of fossil fuels leads to ocean acidification, (OA), which has the potential to affect the growth rates (GR) of marine protists, community composition and drive physiological and evolutionary change in the species. The effects of ocean acidification on the planktonic food web were studied in Disko Bay, West Greenland by incubating surface water sampled in July after manipulation of pH in the range of 8.2−7.2 for 8 days after the addition of inorganic nutrients. The effect of acidification was both investigated for the growth of the entire phototrophic protist community using chlorophyll a as proxy, as well as GR of individual species to investigate if there is differentiated response to acidification based on the species' trophic groups (heterotrophic, CM and NCM), and to which extent this will change the food web dynamics. The results demonstrated that while there were significant effects of acidification on the GR of some of the species included in this study, the overall GR of chlorophyll a was not affected. This can mean that acidification causes the protist community composition to change but seen as a whole the protist community is resilient to pH changes in the ocean.

Introduction

Concentrations of CO_2 and bicarbonate in the ocean are increasing due to anthropogenic CO_2 emissions, which has led to a decrease in ocean water pH, a phenomenon known as 'ocean acidification'. Since the industrial revolution the pH of surface ocean waters has declined by about 0.1 pH units, and is expected to decrease an additional 0.3 units by the end of this century (Collins et al., 2013). Even though this might not sound like much, the pH scale is logarithmic, and thus this change represents approximately a 30% increase in acidity in the ocean by now (NOAA, 2020).

Approximately 25% of the emitted atmospheric CO_2 is absorbed into the oceans (Thoisen et al., 2015). When CO_2 is absorbed by seawater, a series of chemical reactions occur resulting in the increased concentration of hydrogen ions. Water and carbon dioxide combine to form carbonic acid (H_2CO_3), which is a weak acid that dissociates into hydrogen ions (H^+) and bicarbonate ions (HCO_3^-). These chemical reactions alter the composition of DIC and while lowering the pH (acidification). Arctic water is shown to be more sensitive to ocean acidification due to the high solubility of CO_2 in cold waters (Hoppe et al., 2018). The increase in CO_2 in the oceans and atmosphere is expected to have numerous effects on marine ecosystems. Ocean acidification has the potential to affect phytoplankton community composition and drive physiological and evolutionary change in the species. Given phytoplankton taxa's phylogenetic breadth, different taxa will likely have different responses (Collins et al., 2013; Thoisen et al., 2015). For example, the response to acidification has been shown to be species-specific with some species being resp. more sensitive and tolerant (Thoisen et al., 2015) and elevated CO_2 concentration been shown to shift the community structure from dinoflagellates to nanophytoplankton under experimental conditions (Keys et al., 2018)
Ocean acidification is impacting and harming many marine species, especially calcifying organisms that struggle to build and maintain their shells, skeletons, and other calcium carbonate structures (NOAA, 2020;). For example, coccolithophores have been suggested to have hindered the ability to generate calcareous plates (Collins et al., 2013). While some species will be harmed, increased CO_2 could potentially increase primary production as the majority of phytoplankton utilize both HCO_3^- and CO_2. The lowered extracellular pH may however influence the intracellular pH of unicellular organisms and affect physiological processes negatively and thus acidification will not enhance primary processes (Thoisen et al., 2015).

Our study area, Disko bay, located in West Greenland, is important as a fishing area, because of its location just below the southern limit of the Arctic winter sea ice (Riisgaard et al., 2015). The coastal waters in the Arctic are characterized by large variation in pH caused by glacial runoff and ice melt, causing plankton to be resilient to changing pH to a certain degree (Hoppe et al., 2018). The dominant plankton species have, in previous studies, been found to be diatoms, heterotrophic dinoflagellates, prymnesiophytes and prasinophytes during spring (Thoisen et al., 2015; Riisgaard et al., 2015).

Many protists, that have traditionally been seen as a part of the phytoplankton, are able to combine photosynthesis with phagotrophic modes of nutrition. These are now considered to belong to a functional group called constitutive mixotrophs. Other protists previously regarded as heterotrophs have been found to be able to gain phototrophic abilities by ingesting prey, and are therefore now called non-constitutive mixotrophs (Mitra et al., 2016). Not much is known about how these mixotrophic species are affected by ocean acidification, although some studies show that mixotrophs might be positively affected by ocean acidification, since it leads to higher abundance of prey (Bach et al., 2017).

The aim of this study is to study how acidification affects the protist community in Disko Bay, Greenland during the summer period. This is investigated both by looking at the effect of acidification on the growth of entire phototrophic protist community using chlorophyll a as a proxy, as wells as on the growth of individual species to see how if there is a differentiated response acidification based on the species trophic groups, and to which extent this will change the food web dynamics.

This study hypothesizes that the growth rates (GR) of constitutive mixotrophs are positively affected by elevated pH, as they are using the increased amount of CO_2 in the water to photosynthesis. GR of non-constitutive mixotrophs will not be affected by increased CO_2, since they are feeding, and they are respiring CO_2. Heterotrophic protists are not expected to be affected by the CO_2, as they are not photosynthesizing organisms.
All in all, we expect that ocean acidification will lead to changes in the composition of the plankton community and result in higher chlorophyll a levels in the ocean waters (Alvarez-Fernando et al., 2018).

Materials and Methods

Sampling and hydrography

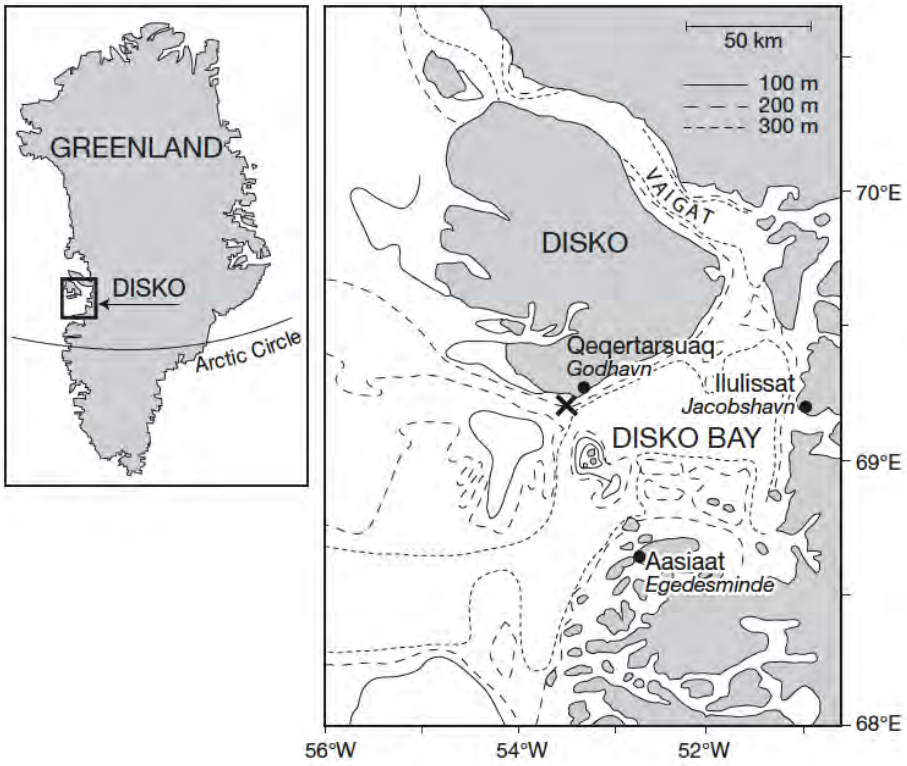

Fig. 1 Location of Qeqertarsuaq on Disko Island, West Greenland, where Arctic Station (X) is situated (Thoisen et al., 2015).

Water was collected from the "Permanent station" (350 m depth) in Disko Bay, west Greenland (69°11mN, 53°31mW) on July 23rd using the RV Porsild belonging to the Arctic Station, Copenhagen University. Water was collected at a 3 m depth at the station from surface water using a 10-L Niskin water sampler. A total of 40 L were collected. A CTD profile was taken with a Seabird SBE19 CTD prior to the sampling of the water. This provided a depth distribution of conductivity, temperature, density and fluorescence were measured with a Seabird CTD.

On land the sample was passed through a cylinder equipped with a 200 µm nitex filter and subsequently added to 2x 20 L containers via a silicon tube to remove mesozooplankton. Immediately after the plankton assemblage was carefully mixed to assure that the organisms were well suspended and 4 L were transferred to 3x 5 L bottles.

Experimental setup

Control and treatments were run in triplicates. A total of 9 different glass bottles (1 L) were used and 3 treatments were conducted with the pH-levels 8.2, 7.7 and 7.2, respectively. pH was adjusted in the bottles by gradually adding drops (approx. 50 µL at a time) of 1 M HCl; if the pH got too low it was increased with addition of small amounts of NaOH. The treatment exposed to pH 7.2 was lowered in steps of 0.5 pH units per 12 h during the first 24 h. Thus the final pH on 7.2 level was reached on July 24th. The bottles with pH 8.2 serve as control bottles in which pH was not adjusted, resembling the pH in Disko Bay at the time of sampling. To ensure that the incubations did not suffer from nutrient limitation nutrients were added to the

water, equivalent to f/20 medium concentrations with silicate addition (see supplement Fig 2). Bottles were incubated at ca. 115 µmol photons $m^{-2}s^{-1}$ in a cooling container which were set to 4°C.

Seawater used for dilution in the treatments during the experiment was collected from the same sampling station and same depth. The water was filtered through a GF/F filter and stored dark and cold (4 ± 2 C°) in a 20 L container. The average pH, temperature and salinity of seawater used for dilution were measured. The water used for dilution was pH adjusted and nutrients added

Zero samples (D0) were taken for quantification of protists and chlorophyll a (Chl a). Every second day, starting from day 2, 100 or 300 mL samples from each of the 9 glass bottles were withdrawn, where after the bottles were refilled with filtered water adjusted to the 3 different pH treatments so that the initial pH setting was achieved to ensure that the pH stays the same throughout the experiment. The bottles were diluted to keep pH at the respective level stable during the incubation. pH was measured with a WTW pH 3210 pH meter equipped with a WTW SenTix 41 electrode. The electrode was regularly calibrated using buffers of pH 7 and 10.

Measurements of Chl a

100 mL sample (except for day one, where 200 mL sample was taken) of the phytoplankton community from each bottle was filtered onto a 0.7 µm GF/F filter and the filter added to a 15 mL falcon tube. 5 mL 96% ethanol was then subsequently added to the falcon tube and the samples were stored in the dark in the refrigerator. The following day the samples were measured using a Turner TD-700 Fluorometer. The growth rate of the phytoplankton community (Chl a) was calculated from the cumulative growth due to the dilution technique.

Identification and enumeration of phytoplankton species

On day two and six 200 mL samples from each of the 9 bottles are transferred to 300 mL brown glass bottles and Lugol's Iodine is added (1 % final concentration). Afterwards the number of protists are counted by using 50 mL sedimentation chambers and an inverted microscope. The sedimentation chamber allows suspended particles to settle out of the water (within 24h) as it slowly flows through the chamber, thereby providing a degree of purification. Dominant species belonging to different protist groups were enumerated covering photoautotrophic, mixotrophic and heterotrophic groups.

Table 1. A list of the species enumerated in this study belonging different algal groups and with indications of their nutritional strategy: Heterotrophs (HET), Constitutive mixotrophs (CM), Generalist non-constitutive mixotrophs (GNCM) and Specific non-constitutive mixotrophs (SNCM).

Class	Species

Dinoflagellates	*Gyrodinium spirale* (HET) *Gyrodinium dominans* (HET) *Protoperidinium bipes* (HET) *Alexandrium* spp. (CM) *Dinophysis* spp. (SNCM)
Chrysophytes	*Dinobryon* spp. (CM)
Cryptophytes	Many species counted together (CM)
Ciliates	*Laboea strobila* (GNCM) *Strombidium* spp. (mix of HET/GNCM) *Strombidium conicum* (GNCM)

All species, except for *Dinobryon* spp and cryptophytes, were enumerated for the whole sedimentation chamber. *Dinobryon* and cryptophytes were enumerated in transects. The specific number of transects varied from sample to sample to ensure that at least 200 cells were counted.

Calculations

The concentration of each phytoplankton species was calculated as the number of cells mL^{-1} using relevant conversion factors for the used microscopes and the knowledge of each sedimentation chamber holding 50 mL. The average of the triplicates samples were used for further data processing.

The growth rates were calculated as an average of the triplicate samples. The growth rates of the entire photosynthetic protist community (Chl a) and the individual species was calculated assuming exponential growth, where μ is the growth rate and N is Chl a or cell concentration at time t_2 and t_1:

$$\mu = \frac{\ln\left(\frac{N_{t2}}{N_{t1}}\right)}{t_2 - t_1}$$

The cumulative concentration (μ') of Chl a and cells were calculated using μ due to the dilution technique, where N is Chl a concentration and μ is the growth rate at time t_2.

$$\mu' = N_{t1} \cdot e^{\mu_{t2} \cdot (t_2 - t_1)}$$

Statistics

The statistical test that has been used for the data of this study is One-Way ANOVA (analysis of variance), which tests for significant differences in the means of two or more independent groups. The tests are made in RStudio, and the significance level is set to 0.050. For the data to have significantly divergent variances, the P value must be below the significance level. The tests have been used for comparison of the cumulative growth in Chl A at the three pH treatments, and the difference in GR of the species as well as nutritional strategy groups at the three pH treatments. Tukey tests (Ad-hoc) were performed when comparing cumulative growth in Chl A and GR of the protists at different pH levels to show between which pH values a significant difference is found.

Results

Hydrography of sampling station in Disko Bay

A CTD profile was performed to measure water parameters in the column of the water from the permanent station (350m depth), used for sampling water to pH experiments. Salinity tended to increase with depth. The salinity was ~32 in the surface water, wherafter it increased to ~34 with the highest value at around 310 meters depth (fig. 2A). The temperature of the surface water was ~7 ºC in the upper water. Temperature dropped steadily with depth to reach the lowest value of close to ºC at ~50 m, where after it increased with depth to reach ~3 ºC at 300 m depth. The chlorophyll fluorescence max was found around 30 m with values in the range of 9-13 raw fluorescence units. The irradiance was ~530 µmol photons m^{-2} s^{-1} at surface level, and reached but decreased to 1 µmol photons m^{-2} s^{-1} at 35 m depth. 1% of incoming radiation was found at ~25 m depth.

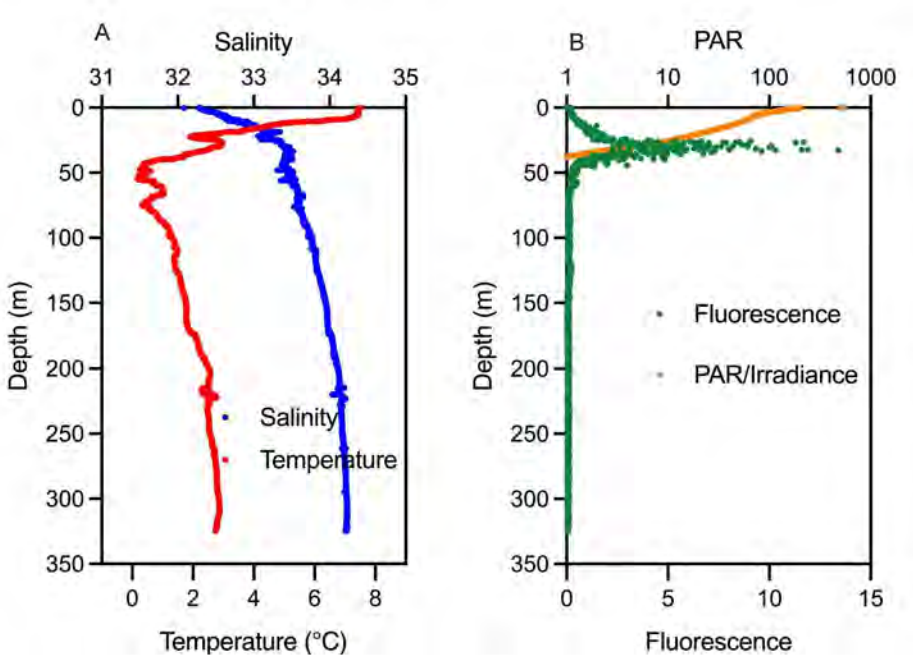

Figure 2: CTD profiles for permanent station (350 m depth) for the sampling day July 23 2022. The data include: Temperature (red line), salinity (blue line), fluorescence (green line) and PAR/irradiance (yellow line) as a function of depths.

Growth of the photosynthetic protist community based on Chl a

All the average measurements of chlorophyll concentrations in the 3 different treatments are presented in Supplement Figure 1. Replicate nr. 3 for 7.2 pH was excluded from calculations on day 6 and 7 as a result of it being a clear outlier with chlorophyll values less than half the other replicates. To keep the individual pH levels, dilutions were done at each sampling occasion (see supplement fig. 1). Cumulative growth of chlorophyll in the different treatments as to see both development in chlorophyll levels and when chlorophyll growth rates had adjusted to regulated pH.

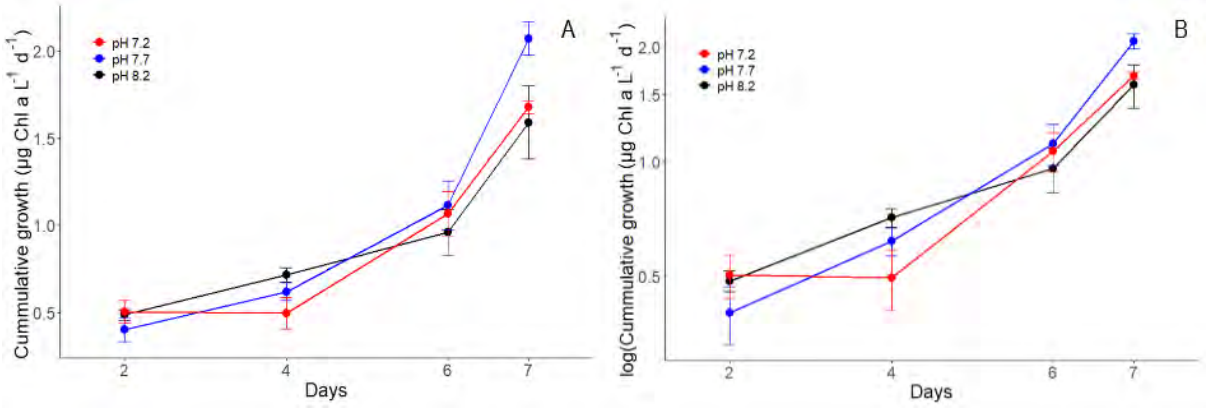

Figure 3. Development of the cumulative growth in Chl A l^{-1} d^{-1} (mean ± SD) with normal (A) and log transformed (B) y-axis during pH experiment in controls (pH 8.2) and 2 pH treatments (pH 7.7 and 7.2).

Growth rates were taken as the average of the growth rates from day 4 and onwards. This was done since the initial acclimation period after pH regulation of the treatments was not over until day 4 (fig. 3B).

Table 2. Average community growth rates based on Chl a for the three treatments.

pH	Growth rate d^{-1}	SD
7.2	0.560	0.002
7.7	0.599	0.179
8.2	0.468	0.202

The growth rate of chlorophyll did not differ much among the 3 treatments. However there is still some variation seen as the growth rate in the treatments with 8.2 pH was lower than in both 7.7 and 7.2. The pH 7.7 treatments had the highest growth rate compared to the others, although it is only significantly different from pH 8.2 ($p<0.05$). No significant difference was found between pH 7.2 and either of the other treatments. All the p-values are found in Supplement Table 3.

Growth rates of the protist species

The growth rates (GR, (organisms d^{-1})) differed a lot among the different groups/species. The GR of *Alexandrium* spp. and *Dinophysis* spp. in the different pH treatments were not statistically different from each other (fig. 4.A), and there is no significant difference ($p>0.05$). The same applies to the GR of *Gyrodinium dominans*, but for *Gyrodinium spirale* the GR is significantly lower at pH 7.2 than at both 7.7 and 8.2. For *Protoperidinium bipes* the GR is significantly lower at both pH 7.2 as well as 7.7 compared to 8.2 ($p<0.05$) (fig. 4.B). The GR of *Laboea strobila* and *Strombidium conicum* were not significantly different at any of the pH treatments, but the growth rate of *Strombidium* spp was significantly lower at pH 7.2 than at pH 8.2 (fig. 4.C). No significant differences are found at the different pH treatments for cryptophytes, but GR of *Dinobryon* spp. was significantly lower at pH 7.2 than 8.2 (fig 4.D). All the p-values are to be found in Supplement Table 1.

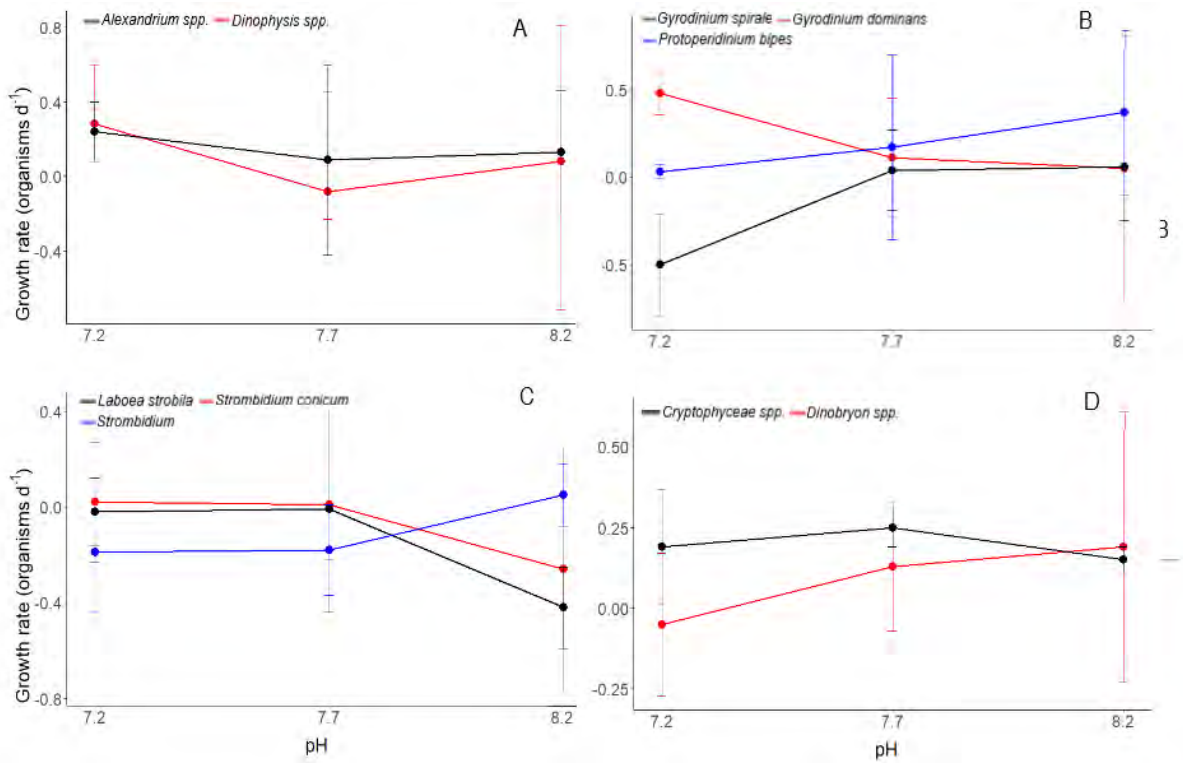

Figure 4: Growth rates of the selected protist species/groups of dinoflagellates (A and B), ciliates (C), and cryptophytes and chrysophytes (D) at pH 8.2, 7.7 and 7.2.

Growth rates of heterotrophic, constitutive mixotrophic- (CM), and non-constitutive mixotrophic (NCM) protists

Heterotrophic, CM and NCM species have been found and enumerated in this study, but photoautotrophic species, although they were observed, were too few to be counted. The abundant heterotrophic protists in our study were *Gyrodinium spirale*, *Gyrodinium dominans*, *Protoperidinium bipes*, *Laboea strobila* and *Strombidium conicum*. The CM protists that were abundant included cryptophytes, the chrysophyte *Dinobryon* spp. and the dinoflagellate *Alexandrium* spp. Only a few NCM protists were observed, *Dinophysis* spp., *Strombidium* spp. and *Mesodinium* spp. We only enumerated the two first of these species (fig. X). In our study *Strombidium s*pp. is considered as a NCM protist, although not all species within this group are mixotrophic, but it has not been possible for us to differentiate mixotrophic from heterotrophic species of this genus. The variances in GR of species within these three nutritional strategies have been tested between the pH treatments, and none of them vary significantly. All the p-values are to be found in Supplement table 2.

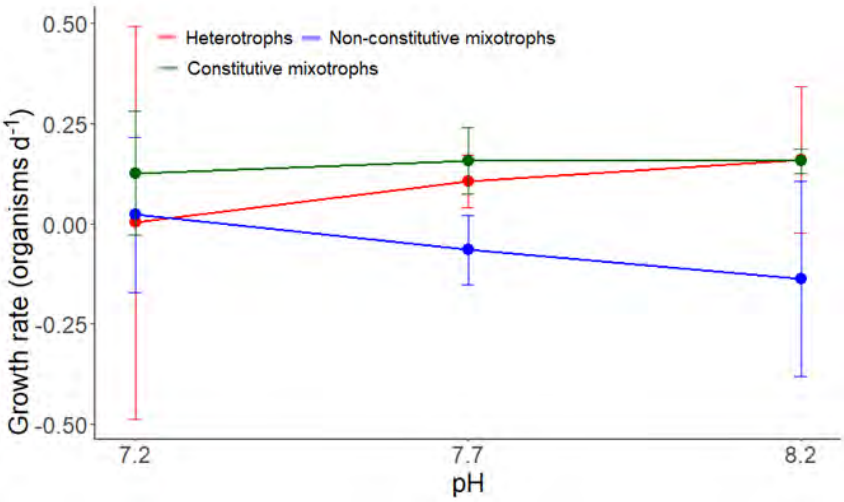

Figure 5: Growth rates (organisms d^{-1}) of the found heterotrophic (HET), Constitutive mixotrophic (CM), and Non-constitutive mixotrophic (NCM) protists at pH 8.2, 7.7 and 7.2.

Discussion

Phototrophic community growth rates based on chlorophyll a measurements

Lowering of pH from 8.2 to 7.2 did not affect phototrophic community growth rates (based on chlorophyll a) in the incubations. In the acclimatization period the chlorophyll levels dropped in the pH 7.2 treatment, but after the acclimatization period it rose to levels similar to those found in the pH 8.2 and 7.7 treatments (fig. 3). We expected to find that the growth rate of chlorophyll a was positively affected by acidification, because of the increased CO_2 levels causing higher photosynthetic rates. But since there are only significant differences in the growth rate of chlorophyll between pH 8.2 and 7.7, it might be a sign that the protist community is positively affected by acidification at very low levels, but this positive effect is already gone at pH 7.2. This means that, when considered as a whole, plankton communities might be insensitive to ocean acidification, which has also been seen in several other studies (Hoppe et al., 2018; Riebesell et al., 2013). However, some studies have seen increased primary production after lowering CO_2 (Alverez-Fernandez et al., 2018). This might be due to the increased CO_2-levels leading to a higher degree of inorganic carbon acquisition and thereby enhanced primary production. Some studies have however suggested that low pH will alter physiological processes in the protist cells, which might offset the positive effects (Hoppe et al., 2018; Thoisen et al., 2015). During our experiment, the samples were stored in a cold container with a temperature of 4°C, which might have led to lower productivity than in an in situ situation, since the ocean temperature at sampling time was around 6-7°C.

Growth rates of protist species

Growth rate has been shown to differ among protist species when affected by lowered pH in treatments. The dinoflagellates *Gyrodinium spirale* and *Protoperidinium bipes*, the chrysophyte *Dinobryon* spp. and the ciliate *Strombidium* spp. all responded with a lower GF when exposed to decreased pH. *Gyrodinium spirale* and *Protoperidinium bipes* are

heterotrophs (HET) whereas *Strombidium* spp. and *Dinobryon* spp. are categorized as resp. a non-constitutive mixotroph (NCM) and a specific non-constitutive mixotroph (SNCM). Both HET and NCM/SNCM are expected not to be affected by the rising CO_2 levels and thus acidified conditions, as they are not photosynthesizing organisms (Alvarez-Fernandez et al., 2018). Nevertheless, we see a lower GF. As mentioned above this might be explained by the fact that low extracellular pH values can influence intracellular pH and physiological processes of protists, and thus affect growth rate negatively (Thoisen et al., 2015). As opposed to this the dinoflagellates *Alexandrium* spp., *Gyrodinium dominans*, *Dinophysis* spp., the cryptophytes and the ciliates *Laboea strobila* and *Strombidium conicum* showed no significant differences when exposed to decreased pH. As our hypothesis also suggested, this indicates that different protist species respond to ocean acidification in different ways, which possibly can lead to a change in species composition (Hoppe et al., 2018). Our study only tested the response of growth rate down to a pH of 7.7 and 7.2, because this simulates possible real scenarios of ocean acidification. GR will most likely be affected negatively and show more significant results if pH was decreased even more. However available literature suggests that some species in general seem quite tolerant to lowered pH (Berge et al., 2010; Hoppe et al., 2018; Gaillard et al., 2020). It has for instance been demonstrated that the growth rate of cryptophytes and dinoflagellates species was not significantly affected by pH until it had reached the range of pH ~6.4 to 6.5 (Berge et al., 2010; Gaillard et al., 2020).

Furthermore no significant increased or decreased growth was found for other species of phytoplankton representing diatoms and haptophytes. Nevertheless, our findings indicate that marine phototrophic protist species in general tend to be resistant to climate change in terms of ocean acidification, and do not increase or decrease their growth rates according to ecological relevant ranges of pH and free CO_2 (Berge et al., 2010).

Growth rates of heterotrophic, CM-, and NCM protists

After categorizing the protist species according to their nutritional strategies and testing for the variance in GR between the three pH treatments, the results showed that there are no significant differences in GR for any of the groups (Supplementary table 2). These results are partly surprising. The primary nutritional strategy of many CM protists is phototrophic, due to the fact that they have their own chloroplasts, which is why one would expect their photosynthesis and growth to be stimulated by the increase of CO_2 in the water, and thereby lowered pH, especially if they are carbon limited (Thoisen et al., 2015). However, it is possible that the CM protists were being affected themselves by the low pH. According to another study (Alvarez-Fernandez et al., 2018), the growth of the phototrophic protists was being stimulated as well, but mostly pronounced in smaller-sized taxa. It is possible that the CM's in our study are simply too large to be affected. Furthermore, the experiment did only run for a week, which may not have been enough time for the protists to respond to the lowered pH.

The NCM protists are less dependent on CO_2, since they are feeding on other protists and bacteria and they are respiring CO_2 (Mitra et al., 2016). It was not expected that this group would be affected much by the lowered pH. The same expectations applied to the heterotrophic protists, as they are feeding and not photosynthesizing. Results from a previous study (Alvarez-Fernandez et al., 2018) shows that the heterotrophic protists (small ciliates) were negatively

affected by simulated ocean acidification (lowered pH) at nutrient rich conditions, but they showed higher abundances when nutrients were depleted. The study's explanation to this is that N depletion, along with an excess of carbon, will cause an increase in phytoplankton's production of transparent exopolymer particles (TEP). Bacterial growth efficiency relies strongly on these TEP's, and the higher bacterial biomasses could possibly have led to higher bacterivore ciliate abundances. Our study did not focus on nutrient manipulations, but the protists had enough nutrients available to live. There might have been a significant difference in the growth of the heterotrophic protists, if the experiments also had focused on nutrient manipulations.

Conclusion

Simulating ocean acidification by lowering pH from 8.2 to 7.2 did not show any significant results towards having an effect on phototrophic community growth rates (based on chlorophyll a), even though the opposite was expected. Plankton communities, considered as a whole, might thus be insensitive to ocean acidification in this range of pH change.
Growth rate has, however, been shown to be species-specific. The *Gyrodinium spirale* (HET) and *Protoperidinium bipes* (HET), *Dinobryon* spp. (SNCM), and *Strombidium* spp. (NCM) responded with a lower GF when exposed to decreased pH. Opposed to this species like *Alexandrium* spp., *Gyrodinium dominans*, *Dinophysis* spp., the cryptophytes, *Laboea strobila* and *Strombidium conicum* showed no significant differences in GR. Phototrophs and constitutive mixotrophs are expected to be positively affected by elevated pH, as they are using the increased amount of CO_2 in the water for photosynthesis, but heterotrophs and non-constitutive mixotrophs are not expected to respond with a lower GF as we see in our results. When categorizing the protist species according to their nutritional strategies and comparing GR between pH treatments, results showed no significant differences in GR. For further studies, it could be interesting to focus more on nutrient manipulations, as this might show significant differences in the growth rates. In general, our findings indicate that OA can have species-specific effects and has the possibility to change the species composition, but also that many marine phototrophic protist species tend to be resistant to OA, as they do not increase or decrease their growth rates according to ecological relevant ranges of pH.

References

Alvarez-Fernandez, S., Bach, L. T., Taucher, J., Riebesell, U., Sommer, U., Aberle, N., Brussard, C. P. D., & Boersma, M., 2018. Plankton responses to ocean acidification: The role of nutrient limitation. *Progress in Oceanography*, 165, 11-18. https://doi.org/10.1016/j.pocean.2018.04.006.

Bach, L.T., Alvarez-Fernandez, S., Hornick, T., Stuhr, A., Riebesell, U., 2017. Simulated ocean

acidification reveals winners and losers in coastal phytoplankton. *PLOS ONE* 12(11). https://doi.org/10.1371/journal.pone.0188198

Berge, T., Daugbjerg, N., Balling Andersen, B. & Hansen, P. J., 2010. Effect of lowered pH on marine phytoplankton growth rates. *Marine Ecology Progress Series*, 416, 79- 91. https://www.int-res.com/abstracts/meps/v416/p79-91/

Collins, S., Rost, B., & Rynearson, T. A., 2013, Evolutionary potential of marine phytoplankton under ocean acidification. *Evolutionary Applications*, 7(1), 140–155. https://doi.org/10.1111/eva.12120

Gaillard, S., Charrier, A., Malo, F., Carpentier, L., Bougaran, G., Hégaret, H., Réveillon, D., Hess, P. & Séchet, V., 2020. Combined Effects of Temperature, Irradiance, and pH on Teleaulax amphioxeia (Cryptophyceae) Physiology and Feeding Ratio For Its Predator Mesodinium rubrum (Ciliophora)1. *Journal of Phycology*, 56(3), 775–783. https://doi.org/10.1111/jpy.12977

Hoppe, C. J. M., Wolf, K. K. E., Schuback, N., Tortell, P. D., & Rost, B, 2018. Compensation of ocean acidification effects in Arctic phytoplankton assemblages. *Nature Climate Change*, 8(6), 529–533. https://doi.org/10.1038/s41558-018-0142-9

Keys., M., Tilstone, G., Findlay, H., Widdicombe, C. E., & Lawson, T., 2018. Effects of elevated CO2 and temperature on phytoplankton community biomass, species composition and photosynthesis during an experimentally induced autumn bloom in the western English Channel. *Biogeosciences*, 15(10), 3203–3222. https://doi.org/10.5194/bg-15-3203-2018

Mitra, A., Flynn, K. J., Tillmann, U., Raven, J. A., Caron, D., Stoeck, D. K., Not, F., Hansen, P. J., Hallegraeff, G., Sanders, R., Wilken, S., McManus, G., Johnson, M., Pitta, P., Våge, S., Berge, T., Calbet, A., Thingstad, F., Jeong, H. J., Burkholder, J., Gilbert, P. M., Granéli, E., & Lundgren, V., 2016. Defining Planktonic Protist Functional Groups on Mechanisms for Energy and Nutrient Acquisition: Incorporation of Diverse Mixotrophic Strategies. *Protists*, 167(2), 106-120. https://doi.org/10.1016/j.protis.2016.01.003.

NOAA, National Oceanic and Atmospheric Administration (April 1, 2020), Ocean acidification, https://www.noaa.gov/education/resource-collections/ocean-coasts/ocean-acidification (Visited 07-08-2022).

Riisgaard, K., Nielsen, T., & Hansen, P. J., 2015. Impact of elevated pH on succession in the Arctic spring bloom. *Marine Ecology. Progress Series (Halstenbek)*, 530, 63–75. https://doi.org/10.3354/meps11296

Thoisen, C. V., Riisgaard, K., Lundholm, N., Gissel Nielsen, T., & Hansen, P. J., 2015. Effect of acidification on an Arctic phytoplankton community from Disko Bay, West Greenland. *Marine Ecology - Progress Series,* 520, 21-24. https://doi.org/10.3354/meps11123

Supplements

Supplement figure 1. Development of the Chl A µg/L (mean ± SD) during pH experiment in controls (pH 8.2) and 2 pH treatments (pH 7.7 and 7.2).

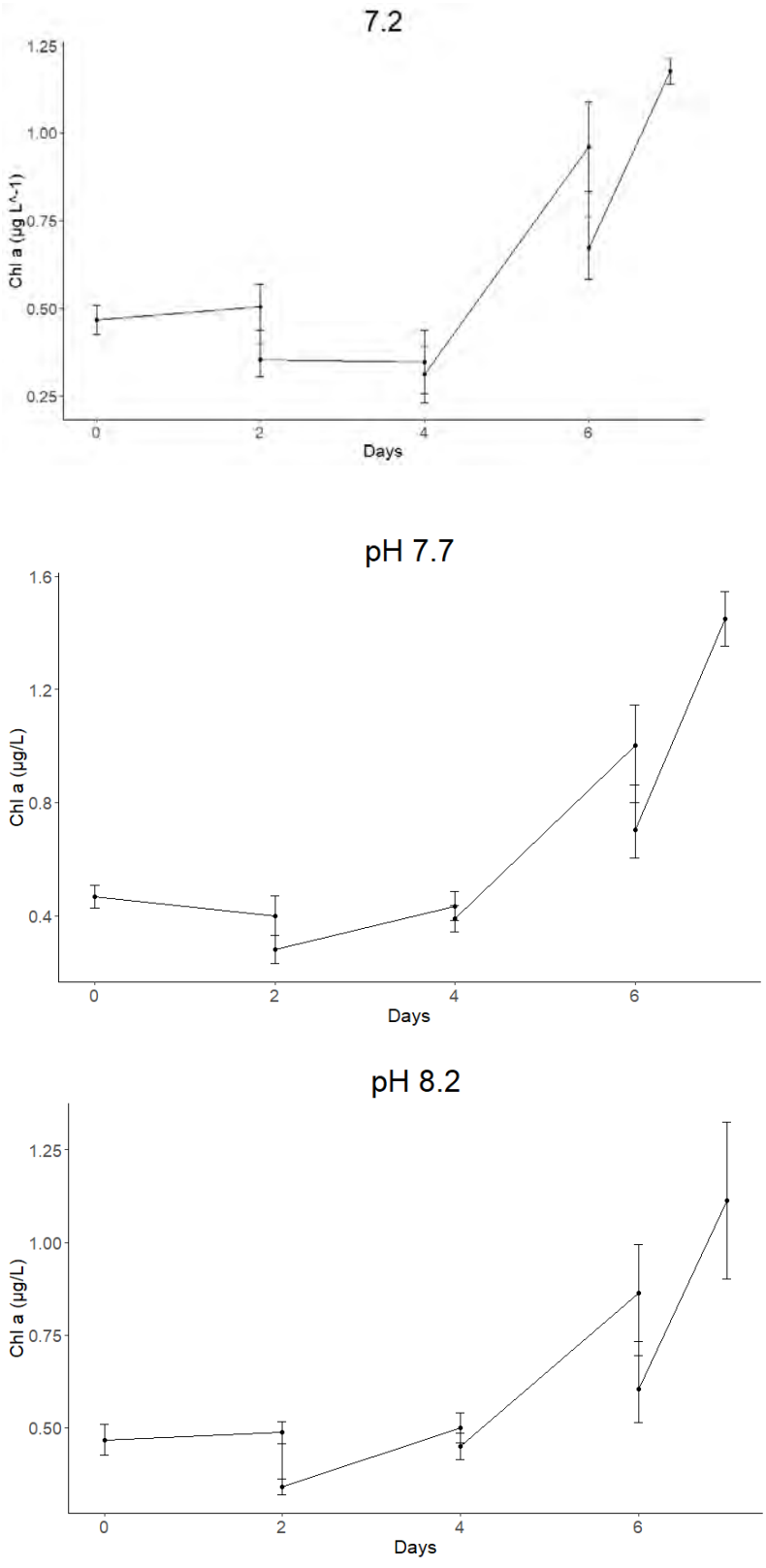

Supplement table 1. One-Way ANOVA tests for the variance in growth rates of the individual species between the three pH treatments followed by Tukey's tests. P values are given in the appendixes, and significant p values ($p<0.05$) are marked.

Species	pH comparison	P value (>/</= 0.050)
Gyrodinium spirale	7.7 vs. 7.2	**0.047**
	8.2 vs. 7.2	**0.010**
	8.2 vs. 7.7	0.446
Laboea strobila	7.7 vs. 7.2	0.399
	8.2 vs. 7.2	0.792
	8.2 vs. 7.7	0.178
Strombidium conicum	7.7 vs. 7.2	0.993
	8.2 vs. 7.2	1.000
	8.2 vs. 7.7	0.993
Protoperidinium bipes	7.7 vs. 7.2	0.096
	8.2 vs. 7.2	**0.001**
	8.2 vs. 7.7	**0.017**
Alexandrium sp.	7.7 vs. 7.2	0.385
	8.2 vs. 7.2	0.261
	8.2 vs. 7.7	0.942
Gyrodinium dominans	7.7 vs. 7.2	0.629
	8.2 vs. 7.2	0.997
	8.2 vs. 7.7	0.667
Dinophysis sp.	7.7 vs. 7.2	0.430
	8.2 vs. 7.2	0.982
	8.2 vs. 7.7	0.350
Strombidium	7.7 vs. 7.2	0.129
	8.2 vs. 7.2	**0.005**
	8.2 vs. 7.7	0.073
Cryptophyseae sp.	7.7 vs. 7.2	0.795
	8.2 vs. 7.2	0.877
	8.2 vs. 7.7	0.985
Dinobryon sp.	7.7 vs. 7.2	0.076
	8.2 vs. 7.2	**0.031**
	8.2 vs. 7.7	0.758

Supplement table 2. One-Way ANOVA tests for the variance in growth rates of heterotrophic-, constitutive mixotrophic-, and non-constitutive mixotrophic protists between the three pH treatments followed by Tukey's tests. P values are given in the appendixes.

Nutritional strategy	pH comparison	P value (>/</= 0.050)
Heterotrophy	7.7 vs. 7.2	0.287
	8.2 vs. 7.2	0.144
	8.2 vs. 7.7	0.918
Constitutive Mixotrophy	7.7 vs. 7.2	0.189
	8.2 vs. 7.2	0.100
	8.2 vs. 7.7	0.935
Non-constitutive Mixotrophy	7.7 vs. 7.2	0.765
	8.2 vs. 7.2	0.336
	8.2 vs. 7.7	0.746

Supplement table 3. One-Way ANOVA tests for the variance in growth rates of the chlorophyll levels between the three pH treatments followed by Tukey's tests. P values are given in the appendixes, and significant p values ($p<0.05$) are marked.

GR chl a	pH comparison	P value (>/</= 0.050)
Both day 6 and 7	7.7 vs. 7.2	0.811
	8.2 vs. 7.2	0.795
	8.2 vs. 7.7	0.359
Mean of day 6 and 7	7.7 vs. 7.2	0.399
	8.2 vs. 7.2	0.371
	8.2 vs. 7.7	**0.050**
Day 6	7.7 vs. 7.2	0.928
	8.2 vs. 7.2	0.206
	8.2 vs. 7.7	0.253
Day 7	7.7 vs. 7.2	0.410
	8.2 vs. 7.2	0.932
	8.2 vs. 7.7	0.522

Supplement figure 2. A standard phytoplankton growth medium the f/2 growth medium, Guillard, R.,1975

TABLE 1

Composition of Enrichment "f/2"

Major Nutrients (stock solutions are described in Table 4)	
$NaNO_3$	75 mg (883 µM)
$NaH_2PO_4 \cdot H_2O$	5 mg (36.3 µM)
$Na_2SiO_3 \cdot 9H_2O$*	15-30 mg (1.5-3 mg Si or 54-107 µM)
Trace metals (working stock solution is given in Table 6)	
$Na_2 \cdot EDTA$+	4.36 mg (ca 11.7 µM)
$FeCl_3 \cdot 6H_2O$+	3.15 mg (0.65 mg Fe or ca 11.7 µM)
$CuSO_4 \cdot 5H_2O$	0.01 mg (2.5 µg Cu or ca 0.04 µM)
$ZnSO_4 \cdot 7H_2O$	0.022 mg (5 µg Zn or ca 0.08 µM)
$CoCl_2 \cdot 6H_2O$	0.01 mg (2.5 µg Co or ca 0.05 µM)
$MnCl_2 \cdot 4H_2O$	0.18 mg (0.05 mg Mn or ca 0.9 µM)
$Na_2MoO_4 \cdot 2H_2O$	0.006 mg (2.5 µg Mo or ca 0.03 µM)
Vitamins (working stock solution is given in Table 8)	
Thiamin·HCl	0.1 mg
Biotin	0.5 µg
B_{12}	0.5 µg
Seawater ‡	to one liter

Notes: *Silicate may be omitted for organisms other than diatoms. The concentration used for diatom cultures may be adjusted according to the silicate concentration of the seawater used and the need for avoiding precipitation.

Studies of size-fractionated marine phytoplankton and diversity of net-phytoplankton in Disko Bay, Western Greenland (July 2022)

Stine Zander Hagen (tdn480), Katrine Maria Larsen (dxz925), Claudia Charlott Lassen (mzd131)

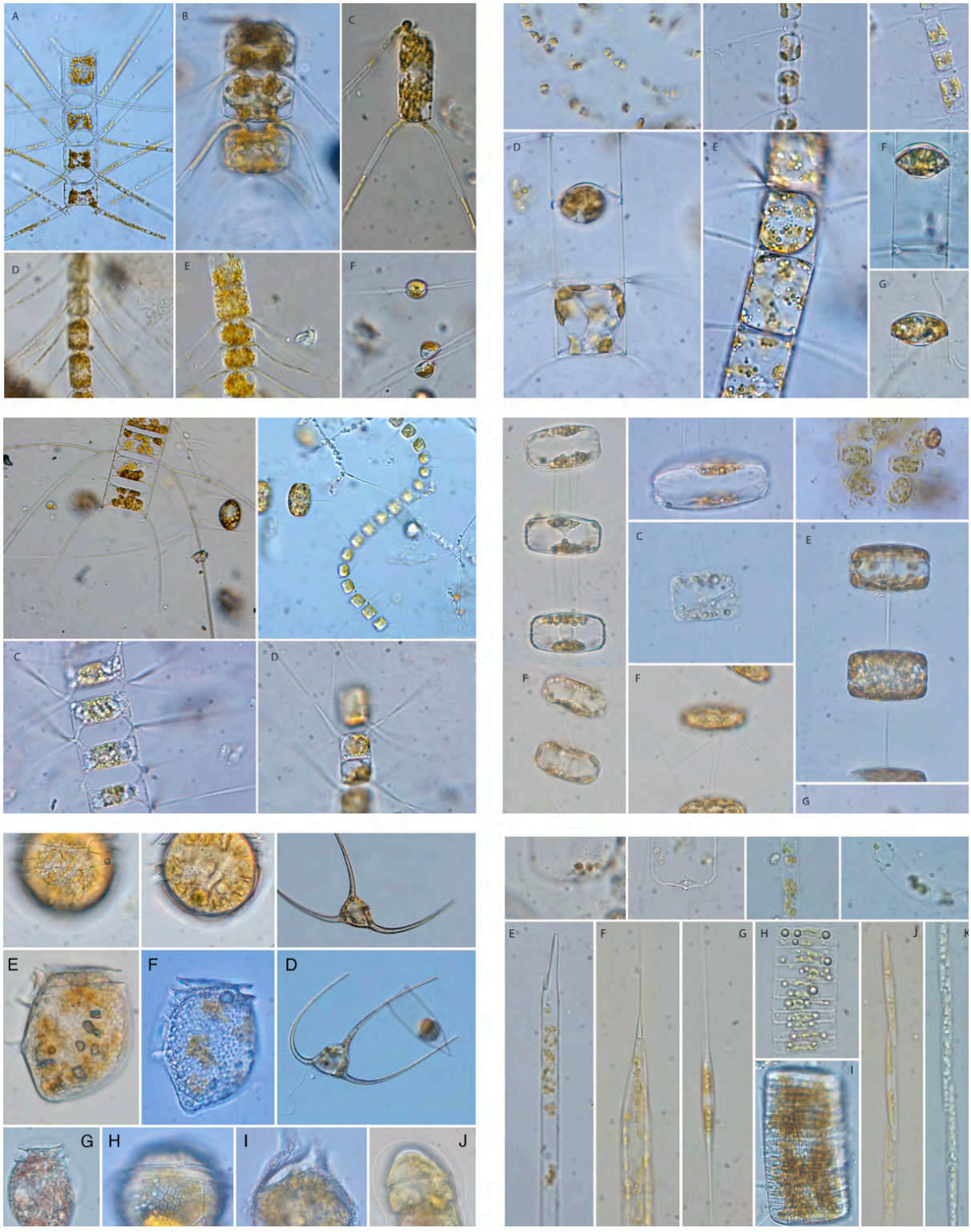

Preface

All fieldwork in this study was conducted during the Arctic Biology Field Course (Course B, Marine Phytoplankton Ecology) with supervision by Niels Daugbjerg and Per Juel Hansen (Dept of Biology) during a 12-day period in July/August 2022. All samples were obtained on board R/V 'Porsild' (belonging to the Arctic Station, University of Copenhagen) at five stations in Disko Bay and in the vicinity of Disko Island, Western Greenland. Environmental samples from 3 well defined depths were analyzed in the laboratories at the Arctic Station. All group members shared the total workload associated with sampling and data analysis equally. Additionally, this report has been written and discussed as a team with an equal contribution from all group members.

Abstract

Climate change is expected to have a profound role in the phytoplankton distribution and dynamics in Arctic marine ecosystems. This study was conducted in Disko Bay near Qeqertarsuaq (western Greenland) to gain an understanding of the dynamics in phytoplankton community composition in a rapidly changing environment. In this study we investigated how three size-fractionated (net-, nano- and pico-plankton) marine phytoplankton each contributed to the total chlorophyll *a* concentration at six locations around Disko Bay. Species diversity of net-phytoplankton was analyzed using light microscopy and species were photographed for comparison with studies conducted in the last 12 years. Pico-plankton had the highest relative abundance at all stations from fluorescence maximum samples and contributed with 45.5% - 71.3% (mean 61.9 ± 9.2%) to the total chlorophyll *a* across three sampled depths at all stations. Confirming our hypothesis, the mean contribution of pico-plankton was higher compared to results from previous years. Permanent Station 1 had the highest phytoplankton biomass and was significantly different from all other stations. Net-phytoplankton samples were dominated by the centric diatom genera *Chaetoceros* and *Thalassiosira*. Large numbers of lipid droplets were detected in all individual species within these two genera, as well as resting spore formation in some of the *Chaetoceros* species. These findings are seen as an indication of a decline of the summer bloom. All results coming from this study support previous studies conducted in the same area and contributes to the insight of potential phytoplankton changes in the Arctic Ocean.

Introduction

Marine phytoplankton play a significant role in global primary production, as they are responsible for up to 50% of the total net primary production in the world with ~10-15% of the total net production taking place on the continental shelves (Field et al. 1998; Finkel et al., 2009; Müller-Karger et al., 2005). Thus, primary production is a key process within the marine environment as the phytoplankton form the base of the entire ocean food web. As primary production depends on light availability and presence of nutrients, photosynthesis in the Arctic regions is highly seasonal due to the shifting light regime between summer (high activity) and winter (low activity) (Barber et al., 2015). Furthermore, impacts of climate change are expected to have a profound effect on the ecosystem in the Arctic regions which cause a different response in the primary production and hence higher trophic levels (Simo-Matchim et al., 2016). Some of the changes include increased air and surface water temperatures, increased precipitation, increased water column stratification, decreased salinity and decreased sea-ice coverage (Li et al., 2009; Coupel et al., 2015). Potential effects of climate change on primary production include earlier phytoplankton spring blooms due to less ice-coverage and increased activity in surface waters due to increased nutrient concentration from sea ice melt and discharge from land. All of this is expected to result in an overall change in phytoplankton community composition. As the Arctic Ocean is a significant contributor to the global carbon cycle and accounts for 10-14% of the total oceanic carbon dioxide sink (Bates and Mathis, 2009; Manizza et al., 2019) the changes mentioned above have the potential to affect the global carbon sequestration and the carbon cycle itself. Carbon export rates depend on the phytoplankton community size structure as the smaller size fraction increases the fast carbon turnover rate, whilst larger size fractions increase carbon sedimentation rates and storage (Finkel et al., 2009). Hence, Arctic phytoplanktonic size fractions and their contribution to the overall primary production are of great importance.

Phytoplankton is divided into three main size fractions; net-phytoplankton (20-200 µm), nano-plankton (2-20 µm) and pico-plankton (< 2 µm) (Sieburth et al., 1978). In general, the fate of phytoplankton varies depending on their size. Smaller sized phytoplankton e.g., pico-

plankton, has an advantage due to their larger surface area per unit volume making nutrient uptake more efficient (Raven, 1998; Li et al., 2009). Several studies have revealed that pico-plankton production and biomass is the greatest contributor to total phytoplankton production and biomass in nutrient depleted waters (Agawin et al., 2000; Tremblay et al., 2009). Even with their small size and biomass, pico-plankton is thought to be responsible for ~10% of the total marine net primary production (Raven, 1998). However, extensive knowledge on their distribution and contribution to the total biomass in the Arctic is yet to be fully understood (Metfies et al., 2016) and with climate change proceeding at accelerated speed the patterns in phytoplankton size fractions are expected to change. This makes determination of phytoplankton biomass and contribution in the Arctic Ocean an important parameter to explore in greater detail. To investigate phytoplankton biomass the most common method is extraction of chlorophyll a (from now on chl *a*) from environmental samples as these two parameters are well correlated (Huot et al., 2007). Previous studies using this method in the Disko Bay region (western Greenland) have shown the most dominating size fractions were net- and nano-phytoplankton (Lett et al., 2010; Salamon, 2019). However, Daufresne and colleagues (2009) explored that climate change will increase pico-plankton biomass and their experimental data revealed that pico-plankton was the greatest contributor to primary production in temperate and tropical regions. Knowledge and studies investigating this in the Arctic region is sparse but should be considered a high priority due to the Arctic waters being highly sensitive to increasing temperatures and sea-ice reduction due to decreasing albedo effect.

Disko Bay is located on the western coast of Greenland with an average depth of 400 meters. In the inner part of Disko Bay, Ilulissat Glacer, one of the most productive glaciers in the northern hemisphere, is located and creates large freshwater run off to the bay. The hydrography of Disko Bay is unique due to mixing of significant different water masses, formed by currents, temperature, and salinity differences. Large differences in water hydrography create strong water column stratifications which during summer divides the water column in Disko Bay into

different dynamic layers. The water column in Disko Bay is formed by the mixing of two distinct water currents - West Greenland Current (WGC) and Irminger Current (IC) in Davis Strait. These two water currents create a surface layer with low salinity due to high freshwater input and a saline water mass below 150 m. A cold winter layer is formed in between surface and deep water at ~100-150 m and the temperature gradient between the layers range from 1-2°C (Nielsen et al., 2005; Mascarenhas et al., 2019).

In this study we investigated how three size fractions net- (20-200 µm), nano- (3-20 µm) and pico-plankton (< 3 µm) contribute to the total biomass of the phytoplankton community in Disko Bay, south of Disko Island (Western Greenland) at different stations and three different depths using chl *a* extractions. Our results were compared to similar studies conducted in the same area for a thorough comparison of data during the last two decades. Furthermore, we identified net-phytoplankton species from all sample stations to gain knowledge on the species diversity and composition. In brief our hypotheses were (I) Picoplankton has an increasing relative biomass independent of geographic position and depth. (II) The highest biomass of phytoplankton will be found at the sewage discharge station due to the increased nutrient availability. (III) The lowest biomass of phytoplankton will be found at the Red River due to expected low light availability and high turbidity.

Materials and methods

Collection of water samples in Disko Bay

All samples were obtained onboard R/V 'Porsild' as part of the Arctic Biology Field Course in Disko Bay (July 2022). To determine chl *a* concentration, samples were collected in 2 l bottles from five stations at three depths depending on fluorescence measurements from the CTD profile. Water samples were collected during midday and represented both in open water and coastal stations (Fig. 1). Bottles were rinsed with water from the collected depths prior to sampling. The three depths constituted surface samples, samples at the fluorescence maximum and samples above or below the fluorescence maximum. Note that the permanent station (station 1 and 5) was sampled twice (beginning and end of the field campaign). Samples

from all depths were obtained in triplicates from individual Niskin casts to obtain an understanding of the biological variation. Profiles of temperature, salinity, light and fluorescence were measured with a Conductivity-Temperature-Depth-Profiler (CTD, Seabird SBE 19plus V2) and all environmental data was analyzed on board and provided for further analysis in this project. To interpret the species composition of net-phytoplankton, water was collected at all sampling stations through a 20 µm plankton net towed from 40-50 m to the surface. All sea water samples were stored in a cooling box aboard Porsild and upon return to Arctic Station stored at 4°C until further processing (within a maximum of 3 hours).

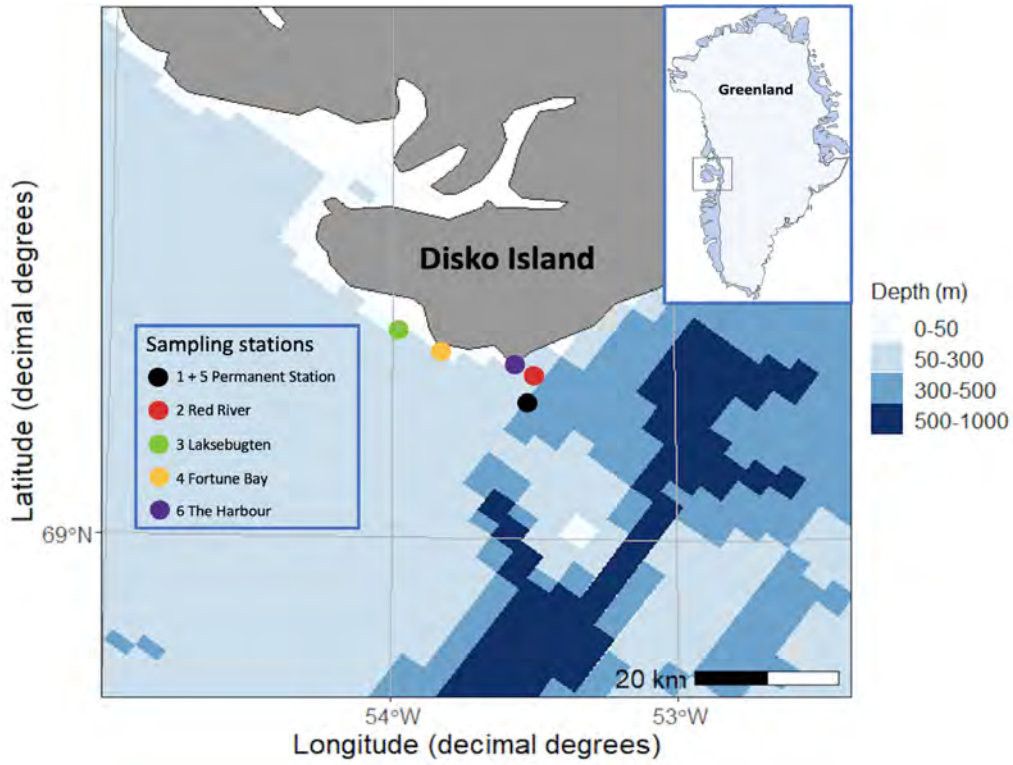

Fig. 1. Bathymetry in Disko Bay. Sampling stations are highlighted with colored dots.

Map is generated in RStudio with the package "ggOceanMaps" (Vihtakari, 2020).

Sampling stations

Sampling stations were chosen to target different water masses for comparison of net-phytoplankton species diversity and concentrations of chl *a*. To investigate biological variation over a 5-day period, samples from the permanent station (station 1 and 5) were obtained at the start (day 1) and end (day 6) of the field trip. This station was chosen due to its unique

hydrography as described in the introduction. Furthermore, the permanent station is frequently monitored and used as a fixed station for phytoplankton studies around Disko Bay which provides an opportunity for comparison of results. The Red River (station 2) was chosen due to its "red run-off"-particles from the mainland, including iron (Hauptmann et al., 2016). The red particles in the water column affect light conditions and nutrient availability which provides an opportunity to investigate how these factors affect phytoplankton biomass and diversity. A station close to the harbor in Qeqertarsuaq was chosen to determine the effects of sewage discharge. Laksebugten and Fortune Bay were chosen to investigate the diversity in a broader range around Disko Bay. Furthermore, sampling at these stations provides another opportunity for comparison of results to previous studies conducted in this area.

Measuring chlorophyll *a* concentrations

A filtration system using a combination of hand-operated vacuum-pumps and one electric vacuum pump was used (Fig. 2) to filter triplicate samples onto filters with three different sizes (20, 3 and 0.7 µm). However, all 2 l samples were pre-filtered through a 200 µm filter to remove zooplankton first, e.g., copepods. All sample volumes were noted prior to filtrations

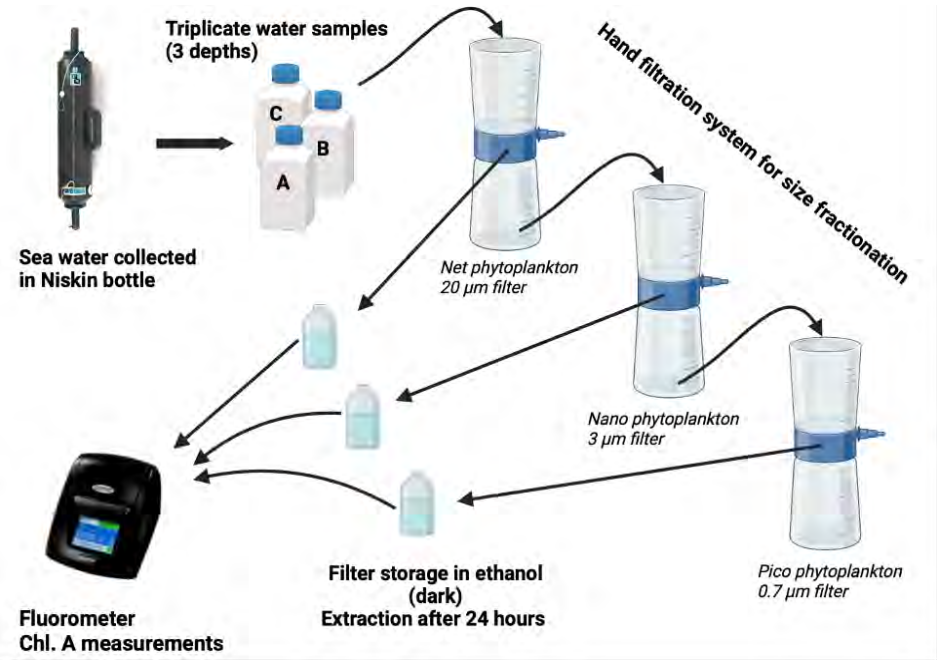

Fig. 2. Filtration and chlorophyll *a* measurements set-up.

Figure produced in BioRender.

and before filtrated through the different size fractionations. By hand-filtration all samples were pumped through the filtration system in a storage room with open doors. Hence, filtrations were performed at ~7 °C to assure temperature control. Straight after filtration, filters were removed and stored in 15 ml Falcon tubes wrapped in tinfoil for chl *a* extractions. All Falcon tubes were filled with 5 ml ethanol (96%) and stored in 4°C for approx. 24 h (following Jespersen and Christoffersen, 1987). At last, chl *a* was measured using a Trilogy Laboratory Fluorometer (Turner Designs, San Jose, USA) with ~1.2 ml pipetted from Falcon tubes to glass vials. Filtration and extraction volume (5 ml ethanol) from each individual sample were registered on the fluorometer to gain actual chl *a* values (µg l^{-1}), which provided the wanted proxy for the size-fractionated phytoplankton biomass. The fluorometer chl *a*-concentration was measured based on equation 1 (Turner Designs, 2019).

$$\text{Chlorophyll } a \text{ concentration} = C_{stand[1]} * [(F_{samp} - F_{blank})/ (F_{stand[1]} - F_{blank})] * (V_{solvent}/ V_{water})$$

Equation 1. Chlorophyll *a* end-calculations from the calibrated 'Non-Acidification'-method. $C_{stand[1]}$: standard concentration (calibrated), F_{samp}: sample fluorescence, F_{blank}: blank fluorescence (calibrated), $V_{solvent}$: ethanol solvent volume, V_{water}: filtered sample volume.

Statistical analyses

Statistical analyses were performed in RStudio version 2022.02.3 (R Core Team, 2022; RStudio Team, 2022). To explore differences in chl *a* concentration, data was grouped in two ways (I) station and depth, (II) station and phytoplankton size fraction. First a Shapiro-Wilk test was conducted to determine normal distribution followed by a Levene test to check the homogeneity of variance. If both assumptions were met a one-way ANOVA test was run. If data did not meet assumptions, a one-way ANOVA test was still included in the analysis and test results were marked. At last, a Tukey-HSD post hoc test was performed to find significance in between the specific groups.

Species diversity of net-phytoplankton

For collection of live net-phytoplankton samples, a plankton net with attached mesh (20 µm) was lowered into the water column and towed from ~40-50 m vertically up at all stations. The

collected water was transferred to a 0.5 l bottle and stored in 4°C at in situ light conditions. To determine species diversity and composition of live net-phytoplankton an Olympus BX51 light microscope was used. The microscopy was equipped with Nomarski differential interference. Species were identified using (I) Marine plankton diatoms of the west coast of North America, (II) The *Chaetoceros* Ehrenberg (Bacillariophyceae) Flora of Narragansett Bay, (III) Identifying Marine Phytoplankton and (IV) 'Norsk Kystplankton Flora' as the main identification guides. Photographs were taken with a digital camera (DP10) and photographic plates were assembled in Adobe Photoshop 2022.

Results

Sample conditions and environmental parameters in Disko Bay

Prior to sampling, CTD-profiles were analyzed to determine fluorescence max for the specific sampling station. Additionally, weather conditions, latitude, longitude, and bottom depth for all stations were noted prior to sampling (Table 1).

Station ID and name	Date	Weather	Sample depths, m	Latitude Longitude	Bottom depth, m
1 Permanent Station (Day 1)	23.07.22	Cloudy, foggy but calm water	Surface: 3 Chl. max: **31** Last: 20	69.1862 53.509933	340
2 Red River	23.07.22	Cloudy, foggy but calm water	Surface: 3 Chl. max: **19** Last: 31	69.221567 53.499333	137
3 Laksebugten	26.07.22	Sunshine, calm water	Surface: 3 Chl. max: **25** Last: 35	69.281 53.9723	88
4 Fortune Bay	26.07.22	Sunshine, calm water	Surface: 3 Chl. max: **30** Last: 40	69.251883 53.829333	77
5 Permanent Station (Day 6)	28.07.22	Sunshine, windy, waves, medium to strong currents	Surface: 3 Chl. max: **37.5** Last: 20	69.18565 53.522	340
6 Qeqertarsuaq Sewage discharge	28.07.22	Sunshine, windy, waves, medium to strong currents	Surface: 3 Chl. max: **30** Last: 20	69.236183 53.563733	75

Table 1. Schematic overview of environmental parameters at all stations (1-6)

The salinity and temperature profiles from the permanent station (station 1 and 5) at day 1 and day 6 present the unique hydrography of Disko Bay (Figs 3A; 4A) described in the introduction. The upper layer is classified as a less salty layer with lower salinity values and higher

temperature (~0-30 m). In the mid layer (~30-100 m) temperature decreases and salinity increases. At last (100-bottom), the temperature starts to increase as the water mixes with warm Atlantic water input from the Irminger Current.

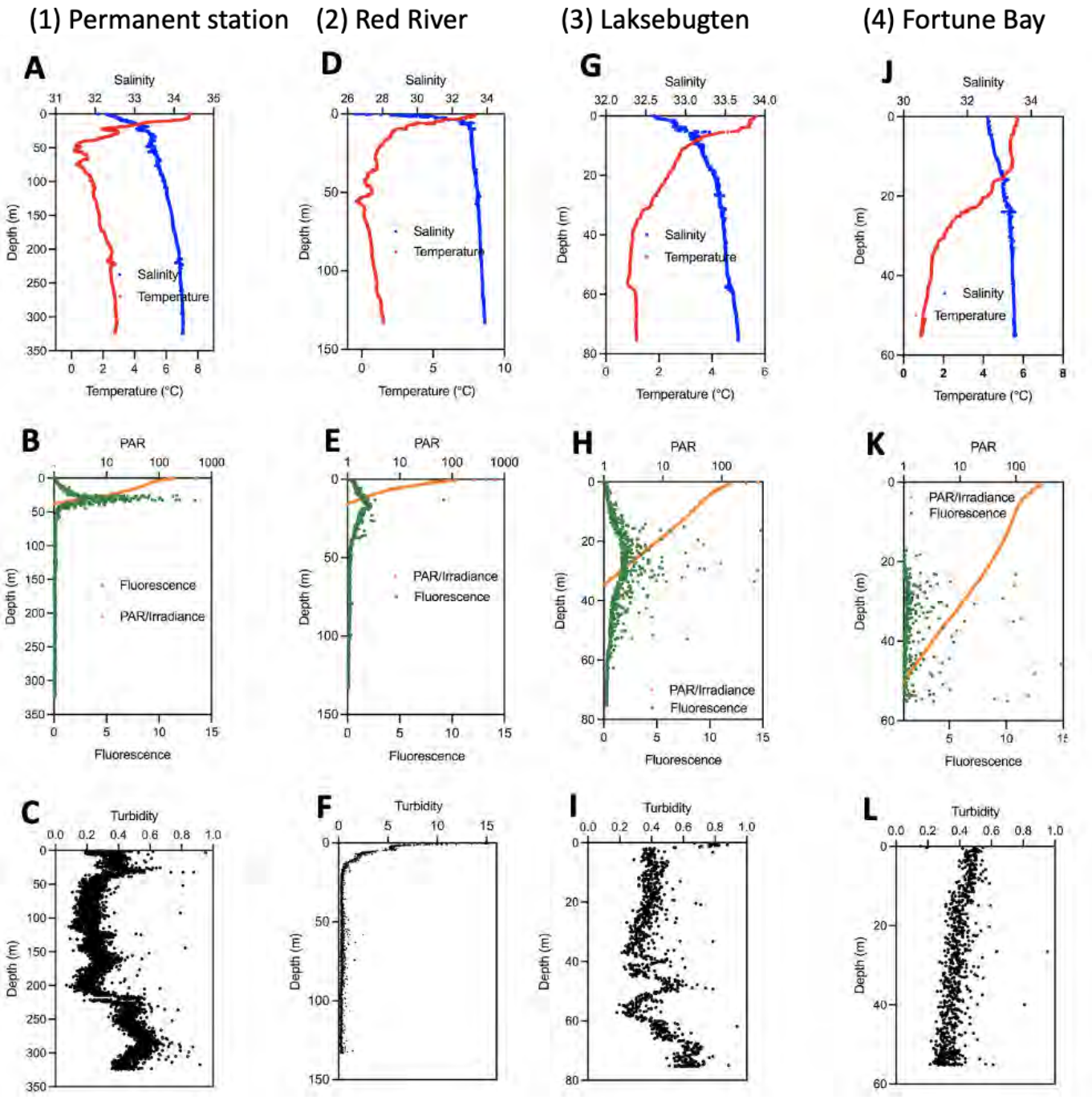

Fig. 3. CTD-profiles prior to sampling at stations 1-4. **A-C)** Permanent Station (Day 1). **D-F)** The Red River. **G-I)** Laksebugten. **J-L)** Fortune Bay. Salinity and temperature profiles are shown in **A, D, G, J.** Light measurements in terms of PAR and fluorescence are shown in **B, E, H, K**. Turbidity is shown in **C, F, I, L.**

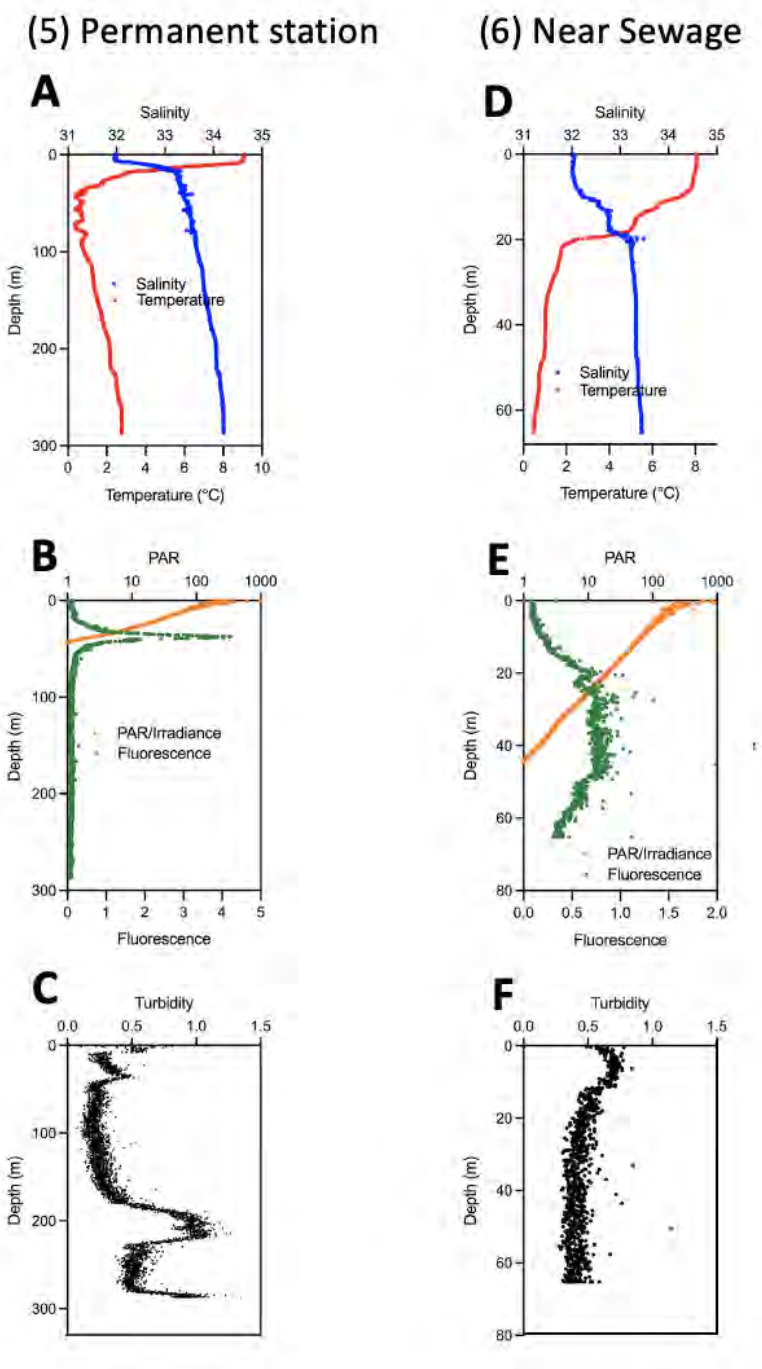

Fig. 4. CTD-profiles prior to sampling at stations 5 and 6. **A-C)** Permanent Station (Day 6). **D-F)** Station (6) Near Qeqertarsuaq sewage discharge. **A, D)** Temperature and salinity profiles. **B, E)** Light measurements in terms of PAR and fluorescence and irradiance profiles. **C, F)** Turbidity profiles.

All stations showed similar salinity patterns in salinity increasing with increased depth and displayed a surface salinity value of ~32, except for the Red River which had a value of 26 (Fig.

3D). The low salinity in the Red River reflects the freshwater run-off from the coast. Furthermore, all stations had similar turbidity profiles except the Red River station, where the turbidity was ten-fold higher due to the run-off from the coast (Fig. 3F). The PAR/Irradiance profiles showed light availability down to 50 meters depth at Fortune Bay (Fig. 3K) and down to 20 meters depth at the Red River station (Fig. 3E). All other stations had PAR/Irradiance values ranging between 35-42 meters depth. The highest measured fluorescence value was seen at the permanent station day 1 where fluorescence maximum was located where the PAR/Irradiance ends at almost all stations.

Phytoplankton biomass distribution

For all surface samples pico-plankton had the highest biomass (relative abundance) except for station 2 (Red River) where nano-plankton was the most dominating size-fraction (Fig. 5a). Furthermore, pico-plankton also dominated the relative biomass in samples collected from fluorescence max at all stations (Fig. 5b). The contribution of pico-plankton to the total chl *a* across the three depths ranged from 45.51% to 71.29% with a mean of 61.98 ± 9.24%. For surface samples taken at day 1 and 6 at the permanent station no significant differences were found in between the different size-fractions. However, the relative biomass in fluorescence max samples at the permanent station showed large differences from day 1 to day 6

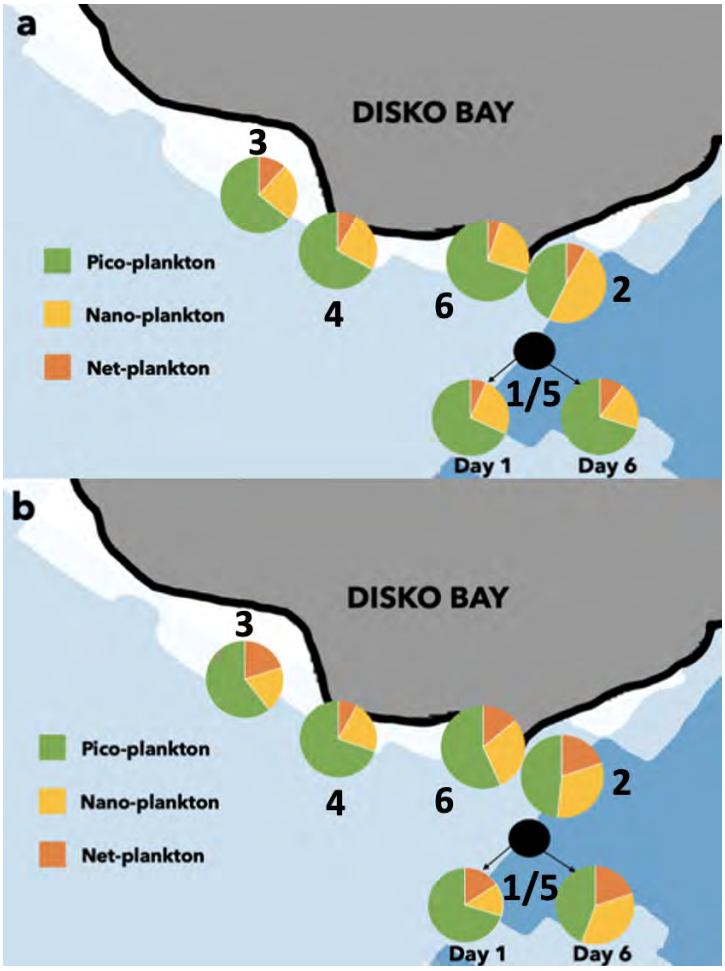

Fig. 5. Biomass distribution of net-, nano- and pico-plankton across the six sample stations (indicated with numbers 1-6) **a)** Biomass distribution for surface samples (3 m) **b)** Biomass distribution for chl max samples

with pico-plankton biomass being significantly different (Student T-test, p = 0.0018). However, no significance was found when comparing the change in biomass of net-phytoplankton and nano-plankton (Student t-test, p>0.05). Significant differences in total chl *a* concentration from all surface samples were found when comparing station 2 and 6, and station 2 and 3 (Fig. 6a). For samples collected at fluorescence max, the concentration of total chl *a* was highest at the permanent station (day 1) which resulted in this station being significantly different compared to all other stations (Fig. 6b). Additionally, station 2, 3 and 5 had significantly higher concentrations in total chl *a* compared to station 4 and 6 (Fig. 6b). Net-phytoplankton were the fraction with the lowest relative abundance at all stations and depths but had higher relative abundance in fluorescence max samples compared to surface samples at all stations except at station 4 (Fortune Bay). Statistical analysis on differences in total chl *a* between the three different size-fractions showed that pico-plankton had significantly higher chl *a* concentration compared to nano- and net-phytoplankton in nearly all samples, and especially in fluorescence max samples (although, one exception at the permanent station day 6) (Fig. 7). In general, nano-plankton showed higher chl *a* concentration compared to net-phytoplankton which especially was seen at station 2 and 6, where significant differences were found at all depths except for 19 m at station 2 (Fig. 7). The two highest chl *a* concentrations were found at the permanent station (day 1) from fluorescence max and 20 m samples with means of 1.37 ± 0.2 µg l^{-1} and 0.92 ± 0.1 µg l^{-1}, respectively. Chl *a* max values ranged between 19-37.5 m at the Red River and

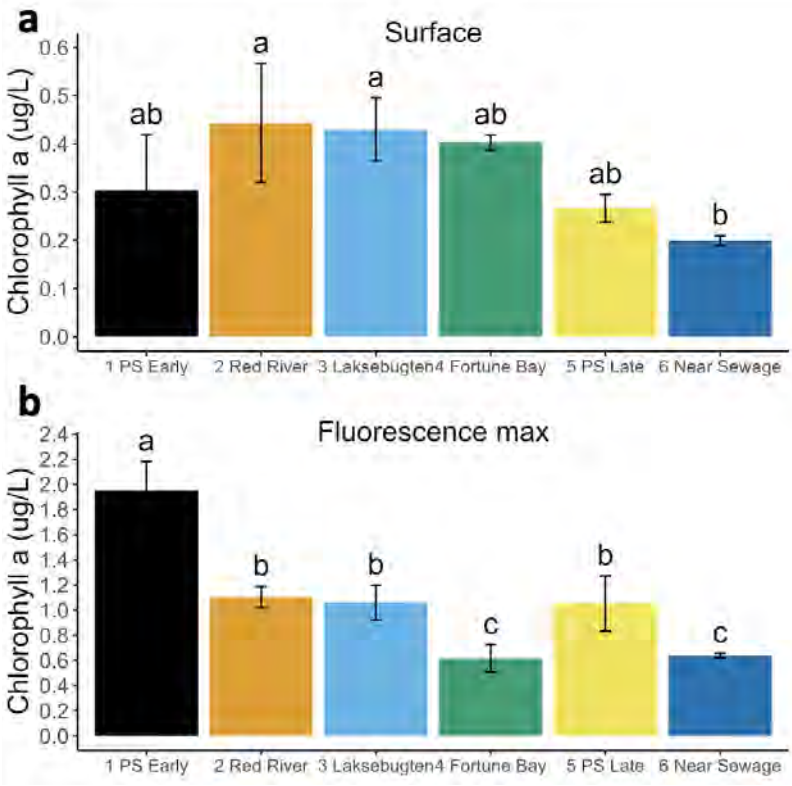

Fig. 6. Total chlorophyll a concentration for all stations at (**a**) surface level (3m) (**b**) fluorescence maximum. Error bars display standard deviation from each station. Significance between stations is marked with a different letter when p < 0.05.

permanent station day 1, respectively (Fig. 8). These depths were significantly different in all size fractions from the two other sample depths at the stations. All stations had the highest

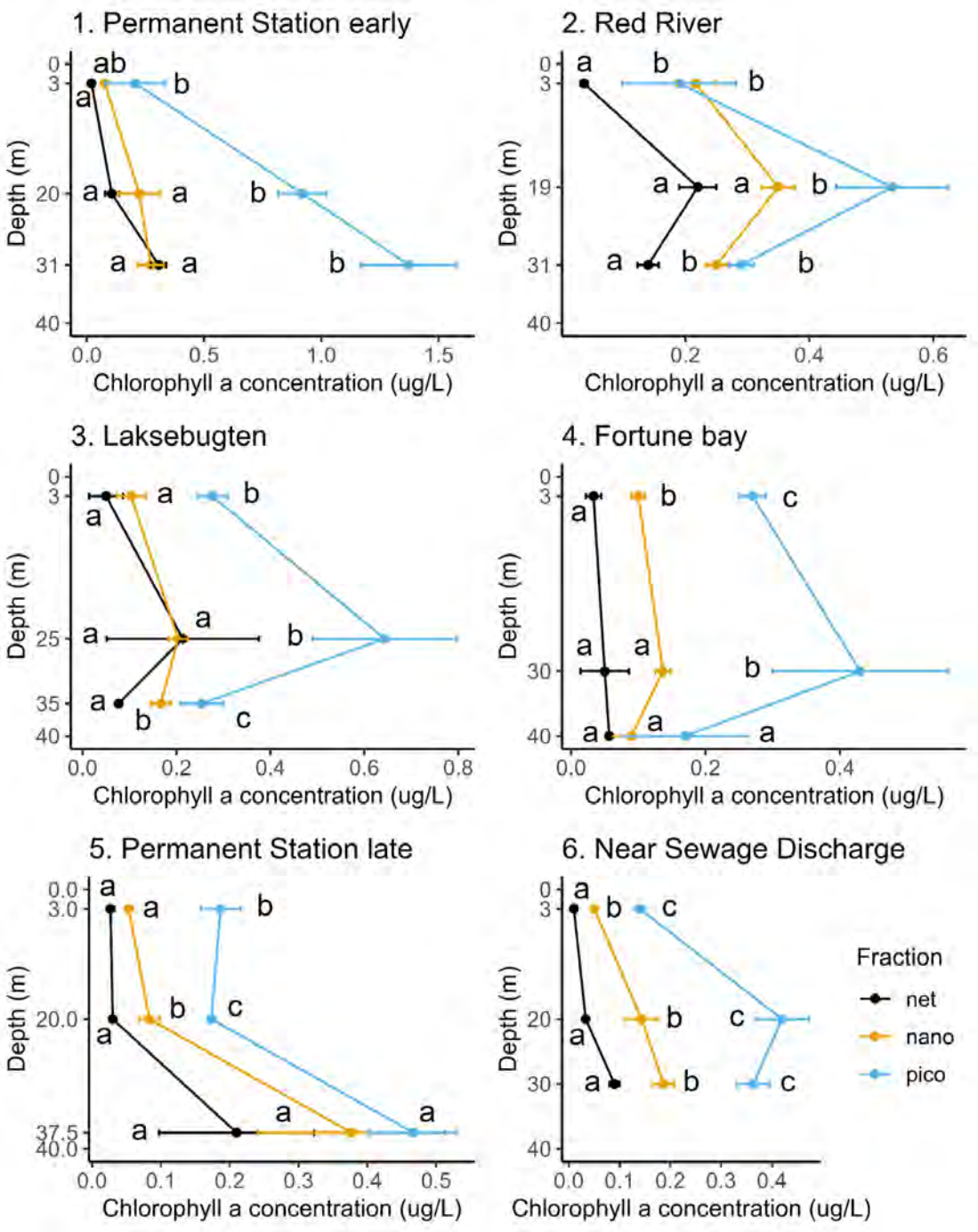

Fig. 7. Chlorophyll *a* concentration in net-, nano- and pico-phytoplankton size-fractions across all six stations from three different depths. Error bars display standard deviation (SD) from each station. Significance between size-fractions at individual depths at all six stations is shown with a different letter when $p < 0.05$.

For specific p-values see Supplementary material 2

chl *a* concentration in samples collected from fluorescence max depth (as expected) resulting in these samples being significantly different from other sample depths in at least one of the size fractions. At station 6 fluorescence max was unclear to determine as picoplankton had its highest chl *a* concentration at 20 m whereas net- and nanoplankton had max chl *a* at 30 m. Although, no statistical differences between these two depths were found (Fig. 8).

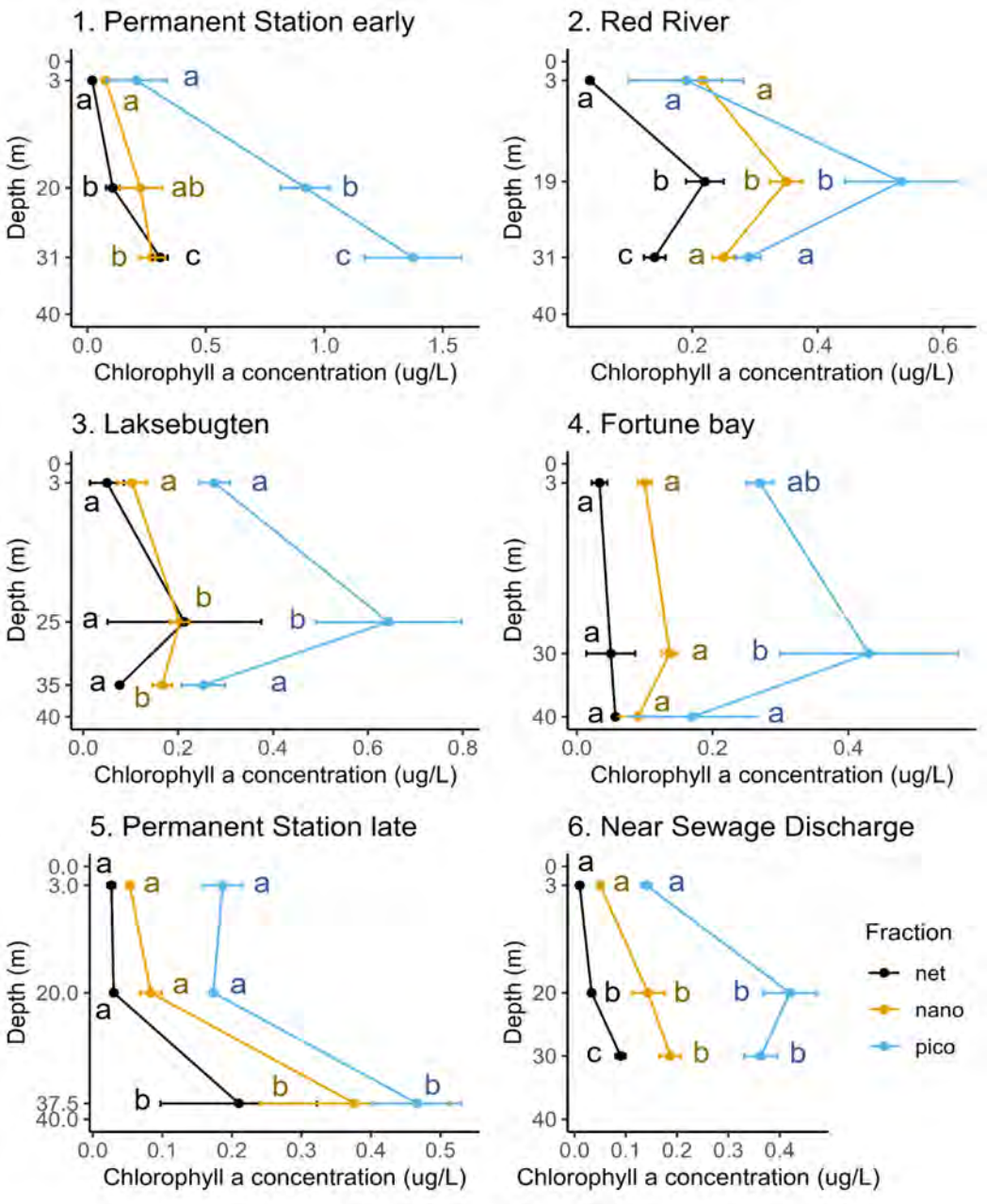

Fig. 8. Chlorophyll concentrations in net- nano- and picoplankton fractions across all six stations from three different depths. Error bars display standard deviation from each station. Significance between depths for each size fraction at all six stations is shown with a different letter when $p < 0.05$.

For specific p-values see Supplementary material 3.

Net-phytoplankton species diversity

Diatoms (Plates 1-5) and dinoflagellates (Plate 6) were the two major groups dominating all net-phytoplankton samples across our six stations with diatoms being the most diverse group with a total of 25 species identified. Overall, *Chaetoceros* was the most abundant and diverse group observed with a total of 12 different species identified (Plate 1-3). In general, all stations (except for station 5) showed similar diversity with an average of 10 diatom species present at each station. The Permanent Station sampled over a 5-day period (station 1 and 5) showed a massive change in species diversity (Table 2) with e.g., 5 species of *Chaetoceros* present at day 1 but none at day 6. Individual diatom species were mainly present in samples from 1-3 stations, whereas only 4 species were located at 5 of 6 stations. *Thalassiosira* cfr. rotula was the only diatom found at all stations. Individual species of dinoflagellates were present at more stations than diatoms. More than half of the identified dinoflagellate species e.g., *Dinophysis norvegica* and *Ceratium arcticum* were found in samples from 4/5 stations out of all 6 stations. Furthermore, *Dinophysis acuta* was the only dinoflagellate species found at all six stations. The Permanent Station (station 1 and 5) had the highest dinoflagellate diversity out of all stations with *Gonyaulax* cysts only found here. Laksebugten (station 3) was the station with lowest dinoflagellate diversity with 3/10 identified species present. Some

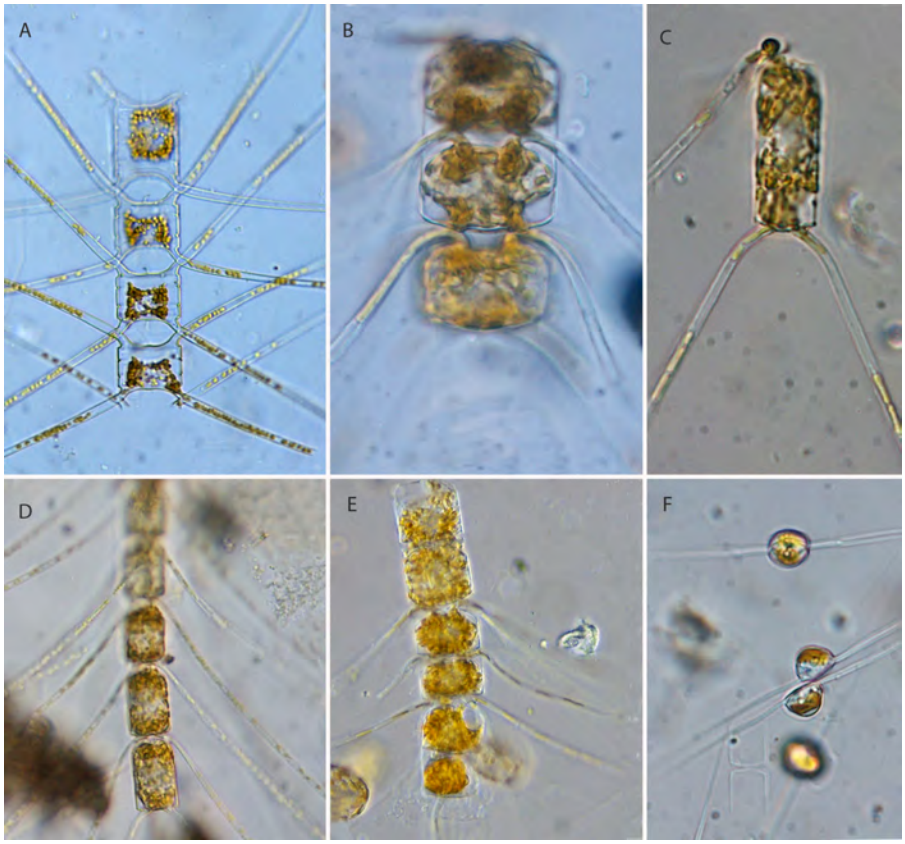

Plate 1. Live cells photographed in Nomarski interference contrast microscopy. **Centric diatoms. A**. *Chaetoceros atlanticus.* **B**. *Chaetoceros concavicornis*. **C**. *Chaetoceros trondsenii* var. *trondsenii.* **D-E**. *Chaetoceros convolutus*. **F**. *Chaetoceros furcellatus* (resting spores).

species were only observed at Station 6, e.g., *Eucampia groenlandica* and *Leptocylindrus danica*. We refrain from giving detailed morphological descriptions of all net-phytoplankton species identified during this project as these have already been given in several previous projects addressing the diversity of the phytoplankton community in Disko Bay (see e.g., Backhause et al., 2014, Helmark et al., 2018). During our light microscopical survey of all six net samples we also encountered numerous heterotrophic protists. These mainly belonged to thecate and athecate dinoflagellates. The most abundant species of thecate dinoflagellates belonged to the genus *Protoperidinium*. This genus was represented by at least 5 different species (qualified estimate based on the micrographs taken). Among the heterotrophic athechate dinoflagellates the genus *Gyrodinium* was abundant with relatively high numbers of *G. spirale* and *G. gracile*. Interestingly, ciliates were not

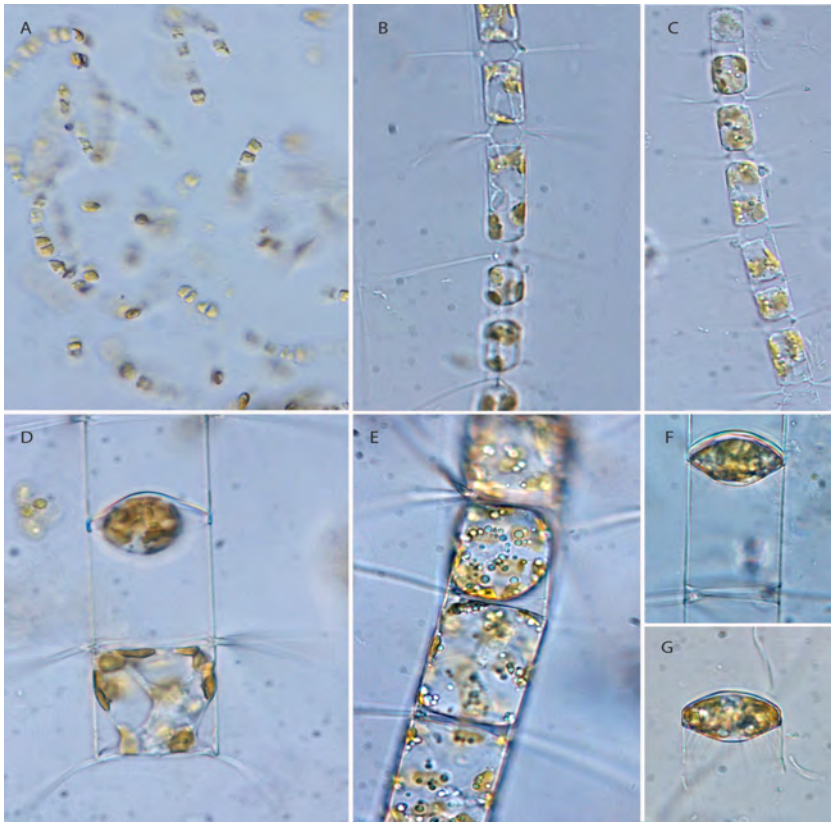

Plate 2. Live cells photographed in Nomarski interference contrast microscopy. **Centric diatoms. A**. *Chaetoceros gelidus.* **B-C**. *Chaetoceros contortus*. **D-G**. *Chaetoceros teres*. **D-E**: vegetative cells. **F-G**: resting spores.

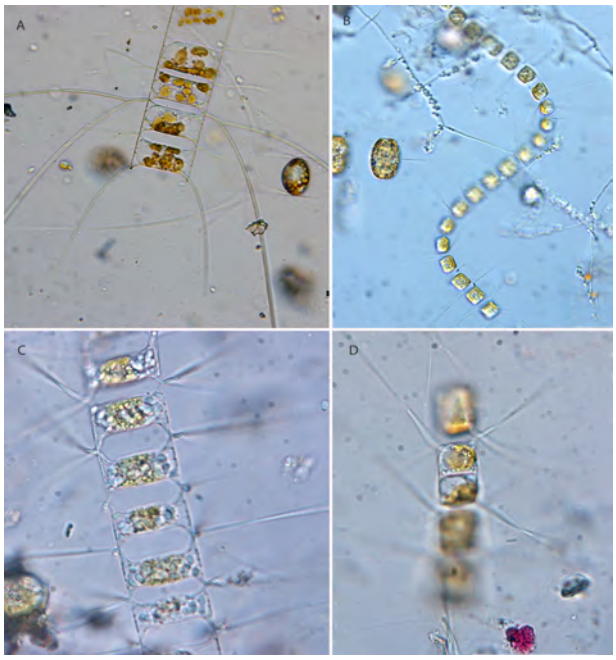

Plate 3. Live cells photographed in Nomarski interference contrast microscopy. **Centric diatoms. A**. *Chaetoceros decipiens*. **B**. *Chaetoceros debilis*. **C**. *Chaetoceros* sp. 1. **D**. *Chaetoceros* sp. 2.

abundant in our net-phytoplankton samples, which may be explained by the physical treatment of the water samples during collection.

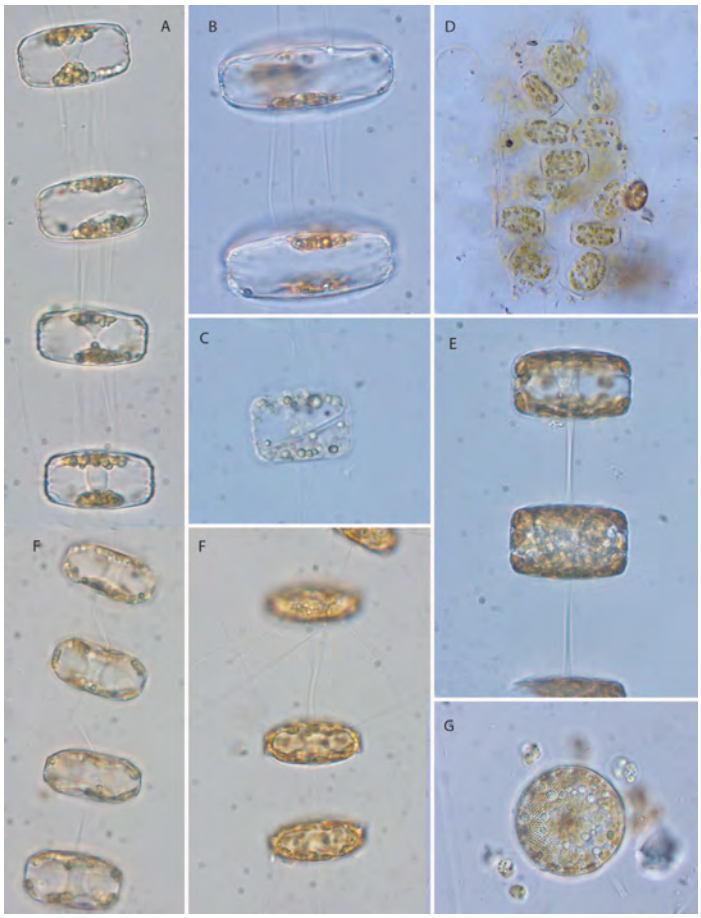

Plate 4. Live cells photographed in Nomarski interference contrast microscopy. **Centric diatoms. A-C**. *Thalassiosira anguste-lineata*. **D**. *Thalassiosira subtilis*. **E**. *Thalassiosira* cf. *rotula*. **F**. *Thalassiosira nordenskioeldii.* **G**. *Thalassiosira* sp. (valve face).

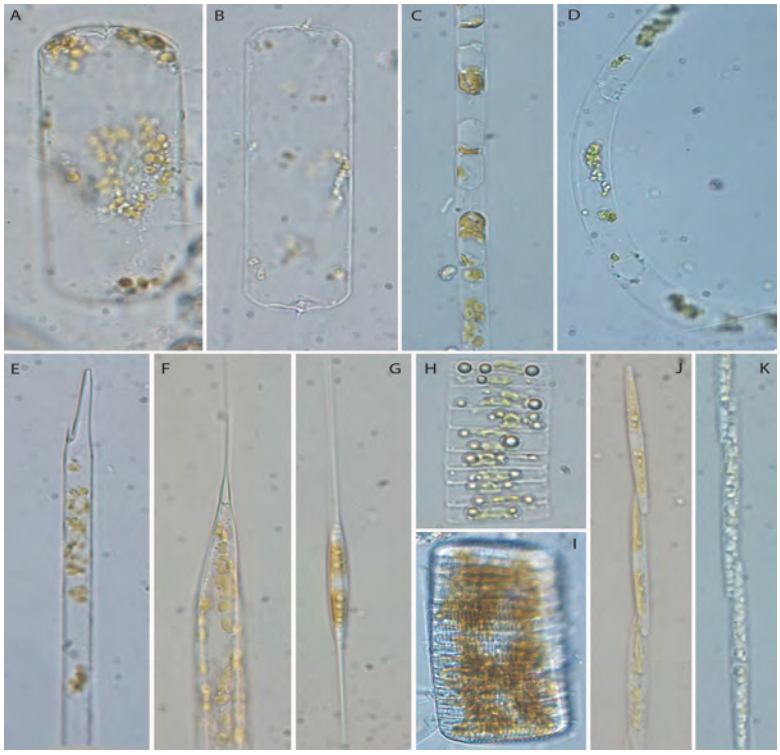

Plate 5. Live cells photographed in Normarski interference contrast microscopy. Centric and pennate diatoms. **A-B**. *Dactyliosolen fragilissimus*. **C**. *Leptocylindrus danicus*. **D**. *Eucampia groenlandica*. **E**. *Proboscia alata*. **F**. R*hizosolenia hebetata* f. hebetata. **G**. *Nitzschia longissima*. **H**. cf. *Fragilariopsis* sp. **I**. Unidentified pennate diatom. **J-K**. *Pseudo-nitzschia* sp.

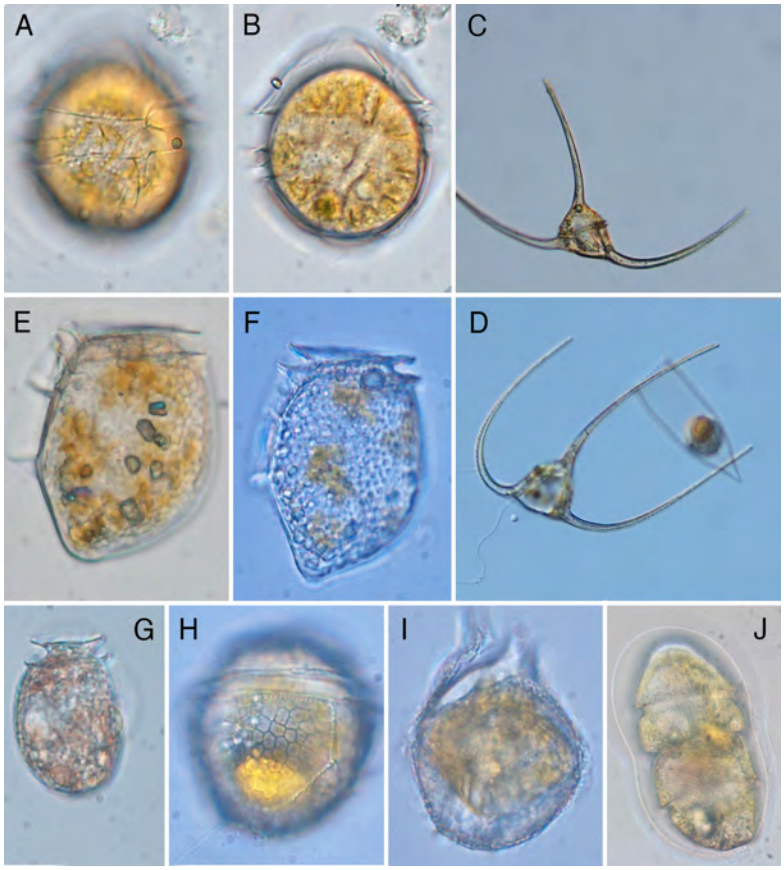

Plate 6. Live cells photographed in Nomarski interference constrast microscopy. Thecate and athecate dinoflagellates. **A-B**. *Alexandrium* sp. **C**. *Ceratium arcticum*. **D**. *Ceratium longipes.* **E**. *Dinophysis acuta*. **F**. *Dinophysis norvegica*. **G**. *Dinophysis acuminata*. **H**. *Protoceratium reticulatum*. **I**. *Gonyaulax* cf. *digitale*. **J**. *Warnovia* sp.

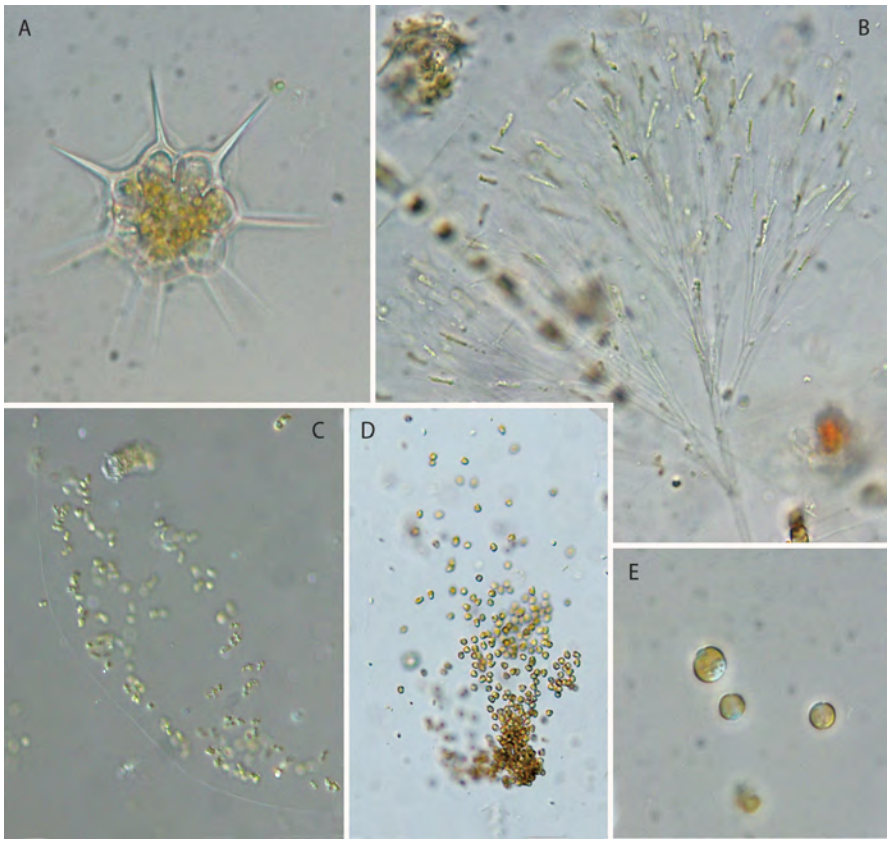

Plate 7. Live cells photographed in Nomarski interference contrast microscopy. Nanoflagellates.
A. *Dictyocha speculum*.
B. *Dinobryon balticum*. **C-E**. *Phaeocystis pouchetii.*

Stations	Station 1	Station 2	Station 3	Station 4	Station 5	Station 6
Dinopohyceae (dinoflagellates)						
Alexandrium sp.	X			X	x	X
Ceratium arcticum	X	X		X	X	X
Ceratium longipes					X	X
Dinophysis acuminata	X	X		X	X	X
Dinophysis acuta	X	X	X	X	X	X
Dinophysis norvegica	X	X	X	X		X
Gonyaulax cyst	X				X	
Gonyaulax cfr. *digitale*	X		X		X	
Protoceratium reticulatum	X			X	X	
Warnovia sp.	X				X	X
Bacillariphyceae (diatoms)						
Chaeotoceros atlanticus				X		
Chaeotoceros convolutus	X		X			
Chaeotoceros decipiens		X	X	X		
Chaeotoceros gelidus			X			
Chaetoceros concavicornis	X					
Chaetoceros contortus	X	X	X	X		
Chaetoceros debilis			X			X
Chaetoceros furcellatus				X		
Chaetoceros sp. 1				X		
Chaetoceros sp. 2				X		
Chaetoceros teres (with resting cysts)	X		X	X		
Chaetoceros trondsenii var. trondsenii	X					
Dactyliosolen fragilissimus				X		X
Eucampia groenlandica						X
Leptocylindrus danicus						X
Nitzschia longissima		X				
Proboscia alata				X		X
Pseudo-nitzschia sp.		X	X		X	
Rhizosolenia hebetata f. hebetata	X		X	X	X	
Thalassiosira anguste-lineatum	X	X		X	X	X
Thalassiosira cfr. rotula	X	X	X	X	X	X
Thalassiosira nordenskioeldii	X	X	X		X	X
Thalassiosira subtilis		X				
cfr. *Fragillariopsis* sp.	X	X				X
Unidentified pennate diatom						X
Dictyochophyceae (silicoflagellates)						
Dictyocha speculum	X					X
Chrysophyceae (golden algae)						
Dinobryon balticum	X			X		X
Haptophyceae						
Phaeocystis pouchetii	X	X	X			

Table 2. Schematic overview of identified net-phytoplankton species at all stations (1-6).

Discussion

Phytoplankton biomass distribution

We expected the Red River station to have the lowest phytoplankton biomass of all stations due to low light availability as well as high turbidity. CTD profiles from this station confirmed our hypothesis about the conditions at the station (Fig. 3 E+F), however the biomass was still significantly higher. Weather conditions on the sample day were overcast and foggy, hence this could not have contributed to the significantly higher biomass. The reason for the biomass being higher than we expected could be due to the high run-off containing melting water with silt, mud, nutrients, and organic matter. This would enable a big number of phytoplankton even though the light only travels a short distance through the water column. To test if this was true, determination of nutrient concentrations could have been conducted.

At fluorescence max samples, the phytoplankton biomass from the Sewage discharge station was significantly lower compared to all stations except Fortune Bay where no significant differences in biomass were found (P-values in S5). The biomass at the surface in the Sewage discharge station was only significantly lower than Red River and Laksebugten ($p = 0.028$, $p = 0.049$). These results were opposite to our expectations, as we assumed the sewage discharge would increase the biomass of phytoplankton due to increased levels of nutrients. The biomass appears to be lower, due to a less clear spike in fluorescence resulting in a lower biomass at the fluorescence maximum. This unclear spike is displayed in both the CTD (Fig. 4E) and the chl *a* measurements (Fig. 8). To test whether this could explain the lower biomass an integrated chl *a* sample would be needed, or chl *a* measurements at several depths collected and analyzed.

The total phytoplankton biomass at the permanent station early and late were significantly different ($p = 0.0001$) at fluorescence max. The total chl *a* concentration at the permanent station early was 1.9 µg l^{-1}, whereas permanent station late was 0.6 µg l^{-1}. This station was sampled twice to investigate the dynamics during a 5-day period. The permanent station was considered an open water station where a lower biomass is expected compared to other stations which are shallower and more coastal e.g., Laksebugten and Fortune Bay. Coastal stations are expected to have higher nutrition levels due to run-off from land. However, our

results contradicted this hypothesis. Permanent Station early had a significantly higher biomass compared to all other stations (S5) at the fluorescence max depth (Fig. 6b). We suggest, this could have been different if samples were conducted at the beginning of the spring/summer bloom and that our results may reflect the decline of the summer bloom. The difference in biomass from day 1 to 6 at the Permanent Station demonstrates how dynamic the community is during the decline of the bloom. Also, it emphasizes that the biomass and species diversity results from this and previous year's reports should be seen as a momentary picture of the community, as the community can change rapidly. Finally, the water column at the Permanent Station cannot be considered stagnant as local currents most likely transport "new" water to and "old" water away from the area. Transport of water bodies due to currents may of course also introduce a phytoplankton biomass which essentially was built in another geographical area.

Net-phytoplankton species diversity

Diatoms and dinoflagellates were the most common net-phytoplankton groups observed. *Chaetoceros* was the most abundant and diverse genus found in our samples (Plates 1-3) and were found at all stations except for Permanent Station late (Table 2, Station 5). *Thalassiosira* was another diatom genus which was found at all stations (Plate 4 and Table 2). This was anticipated, as studies from Disko Bay in 2014 as well as 2018 found a community dominated by the exact same genera (Backhaus et al., 2014, Helmark et al., 2018). According to Krawczyk et al., a study from 2007, also found a *Thalassiosira* dominated community, this composition reflects the summer/autumn bloom (Krawczyk et al., 2015). Most of the net-phytoplankton samples contained phytoplankton with lipid droplets, which indicates a declining bloom. The only station that deviated from this was station 6, Sewage Discharge Station. Phytoplankton from this station did not reflect any signs of nutrition depletion. They appeared healthier with more yellow-brown colors. Though we did only detect one species of *Chaetoceros*, *Chaetoceros debilis* (Plate 3 b). Other signs of the bloom declining included resting spores.

No station stood out as having less species diversity than others, as station 2; Red River, 3; Laksebugten, and 5; Permanent Station late, all had 14 species observed, which was lower than the three other stations. The biggest species diversity was observed at the Permanent Station early. Five different species from the *Chaetoceros* genus were observed in the net-

phytoplankton sample on day 1. However, no *Chaetoceros* sp. were found when returning on day 6 which indicated the sedimentation of resting spores (Table 2). On the other hand, this could explain the biomass differences between Permanent Station early and late.

A pico-plankton dominated Bay - First sign of climate change?

The pico-plankton fraction was expected to dominate the stations independent of depth. Our results mainly support this hypothesis as pico-plankton chl *a* was significantly higher than the other fractions at least two depths except for the Red River (Fig. 7). The Red River also contained a large amount of the nano-plankton fraction. The environmental conditions at the Red River could explain the differences from other stations as discussed previously. We expected pico-plankton to dominate due to the increasing abundance of picoplankton throughout recent years in both Arctic marine ecosystems, but specifically in Disko Bay (Booth et al., 1997, Helmark et al., 2018, Sørensen et al., 2011). In our study, the relative chl *a* concentration by pico-plankton to the total concentration ranged between 45.51% and 71.29% with a mean of 61.98%. This mean was larger than the study conducted in 2018 where the study estimated the mean to be 50.44% with a range of 11.37% to 84.34%, and almost a three-fold increase from the Arctic Field Course 2010 Lett *et al.* where the mean was estimated to be 21.4% with a range from 3.2% to 61.5%. It should be noted that all these studies were conducted at almost the same dates in July. A possible explanation to this tendency could be that they are better adapted to the changing Arctic marine ecosystem due to their smaller surface-area-to-volume ratio (Li et al. 2013).

Conclusion

In conclusion, pico-plankton was the overall largest contributing fraction to the total chl *a* concentration and had a higher relative abundance in comparison to previous studies from this area. Permanent Station early had the highest overall biomass and the highest pico-plankton biomass at fluorescence max. Net-phytoplankton samples were quite similar in diversity however, significant differences between sampling at the permanent station over 5 days, were noticed. Interestingly no species of *Chaetoceros* were detected at Permanent Station late, suggesting that these colony-forming diatoms had sunken out of the water column. Furthermore, differences in the lipid content were detected in the phytoplankton sample from the Sewage discharge station where no lipids were noticed, possibly due to higher nutrient

availability offsetting the decline of the bloom. The most common genera were *Chaetoceros* and *Thalassiosira*, but in general the diversity of diatoms was rather large.

Acknowledgements

The authors would like to thank Niels Daugbjerg for valuable supervising and for sharing his incredible knowledge on phytoplankton species diversity. We would also like to thank both Per Juel Hansen and Niels Daugbjerg for motivating us during our stay and field excursions. Furthermore, we thank our captain Jørgen-Peter, and the crew Erik and Eli on board R/V 'Porsild' for helping us collect our samples and sharing their exceptional knowledge on the Disko Bay region. Lastly, we would like to thank Morten Rasch and Emilie Henningsen for a pleasant stay at the Arctic Station and for helping with water collection and CTD data as well as fun hikes in the area.

Supplementary Data

S1 - Relative chlorophyll percentage in the three different fractions across all stations

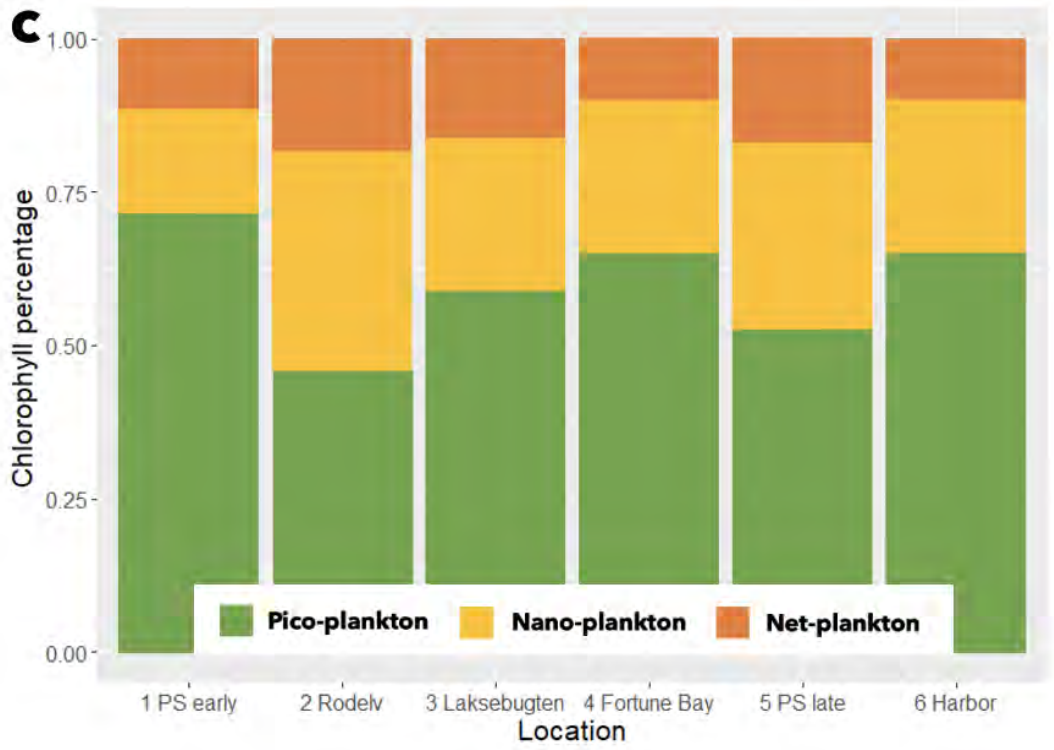

S2 - P values for Tukey HSD tests for individual stations and fractions, across depths

Values marked with gray did not meet the assumptions for conducting a one-way ANOVA test.

Station	Fraction	P-value 3 ~ 31	P-value 3 ~ 20	P-value 31 ~ 20
1	Net	0.0000229	0.0142521	0.0001834
1	Nano	0.0189266	0.0615005	0.6096096
1	Pico	0.0001981	0.0028591	0.0244271
Station	Fraction	P-value 3 ~ 19	P-value 3 ~ 31	P-value 31 ~ 19
2	Net	0.0000797	0.0019013	0.0069406
2	Nano	0.0016222	0.3128791	0.0069953
2	Pico	0.0033425	0.3047429	0.0173698
Station	Fraction	P-value 3 ~ 25	P-value 3 ~ 35	P-value 25 ~ 35
3	Net	0.1728675	0.9386559	0.2647471

3	Nano	0.0058769	0.0443186	0.2377437
3	Pico	0.0073968	0.9509036	0.0054746
Station	Fraction	P-value 3 ~ 30	P-value 3 ~ 40	P-value 30 ~ 40
4	Net	0.6468154	0.4490117	0.9284607
4	Nano	0.1300085	0.8097090	0.0585608
4	Pico	0.1758659	0.4473860	0.0347003
Station	Fraction	P-value 3 ~ 37,5	P-value 3 ~ 20	P-value 37,5 ~ 20
5	Net	0.0316429	0.9978382	0.0340943
5	Nano	0.0059400	0.8906451	0.0094916
5	Pico	0.0003805	0.9167659	0.0002935
Station	Fraction	P-value 3 ~ 30	P-value 3 ~ 20	P-value 30 ~ 20
6	Net	0.0000151	0.0122323	0.0001135
6	Nano	0.0006754	0.0049834	0.1159215
6	Pico	0.0006833	0.0001942	0.2142658

S3 - P values for Tukey HSD tests for individual stations and depths, across fractions

Values marked with gray did not meet the assumptions for conducting a one-way ANOVA test.

Station	Depth	P-value Net~Nano	P-value Nano~Pico	P-value Net~Pico
1	3	0.6407216	0.1610509	0.0494970
1	20	0.2630225	0.0001105	0.0000453
1	31	0.9420431	0.0000865	0.0001032
Station	Depth	P-value Net~Nano	P-value Nano~Pico	P-value Net~Pico
2	3	0.0177911	0.8331693	0.0350438
2	19	0.0702342	0.0178581	0.0012686
2	31	0.0007765	0.0808828	0.0001378
Station	Depth	P-value Net~Nano	P-value Nano~Pico	P-value Net~Pico

3	3	0.1980096	0.0016214	0.0003773
3	25	0.9950644	0.0138776	0.0153978
3	35	0.0223511	0.0262417	0.0007934
Station	Depth	P-value Net~Nano	P-value Nano~Pico	P-value Net~Pico
4	3	0.0032747	0.0000176	0.0000024
4	30	0.4213323	0.0090619	0.0025028
4	40	0.7728627	0.2878084	0.1194806
Station	Depth	P-value Net~Nano	P-value Nano~Pico	P-value Net~Pico
5	3	0.2227599	0.0001992	0.0000704
5	20	0.0010921	0.0000583	0.0000035
5	37.5	0.2250714	0.5957865	0.0622852
Station	Depth	P-value Net~Nano	P-value Nano~Pico	P-value Net~Pico
6	3	0.0003597	0.0000030	0.0000006
6	20	0.0.0221378	0.0001980	0.0000288
6	30	0.0049314	0.0001945	0.0000154

S4 - P values for Tukey HSD tests for total chlorophyll at surface level (3m) across stations

Only significant results shown.

Station	**P - Value**
Sewage discharge ~ Red River	0.0184104
Sewage discharge ~ Laksebugten	0.0265448

S5 - P values for Tukey HSD tests for total chlorophyll at maximum fluorescence (see Fig. 3&4) across stations

Only significant results are shown in this tabel.

Station	**P - Value**

Permanent Station Early ~ Red River	0.0002109
Permanent Station Early ~ Laksebugten	0.0001306
Permanent Station Early ~ Fortune Bay	0.0000020
Permanent Station Early ~ Sewage discharge	0.0000024
Permanent Station Early ~ Permanent Station Late	0.0001215
Fortune Bay ~ Red River	0.0201168
Sewage discharge ~ Red River	0.0275923
Fortune Bay ~ Laksebugten	0.0361649
Sewage discharge ~ Laksebugten	0.0495193
Permanent Station Late ~ Fortune Bay	0.0395704

References

Agawin, N. S., Duarte, C. M., and S. Agustí **(2000)**. Nutrient and Temperature Control of The Contribution of Picoplankton to Phytoplankton Biomass and Production. Limnology and Oceanography 45(3): 591-600.

Backhaus, L., Fassel, N. and Jensen, D. B. **(2014)**, Identity, abundance and biomass of diatoms in Disko Bay and fjords, Western Greenland. Arctic Biology Field Course July 2014. University of Copenhagen, Faculty of science, pp. 35-64.

Booth, Beatrice C., and Rita A. Horner **(1997)**: Microalgae on the Arctic Ocean Section, 1994: species abundance and biomass. 44.8 (1997):1607-1622.

Cupp, E. E. **(2004)**. Marine plankton diatoms of the west coast of North America. Berkeley, University of California Press.

Field, C. B., Behrenfeld, M. J., Randerson, J. T. and Falkowski, P. **(1998)**. Primary Production of The Biosphere: Integrating Terrestrial and Oceanic Components. Science, 281, 237-240.

Finkel, Z. V., Beardall, J., Flynn, K. J., Quigg, A., Rees, T. A. V., and J.A. Raven **(2009)**. Phytoplankton In A Changing World: Cell Size and Elemental Stoichiometry. Journal of Plankton Research 32(1): 119-137.

Hauptmann, Aviaja & Markussen, Thor & Stibal, Marek & Olsen, Nikoline & Elberling, Bo & Baelum, Jacob & Sicheritz-Pontén, Thomas & Jacobsen, Carsten Suhr. **(2016)**. Upstream Freshwater and Terrestrial Sources Are Differentially Reflected in the Bacterial Community Structure along a Small Arctic River and Its Estuary. Frontiers in Microbiology. 7. 1474. 10.3389/fmicb.2016.01474.

Helmark, S., Petersen, C. S. W., Christensen, M. S., Gough, I., **(2018)**, Size fraction determination and species assessment of phytoplankton in Disko Bay, Western Greenland. Arctic Biology Field Course July 2018. University of Copenhagen, Faculty of science.

Krawczyk, Diana & Andrzej, Witkowski & Juul-Pedersen, Thomas & Arendt, Kristine & Mortensen, John & Rysgaard, Søren. **(2015)**. Microplankton succession in a SW Greenland tidewater glacial fjord influenced by coastal inflows and run-off from the Greenland Ice Sheet. Polar Biology. 10.1007/s00300-015-1715-y.

Lett, S., Paulsen M. L., and S.S. Larsen **(2010)**. Marine Eukaryote picophytoplankton in the waters around Disko Island (West Greenland): a first attempt to evaluate their relative contribution to total biomass and productivity. University of Copenhagen, Faculty of science, pp. 52-85.

Li, W. K., McLaughlin, F. A., Lovejoy, C., and E.C. Carmack **(2009)**. Smallest algae thrive as the Arctic Ocean freshens. Science 326(5952): 539-539.

Li, Z., L. Li, K. Song, and N. Cassar **(2013)**, Estimation of phytoplankton size fractions based on spectral features of remote sensing ocean color data, J. Geophys. Res. Oceans, 118, 1445–1458,

Mascarenhas, Veloisa & Zielinski, Oliver. **(2019)**. Hydrography-Driven Optical Domains in the Vaigat-Disko Bay and Godthabsfjord: Effects of Glacial Meltwater Discharge. Frontiers in Marine Science. 6. 10.3389/fmars.2019.00335.

Metfies, K., von Appen, W.J., Kilias, E., Nicolaus, A. and E.M. Nöthig **(2016)**. Biogeography and Photosynthetic Biomass of Arctic Marine Pico-Eukaryotes during Summer of the Record Sea Ice Minimum 2012 . PLoS One 11(2): e0148512.

Raven, J. A. **(1998)**. The twelfth Tansley Lecture. Small is beautiful: the picophytoplankton. Functional ecology, 12(4), 503-513.

Rines, J.E.B and Hargraves, P. E. **(1988)**. The Chaetoceros Ehrenberg (Bacillariophyceae) Flora of Narragansett Bay, Rhode Island, USA. Bibliotheca Phycologica Band 79, J. Cramer, Berlin, 196 pp.

*RStudio Team **(2020)**. RStudio: Integrated Development for R. RStudio, PBC, Boston, MA URL http://www.rstudio.com/.*

Simo-Matchim, A. G., Gosselin, M., Blais, M., Gratton, Y. and J. É. Tremblay **(2016)**. Seasonal variations of phytoplankton dynamics in Nunatsiavut fjords (Labrador, Canada) and their relationships with environmental conditions. Journal of Marine Systems 156: 56-75.

Sørensen, N., Daugbjerg, N., & Gabrielsen, T.M. **(2011)**. Molecular diversity and temporal variation of picoeukaryotes in two Arctic fjords, Svalbard. Polar Biology. 35, 519- 533.

T.G. Nielsen **(2005)**: Struktur og funktion af fødenettet i havets frie vandmasser. Doktordisputats. Danmarks miljøundersøgelser. 71 s.

Throndsen, J, Hasle, G.R and Tangen K. **(2003)**. Norsk Kystplankton Flora. Oslo : Almater Forlag.

Tomas, C.R., **(1997)**: Identifying Marine Phytoplankton, Academic Press, Elsevier, 525 B Street, Suit 1900, San Diego, California 92101-4495, USA.

Tremblay, J. É., Anderson, L. G., Matrai, P., Coupel, P., Bélanger, S., Michel, C. and M. Reigstad (**2015)**. Global and regional drivers of nutrient supply, primary production and CO2 drawdown in the changing Arctic Ocean. Progress in Oceanography 139: 171-196.

Turner Designs **(2019)**. Trilogy laboratory fluorometer Product Datasheet Brochure. S-0068 Rev. AA. (http://docs.turnerdesigns.com/t2/doc/brochures /S-0068.pdf)

UNIVERSITY OF COPENHAGEN
FACULTY OF SCIENCE

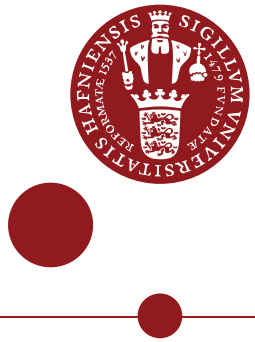

Influence of experimental iron and nutrient additions on chlorophyll *a* growth rate in sediment-rich waters in Disko Bay, Greenland

By Eve Isobel Galen, Anna Maria Klüssendorf, and Timothy Alexander Leslie Nicol

Arctic Biology Field Course 2022

Course code: NBIK18001U
Credit: 7.5 ECTS

Supervisors: Niels Daugbjerg and Per Juel Hansen

Submitted on: 14 August 2022

Abstract

Glacial meltwater and freshwater runoff supply the coastal waters of Disko Island with large volumes of sediment and bioessential iron. The particulate fraction of iron entering the near-shore ecosystem is high, however the lability of the iron for uptake by marine organisms is believed to be low. Few studies have investigated the effect of *in vitro* experimental iron additions on Greenlandic coastal water, and none on the southern coast of Disko Island. As a dominant characteristic of the region is the large annual influx of iron-rich meltwater from the nearby Red River, investigating the role of iron addition is critical for understanding how marine organisms may respond to changes in iron availability in the future. Specifically, this study seeks to understand the influence of experimental iron and iron & nutrient addition on chlorophyll *a* growth rate in late summer. The results of the study indicate that iron addition alone had no significant influence on organism growth rate, while iron & nutrient addition significantly impacted growth rate at two of the sampling sites. In addition, larger organisms (namely diatoms) had higher growth rates compared with smaller organisms, although the overall concentration of cells was lower in the larger size fractionation. Turbidity caused by river discharge, and its consequent influence on mixing in the water column and light availability, appeared to be the dominant limiting factor in our experiment, suggesting that further research into the role of light and macronutrient concentrations is necessary for understanding the influence of increasing freshwater runoff deposition on marine ecosystems under climate change conditions.

1. Introduction

The ocean absorbs roughly twenty-five percent of all anthropogenic carbon dioxide (CO_2) emissions (Watson et al., 2020). The temporal and spatial rate of absorption is governed by the relative partial pressure of CO_2 at the ocean-atmosphere interface, as well as the rate of photosynthesis and subsequent sequestration of carbon to the deep ocean (Galazzo-Boscolo et al., 2018). Downwelling of phytoplankton and the sedimentation of sequestered CO_2 from the biological carbon pump lowers the partial pressure of the ocean, resulting in an increased capacity for CO_2 absorption. This negative feedback has clear implications for atmospheric CO_2 concentrations, the greenhouse effect, and climate change (Doney et al., 2014).

Efficiency of the biological carbon pump is dependent on phytoplankton physiology and community composition (Basu & Mackey, 2018). In turn, phytoplankton net primary production is controlled by physical and chemical properties of the marine environment,

including nutrient availability and trace element concentrations (Basu & Mackey, 2018). Specifically, marine primary production is often controlled by region-specific nutrient and trace element limitation. Iron has been shown to be a key limiting element in marine systems, particularly in the Southern Ocean, and there the causal link between oceanic iron concentration and primary productivity is well understood (Armand et al., 2008). Further investigation into the role of iron in the global marine system, including in the paleorecord, has demonstrated the global importance of iron in marine biological systems, and a coupled relationship between iron and carbon (Williamson et al., 2012).

The paleorecord illustrates a correlation between atmospheric CO_2 concentrations and atmospheric iron flux (dust) over the last 160 thousand years (Fig. 1). Periods of relatively low CO_2 concentrations are synchronous with periods of high atmospheric dust, and vice versa (Street & Payton, 2005). This implies a relationship between a warming climate (high atmospheric CO_2 concentrations) and decreased iron flux into the ocean over the paleorecord. Contemporaneous increases in atmospheric CO_2 concentrations likely have an influence on natural iron fluxes into the global biological systems, including the marine environment.

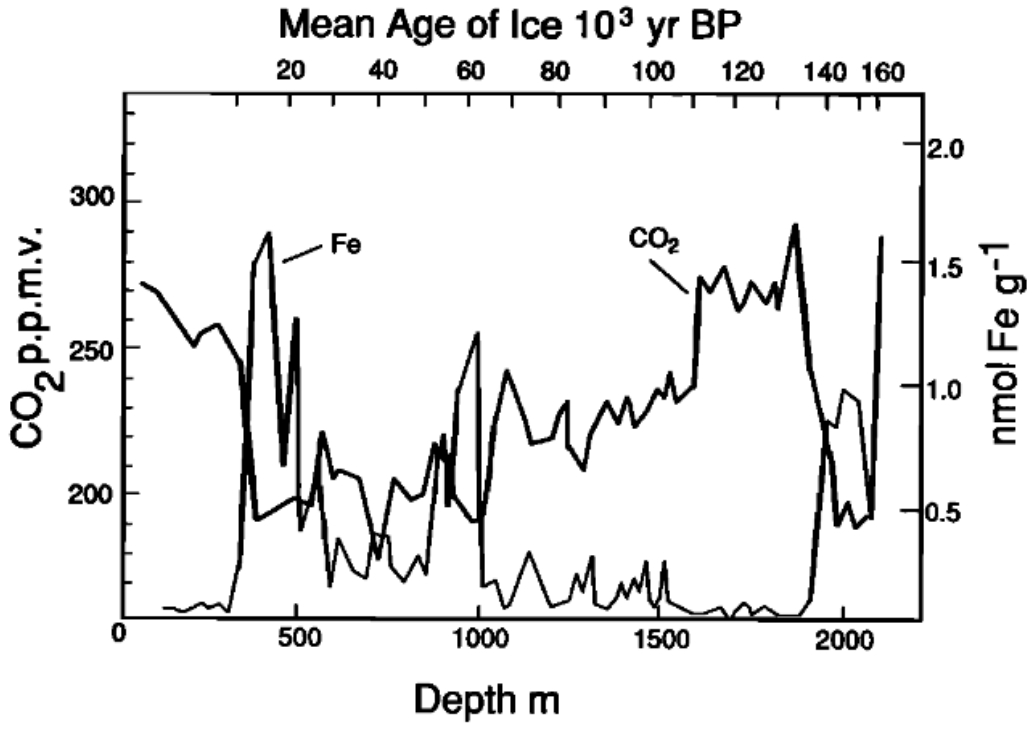

Figure 1. Atmospheric CO_2 measured from trapped air in Antarctic ice as a function of depth of the Vostok ice core, together with the synchronous mean iron flux in atmospheric dust for the past 160 thousand years. Figure taken from Martin (1990).

Present day, large regions of the global ocean have been shown to be experiencing a trace element limitation, including iron, despite high availability of essential nutrients such as nitrogen and phosphorus (Moore et al., 2013). In the Arctic, little research has been conducted beyond a simple understanding that iron is abundant (Wang et al., 2014). The lack of research in this field is surprising given the geology of Greenland's west coast is dominated by iron-rich plateau basalts. These rocks will be increasingly exposed to weathering as the tidewater glaciers retreat, potentially stimulating primary productivity in near-coast marine ecosystems if other nutrients are not limiting (Boyd et al., 2000). This has clear implications for climatic feedback loops and could be a contributing factor to the deceleration of global temperature increase (Wang et al., 2014).

1.1 Field Site

The volume of freshwater discharge from the Greenland Ice Sheet is increasing, with a doubling of mean annual mass loss between 2003-2010 (compared with 1983-2003) from the ice sheet (Kjeldsen et al., 2015). Glacial meltwater originating from the Greenland Ice Sheet and adjacent glaciers supplies the Greenlandic coast with large volumes of freshwater and sediments, including the transport of dissolved organic carbon (DOC), dissolved silicates, and iron and nitrogen to coastal marine ecosystems (Hawkings et al., 2014). However, the fertilization potential of glacial meltwater is still unclear. Recent studies have demonstrated a large supply of labile, and potentially bioavailable, forms of iron to the Arctic Ocean via glacial meltwater, however iron particle redistribution in the Arctic Ocean, and its effect on biological systems, is not well understood (Bhatia et al., 2013; Hawkings et al., 2014; Hopwood et al., 2018). It is relatively well understood that significant losses of glacially sourced dissolved Fe occur upon mixing with seawater due to flocculation, however less well understood are the physical processes linking freshwater input to near-shore ecosystems and mixing of ocean water to induce iron fluxes from upwelling (Hopewood et al., 2018).

Disko Island is situated in a lava basin that runs along the western coast of Greenland. The bedrock is primarily basalt, which serves as a large source of labile iron to the surrounding environment from weathering of the eroding basalt (Markussen et al., 2016). On the island, meltwater originates from the Sermerssuaq Ice Cap. With ice cap retreat, the island's proglacial zones are extending, and meltwater is increasing collecting sediments and material from topsoil and river-bank erosion in its runoff (Markussen et al., 2016). Specifically, meltwater supplies a large quantity of iron-rich sediments to the Davis Strait, and wider Disko Fjord via sub- and

supraglacial runoff and erosion of the Red River riverbank (Markussen et al., 2016). Due to the discharge of the Red River, the area around the south coast of Disko Island is not considered to be limited by iron.

2. Theoretical Background

Several biological, physical and chemical processes control primary productivity. Crucial for photosynthesis, abiotic factors such as light, temperature, and nutrient supply directly influence the rate of cellular growth.

2.1 Nutrition of Phytoplankton: Iron

Besides macronutrients, small quantities of certain trace metal micronutrients are required for phytoplankton growth and structure control. Despite its high crustal abundance, iron is the third most growth-limiting nutrient caused by its low bioavailability in aquatic environments (Rout and Sahoo, 2015). Iron is found in two oxidation states, Fe^{2+} and Fe^{3+}, where the latter is often bound in ferric oxyhydroxides and therefore less soluble in water. In the open ocean, iron is only rarely available to phytoplankton as it is predominantly present in its non-absorbable ferric form or almost completely bound by strong organic ligands (Rue and Bruland, 1995). Iron is, however, highly important for the photosynthetic activity, being involved in several processes in both photosystems. Photosystem I is the largest iron sink in phytoplankton as twelve atoms are related to it, while two to three iron atoms are directly involved in photosystem II (Glibert et al., 2016). Its flexible redox chemistry enables iron to serve as an iron carrier and catalysator in the photosynthetic transport chain. Further, it controls the biosynthesis of, among others, chlorophyll and cytochromes (Rout and Sahoo, 2015), as well as the maintenance of the function and structure of chloroplasts. Conclusively, the amount of chlorosis increases with increased iron uptake, as long as it is the limiting factor, and thereby promotes primary productivity (Smith et al., 2013).

Furthermore, iron limits nitrogen fixation, where the phytoplankton converts nitrogen into ammonia. Multiple studies have shown that the nitrate uptake by phytoplankton cells is less efficient under iron stress (Timmermanns et al., 1994; Milligan and Harrison, 2000; Schoffmann et al., 2015). Therefore, phytoplankton growing on nitrate and those relying on nitrogen fixation require higher cellular iron concentrations.

Besides constraining the overall biomass, low iron availability can influence the phytoplankton community composition since the iron requirements and storage capabilities differ between taxa and thereby impacts the ecological competition (Quigg et al., 2013, Marchetti et al., 2006). For instance, nanoflagellates and picophytoplankton are seen to replace larger plankton such as diatoms under decreasing iron concentrations, especially in combination with other nutrient limitations as the iron quotas are affected by nitrogen availability (Twining et al., 2020).

2.2 Nutrition of Phytoplankton: Nitrogen, Phosphorus and Silicate

Ensuring growth, reproduction, and endurance of algal cells, nitrogen and phosphorus are considerably the most important macronutrients. In marine environments, nitrogen is the primary growth-limiting nutrient mainly because of slow fixation of nitrogen in saltwater (Hecky and Kilham, 1988). Nitrogen both directly and indirectly contributes to photosynthetic processes. Indirectly, it increases the photosynthetic area by expediting the synthesis of essential proteins, which are involved in cell growth, cell division, and the synthesis of cell walls. As a direct component of the photosynthetic enzymes, nitrogen enhances the formation of chlorophyll and affects the amount and size of chloroplasts (Bassi, Menossi, and Mattiello, 2018).

Phosphorus is associated with different components of metabolism and energy transfer. Being closely related to carbon fixation during photosynthesis, it is an essential mineral nutrient for plant growth and development (Rychter and Rao, 2005). The growth rate of phytoplankton is further improved by silicate, which is a crucial part of the structure and remodeling of cell walls. During biosilicification, it forms covalent bonds with cell wall components and thereby ensures phytoplankton growth (Sheng and Chen, 2020). Marine diatoms, for example, are surrounded by a frustule, a silica cell wall, so require dissolved silicic acid in the surface waters to grow (Tréguer et al., 1995). Silicate further has been found to increase the resistance against biotic and abiotic stresses. This protective effect is, however, not yet fully understood (Curry and Perry, 2007).

How the availability of these previously mentioned elements constrains the photosynthesis and remineralization reactions, and consequently the amount of carbon (i.e. biomass of phytoplankton) is defined by the Redfield Ratio. The value of this ratio, relating the most essential elements, can slightly vary between regions and species. However, adding silicon and iron to the original ratio, the most commonly used ratio still is

106C:16N:16Si:1P:0.1-0.001Fe for balanced growth and is said to be nearly constant throughout the world's oceans (Sharp, 2001; Dooney, 2013; Broecker and Peng, 1982).

3. Research Aims

Due to the well-understood link between iron fertilization and increased photosynthesis of marine phytoplankton in nutrient rich ocean water, *in situ* and *in vitro* experimental iron additions is considered a popular method for attempting to increase marine net primary productivity, and consequently increase the ocean's availability to store CO_2, especially in high-nutrient low-chlorophyll regions.

This paper seeks to evaluate the influence of ferric iron on net biomass between two sampling sites in the region around the mouth of the Red River and the open ocean in the south-west of Disko Island both in the surface column and deeper waters. Specifically, the impact of iron addition on two size fractionations from waters considered to be iron-sufficient and waters with potential iron deficiencies. Based on simultaneous co-limitation of nutrients in natural waters, the effect of adding iron individually as well as in combination with other essential nutrients and trace elements is the aim of this study (Browning et al., 2017).

3.1 Hypotheses

1. Due to the impact of the iron-rich discharge of the Red River, we do not expect the biomass to be limited by iron proximate to the river mouth and therefore, iron addition will not change the biomass of the samples. However, enhanced nutrient availability in addition to a higher iron flux will hypothetically increase the chlorophyll *a* concentrations (which is a proxy for the biomass of phytoplankton). Since the growing season is already well advanced at the end of July, the water has been depleted in nutrients and new available nutrients might positively influence the growth rate.

2. At the site further away from the river mouth, we predict iron to be a growth-limiting nutrient and accordingly, iron additions will increase the chlorophyll *a* concentrations in those samples. As a consequence of reduced vertical mixing, we predict that iron is a limiting nutrient lower in the water column both proximate and distal to the river mouth, and iron additions will increase chlorophyll *a* concentrations.

3. The phytoplankton abundance and community composition will be different in iron-abundant waters compared to waters where iron is growth-limiting, as smaller phytoplankton

will be more abundant in waters with a lower iron concentration. More precisely, samples from the distal site as well as samples from the lower in the water column are expected to be dominated by nano- and picoplankton. With iron additions, we predict the relative abundance of the different phytoplankton groups to change. Specifically, microalgae, such as diatoms, are predicted to outcompete smaller taxa.

4. Methods

All fieldwork was undertaken in mid- to late-summer (week 29 and 30 of 2022). Sampling took place on 23rd July, and as such the water body had 24-hour access to sunlight. Disko Bay experienced abnormally late spring sea-ice extent, which fully melted around one month later than is usual.

4.1 Sampling

Two sampling sites are chosen, one nearshore site close to the river mouth and a distal site with lower impact of the iron-rich silt discharge from the Red River. Here, the proximate site is chosen in reasonable distance (3km) to the river mouth, to allow for mixing of the sediments with the sea water, and to avoid the primary productivity of phytoplankton to be suppressed by freshwater influences of low salinity, enhanced turbidity and decreased light penetration from suspended discharged particles (Zhou et al., 2008). Measurements of the salinity and turbidity can be seen in Figure A1.A and A1.D, and A1.C and A1.F for both sampling sites, respectively.

The distal site located 2.9km south of the proximate site is the permanent sampling station of the University of Copenhagen. Both sampling sites can be seen in Figure 2. Due to limited vertical mixing, the bay is highly stratified (Markussen et al., 2016). Iron tends to remain near the surface of the water, with concentrations declining drastically only 10 meters below the surface (Markussen et al., 2016). Therefore, water is sampled from the surface at 3m depth.

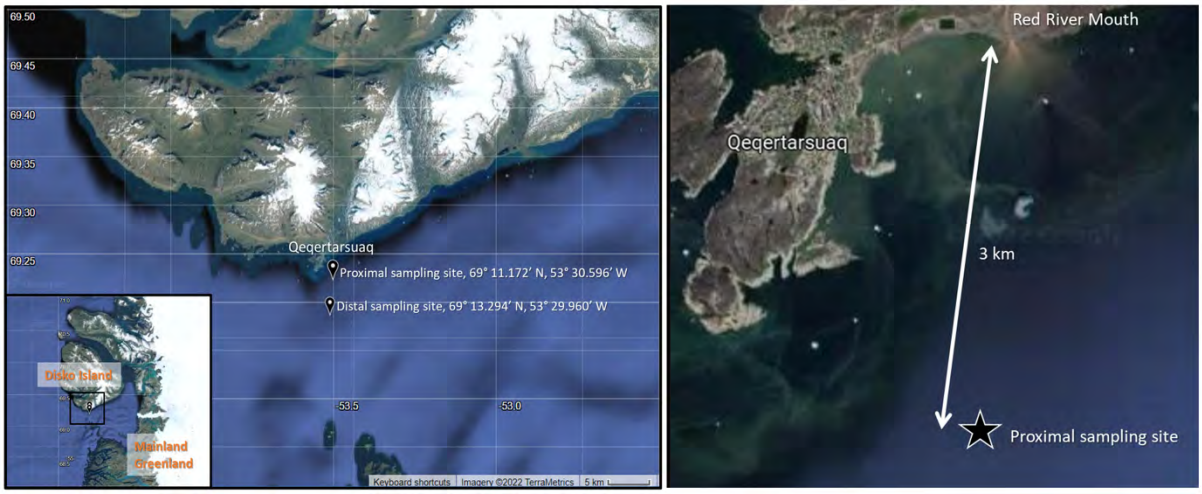

Figure 2: Maps indicating the locations of the two different sampling sites

Based on the fluorescence maximum, determined by the CTD (see Figure B1.B and B1.E), the other samples were taken from 19m and 31m for the proximate and distal site, respectively.

Each sample was collected by filling a 10l Niskin bottle twice from an average depth, namely centered from the middle of the bottle. The depth was previously determined by a mechanical hoist, calibrated to 0m when the Niskin bottle was halfway submerged.

4.2 Preparing the Samples

Filtering the water from all four sampling sites through a 200µm-filter, two controlled experiments were set up for each sample site. See Table 1 for an overview of the different experiments conducted. The water was filtered to remove any debris (such as sediment particles, larger organisms, feces etc.) which could impact the growth of phytoplankton in a closed environment. For the iron addition experiment, the iron concentration was increased by 0.3µmol adding 0.5ml iron (III) chloride hexahydrate ($FeCl_3 \cdot 6H_2O$) stock solution to each sample of 500ml volume. Having a molecular weight of 270.95g mol^{-1}, 0.00811g of $FeCl_3 \cdot 6H_2O$ were dissolved in 100ml of water to obtain this concentration. According to Markussen et al. (2016), this corresponds to doubling the concentration of iron. In order to make the iron bioavailable to phytoplankton, an EDTA buffer ($Na_2EDTA \cdot 2H_2O$) was added to the samples. A stock solution was prepared by adding 0.4352g of $Na_2EDTA \cdot 2H_2O$ (having a molecular weight of 372.24g mol^{-1}) to 100ml of water. Attempting a final concentration of 11.7µmol, finally 0.1ml of the stock solution was added to each sample.

The same procedure was performed for the second experiment. Here, additionally nutrients, vitamins, and trace elements were dissolved in the samples to further enhance primary productivity. The nutrient stock contained 220.5µM of $NaNO_3$, 18.1µM of NaH_2PO_4, and 53.0µM of $NaSiO_3$ in a total volume of 100ml. The vitamin stock solution comprised cyanocobalamin (vitamin B1) and thiamine (vitamin B12) and biotin (vitamin H). In the trace element stock solution, 90.9µM $MnCl_2 \cdot H_2O$, $80.0 \cdot 10^{-1}$µM $ZnSO_4 \cdot 7H_2O$, $50.0 \cdot 10^{-1}$µM $CoCl_2 \cdot 6H_2O$, $10.0 \cdot 10^{-1}$µM $CuSO_4 \cdot 5H_2O$, $82.2 \cdot 10^{-1}$µM $Na_2MoO_4 \cdot 2H_2O$, respectively $10.0 \cdot 10^{-1}$µM of H_2SeO_3, $NiSO_4 \cdot 6H_2O$, Na_3VO_4, and K_2CrO_4 were dissolved in 100ml of water. To each sample of 500ml, 0.5ml nutrient as well as trace element and vitamin stock solution was added. Preparing the stock solutions containing iron, nutrients, and trace elements, it was autoclaved for 20 minutes at 121°C, whereas the vitamin stock was kept at 4°C and filtered through a 0.22µm-filter before being added to the samples.

The samples of the control experiment were kept unchanged throughout the whole experiment. All individual experiments were run in triplicate, resulting in a total of 36 samples of 500ml each. The flasks were arranged in a cold environment of an average temperature of 5°C underneath a LED strip structure with an average photosynthetically active radiation (PAR) of 82.5 $Em^{-2}s^{-1}$, turned on 24 hours a day to mimic the arctic summertime. Due to a discrepancy of light intensity between the flasks, the samples were randomly redistributed twice a day to ensure they received a light amount as equal as possible. To prohibit the heavier organisms from sinking to the bottom of the flasks, they were carefully mixed twice a day.

Table 1. Overview of the different experiments carried out for samples from four sampling sites. Key: Fe = Iron stock solution, EDTA = Collator buffer, N = Nutrient stock solution, V = Vitamins stock solution, TMs = Trace Metals stock solution.

	Proximate, 3m depth P3	Proximate, 19m depth P19	Distal, 3m depth D3	Distal, 31m depth D31
	Addition (0.5ml)			
Control (C1)	No addition (C1P3)	No addition	No addition	No addition
Control (C2)	No addition	No addition (C2P19)	No addition	No addition
Control (C3)	No addition	No addition	No addition (C3D3)	No addition
Iron Addition (I1)	Fe, EDTA	Fe, EDTA	Fe, EDTA	Fe, EDTA (I1D31)
Iron Addition (I2)	Fe, EDTA	Fe, EDTA	Fe, EDTA	Fe, EDTA
Iron Addition (I3)	Fe, EDTA	Fe, EDTA	Fe, EDTA	Fe, EDTA
Iron & Nutrient Addition (N1)	Fe, EDTA, N, V, TMs	Fe, EDTA, N, V, TMs	Fe, EDTA, N, V, TMs	Fe, EDTA, N, V, TMs
Iron & Nutrient Addition (N2)	Fe, EDTA, N, V, TMs	Fe, EDTA, N, V, TMs	Fe, EDTA, N, V, TMs	Fe, EDTA, N, V, TMs
Iron & Nutrient Addition (N3)	Fe, EDTA, N, V, TMs	Fe, EDTA, N, V, TMs	Fe, EDTA, N, V, TMs	Fe, EDTA, N, V, TMs

4.3 Filtration and Chlorophyll a Measurements

From each sample, 100ml was extracted of which 50ml was filtered through a 20µm-filter and 50mL through a 0.7µm-filter using a suction pump. This way, two size fractionations could be monitored for the different treatments and the different sample sites. The filters were added to 5ml ethanol in falcon tubes and stored in a fridge at 4°C for approximately 24 hours before being measured. If left between 15 and 20 hours, the ethanol extracts around 90% of the biomass from the filters, while around 99% of the biomass is extracted after 24 hours.

The chlorophyll *measurements* were carried out by the Trilogy® Fluorometer, irradiating approximate 1.5ml of the ethanol extraction in a glass vial with light at wavelength of 660nm and subsequently quantifying the light which is emitted at longer wavelength than

what is absorbed by the chlorophyll *a* in the sample (Trilogy, 2008). To avoid cross-contamination between samples, new pipettes and new well-sanitized vials were used for each sampling site and each treatment sample, respectively.

4.4 pH Measurements and Dilution

With the nutrient additions and increasing primary productivity, the pH is expected to rise. To maintain a good environment for the phytoplankton to grow, the pH in the samples were controlled every other day (Day 0, 2, 4, and 6). Assuming the triplicates to react equally to the applied changes, the pH was presumed to vary minimally between triplicates, and thus, only one of each of the 12 triplicates was measured. However, if the standard error of the triplicated chlorophyll *a* measurement was >0.03, the pH was measured in all three samples. The pH-measurements were carried out using a calibrated portable WTW pH 3210 ProfiLine Handheld Mater with a pH resolution of 0.001 ± 0.005.

In order to prevent the water alkalinity increasing too much, the samples were diluted when the pH was approaching 8.5 after the second measurement (>40 hours into the experiment). For that, the water sampled at the four different sites was filtered through a 0.7µm-filter to remove the phytoplankton of both size fractionations (i.e., to clear the water from all particles which later were investigated). The filtered water was stored together with the samples at approximately 4.5-5.0°C but with less light impact. Since 100ml were removed for analysis, the same amount was added to sample as well as 0.1ml of the respective stock solution to maintain the same concentration in each sample. To account for the dilution, the measured chlorophyll *a* was multiplied by a factor of 1.25 after Day 2 (i.e., from the third measurement after 92 hours).

Previously, the pH of the sampled water from all four sites without any treatment has been measured applying the same device as described above. The measurement was carried out on Day 1 (0 hours), but is assumed applicable as a baseline value, since approximately all phytoplankton has been removed in filtration and therefore, the pH is thought to be unchanged.

4.5 Data Analysis

Statistical tests were performed using GraphPad Prism (version 9.4.1). P values <0.001 were reported as significant with *** and termed 0.1% significant, p values <0.01 were reported as significant with ** and termed 1% significant, and 0.01 < p values <0.05 were

reported as significant with * and termed 5% significant. The significance level of 5% was used for determining the efficacy of our hypotheses. The effect of site on chlorophyll *a* growth rate was analyzed independently for each treatment at the two size fractionations using a one-way analysis of variance (ANOVA). The effect of treatment on chlorophyll *a* doubling was analyzed independently for each site and size fractionation using a one-way ANOVA. Finally, the effect of size fractionation on chlorophyll *a* growth rate analyzed independently for each treatment and site using a one-way ANOVA. Statistically significant results are reported in graphs in Results.

5. Results

The chlorophyll *a* concentration for two size fractions were measured in triplicate samples for each treatment (control, iron addition, iron & nutrient addition) to follow the growth development over time. The average concentration of the triplicates for the baseline measurement and the four subsequent measurements (taken 40, 92, 140, and 188 hours after the beginning of the experiment) are presented in Figure 3. An averaged concentration has been used since the discrepancy between the replicates was considerably low, as implied by the standard errors marked as error bars in Figure 3 and Figure 4 for the small size fraction (0.7-20µm) and the large size fraction (20-200µm), respectively.

The start concentration was generally low in all the samples from the different sites. With a concentration ranging from 0.03µgl-1 at the proximate site to 0.29µgl-1 at the distal site, the quantity of larger organisms (20-200µm) was substantially lower than the amount of the smaller organisms (0.7-20µm), showing a baseline concentration between 0.70µgl-1 and 2.14µgl-1. Here, the concentrations were higher at the distal site than at the proximate site, valid only for the samples taken from deeper in the water column (at 19m and 31m, respectively), as indicated by the fluorescence measurements of the CTD (Figure B1.B and B1.E). While the concentration of larger size fractionation was equal both at the proximate and the distal site in the surface column, the smaller fraction was lowest concentrated close to the mouth of the Red River in 3m-depth.

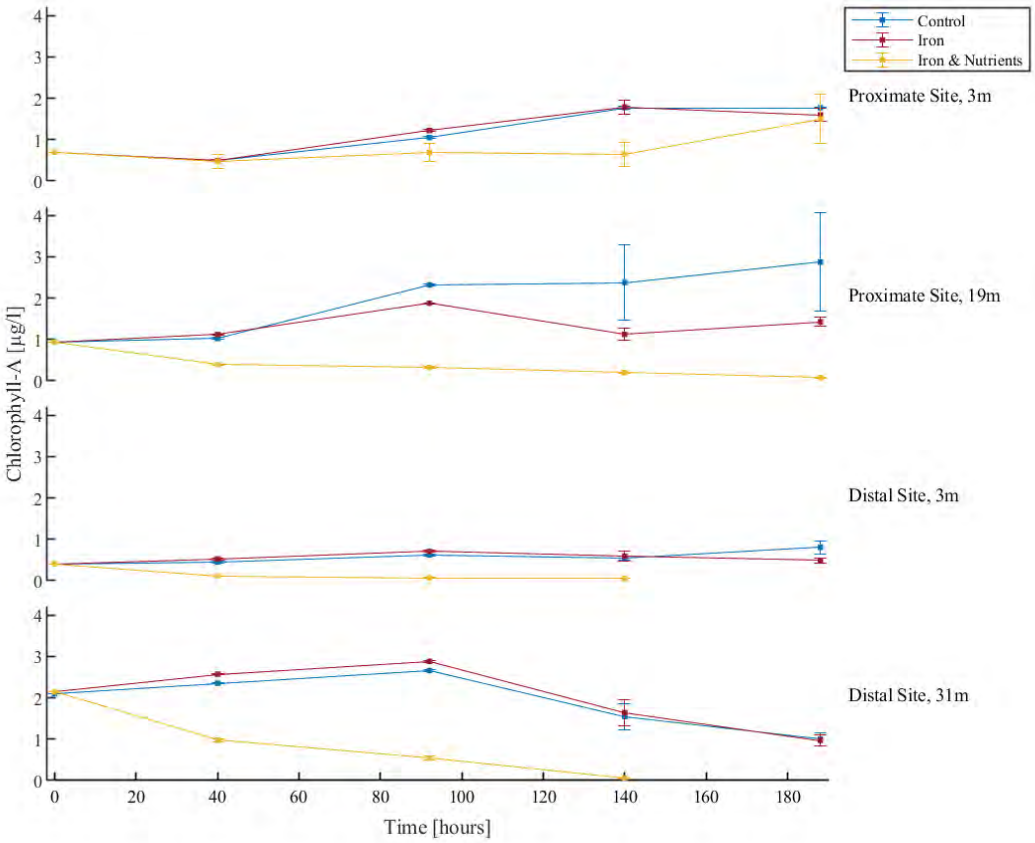

Figure 3. Average chlorophyll *a* concentration in the samples from the four different sampling sites over time for the small size fraction (0.7-20µm) for the control experiment as well as the two treatment experiments (iron addition only and combined iron and nutrient addition). The deviation between the triplicates is determined by the standard error and indicated by the error bars. The values of the standard errors can be found in Table B 1.

During the experiment (188 hours in total), the phytoplankton in the control samples of both size fractions continuously grew, except for the sample taken at 31m depth at the distal site. Here, the chlorophyll *a* concentration of the smaller cells sharply declined after reaching a maximum at 92 hours. Generally, the growth curve in the iron addition experiment is closely following the control samples at all sites and for both size fractions.

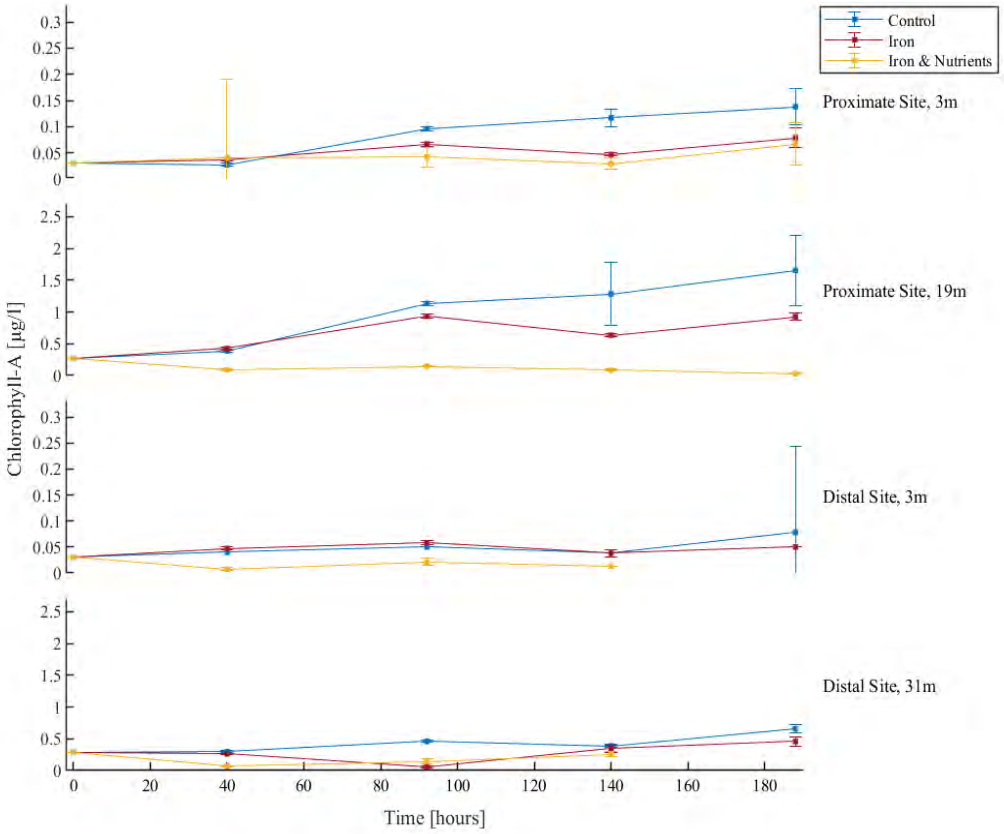

Figure 4. Average chlorophyll *a* concentration in the samples from the four different sampling sites over time for the big size fraction (20-200µm) for the control experiment as well as the two treatment experiments (iron addition only and combined iron and nutrient addition). The deviation between the triplicates is determined by the standard error and indicated by the error bars. Note that the y-axes have different magnitudes for Proximate, 3m and Distal, 3m and also vary from the small size fraction in Figure 3.

The combined iron and nutrient treatment resulted in a steady decline of the chlorophyll *a* concentration in all samples except for the small size fraction sampled from the surface waters near the river mouth and the large size fraction in the deep waters at the distal site. Here, the phytoplankton started distinctly growing after the third measurement 140 hours and 40 hours into the experiment, respectively. Since the concentration had approximately reached 0µg l-1 for both sizes in the samples from the distal site, the experiment was aborted after the third measurement (>140 hours) as no further recovery was expected.

Under the assumption of an exponential growth, the diurnal growth rates for the different experiments and size fractions were determined. For each sample, the chlorophyll *a* concentration has been plotted against time, and an exponential function was fit to the data. Some data points were disregarded, as a lag phase in the early state as well as a stationary phase later in the experiment can disrupt the exponential growing pattern. Therefore, the daily

doubling of the chlorophyll a concentration is only based on the exponential part of the growing curve (see Figure C1 in Appendix C). An averaged growth rate of the sample replicates for both size fractions and all four sampling sites can be seen in Figure 5-7. A negative growth rate (i.e., decline in chlorophyll a concentration) was not quantified.

In Figure 5, the samples are grouped by treatment in order to analyze the two different size fractions with the different sampling sites. For all the treatments, the most distinct differences in the growth rates can be seen between sampling sites. Specifically, there was a significantly higher chlorophyll *a* growth rate (1% significance) in the control experiment for the small size fractionation at the proximate site at 3m depth compared to the distal at 3m and 31m depths. The proximate site at 19m depth had a significantly higher (5% significance) compared with both the distal depths. For the large size fraction, there was a significantly higher chlorophyll *a* growth rate (5% significance) at the proximal 19m site compared with the distal 3m site. In the iron treatment experiment for the small fraction sizes, there was a significantly higher (1%) chlorophyll *a* growth rate at the proximal 3m site compared with 19m depth and significantly higher (0.1%) chlorophyll a growth rate at the proximal 3m site compared with the distal 3m site. The large size fractions show no significant difference between the stations in the iron treatment experiment.

For the iron & nutrient treatment experiment, there was a significantly lower (5% significance) chlorophyll *a* growth rate at the proximal 3m site compared with the distal 31m site for the large size fractionation. Here again, it is noticeable that the combined iron & nutrient treatment resulted in a decline in chlorophyll *a* in five out of eight experiments, as only three out of eight samples showed a positive growth rate.

In conclusion, while the distance to the coast, and thereby distance to the mouth of the Red River, is affecting the growth rates of both size fractions, the depth from where the sample was taken had no significant influence on growth rate for control and nutrient treatments. The iron treatment did, however, show some significant difference between depths.

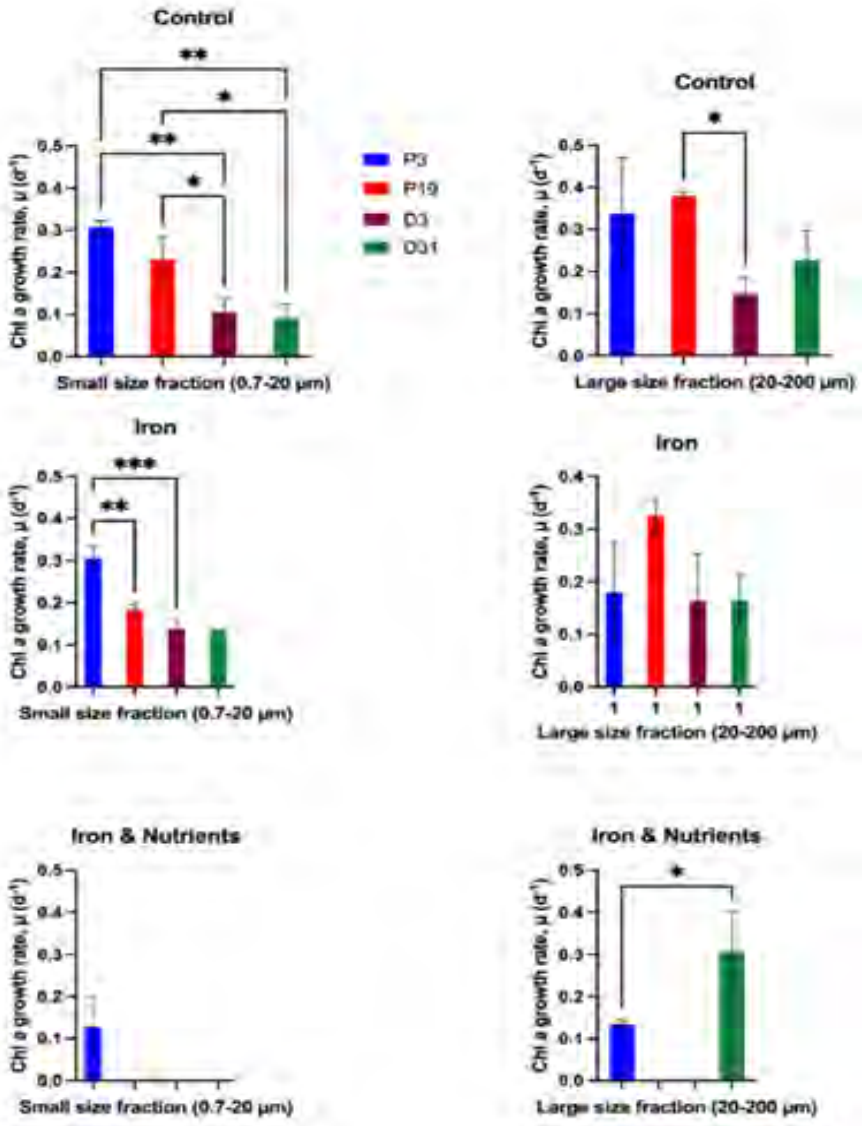

Figure 5. Average daily growth rate of chlorophyll *a* concentration for the small cells (0.7-20µm) and the large cells (20-200µm) in the different treatment experiments (control in upper panel, iron addition only in central penal, and iron and nutrient addition in lower panel) for the proximate site at 3m depth (P3, blue) and 19m depth (P19, red), and at the distal site at 3m depth (D3, purple) and 31m depth (D31, green). No data indicate a negative growth rate. Error bars mark the standard deviation between the triplicated samples and the asterisks denote a significance level of 5% (*) and 1% (**) between the indicated growth rates, respectively. Note the different scales on the y-axes.

In order to analyze how the cells of different size fractions reacted to the different treatments, the small and the large size fractionations from each sampling site were grouped for the different experiments separately. The diurnal growth rates of chlorophyll *concentrations* are presented in Figure 6.

Figure 6 clearly shows that there is no significant difference in the growth rates of both size fraction between the control and the iron treatment. That applies to the two sampling stations as well as the two sampling depths.

The three replicates in which the iron & nutrient treatment resulted in a chlorophyll *a* increase showed a significant decrease (5%) in chlorophyll *a* doubling at the proximate 3m site for the small size fractionation when compared with control and iron, and for the large size fractionation compared with the control. The large size fractionation at the distal 31m site showed a significant increase (5%) in chlorophyll *a* doubling under the iron & nutrient treatment compared with the iron treatment. Here it is noteworthy that the growth rate after the nutrient treatment is highest in the deep-water sample from the distal station.

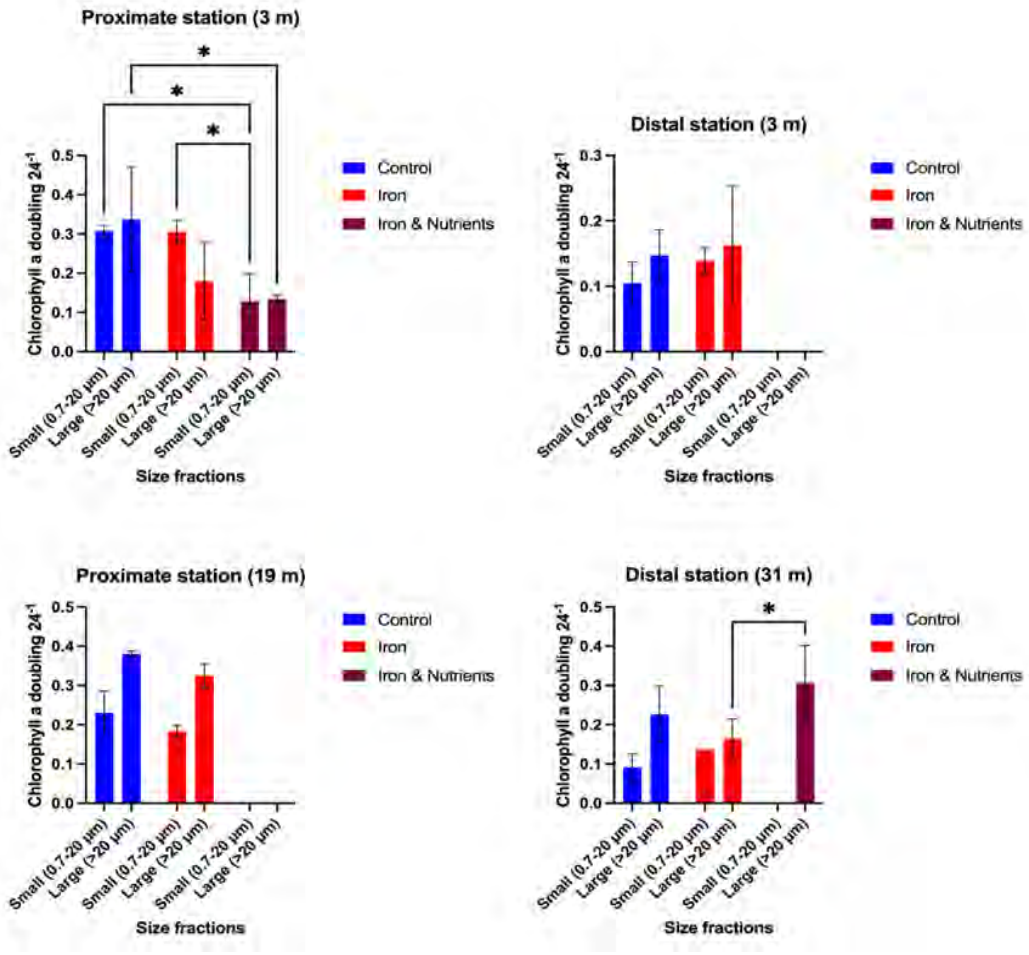

Figure 6. Average diurnal exponential growth rates of the small cells (0.7-20µm) and the large cells (20-200 µm) based on the chlorophyll *a* concentration for three different treatments (control in blue, iron addition in red, and combined iron and nutrient treatment in purple) and two different sampling sites and the corresponding depths. Error bars represent the standard deviation between the triplicates. No data indicate a negative growth rate. Asterisks denote a 5% level of significance of the difference between the two indicated growth rates.

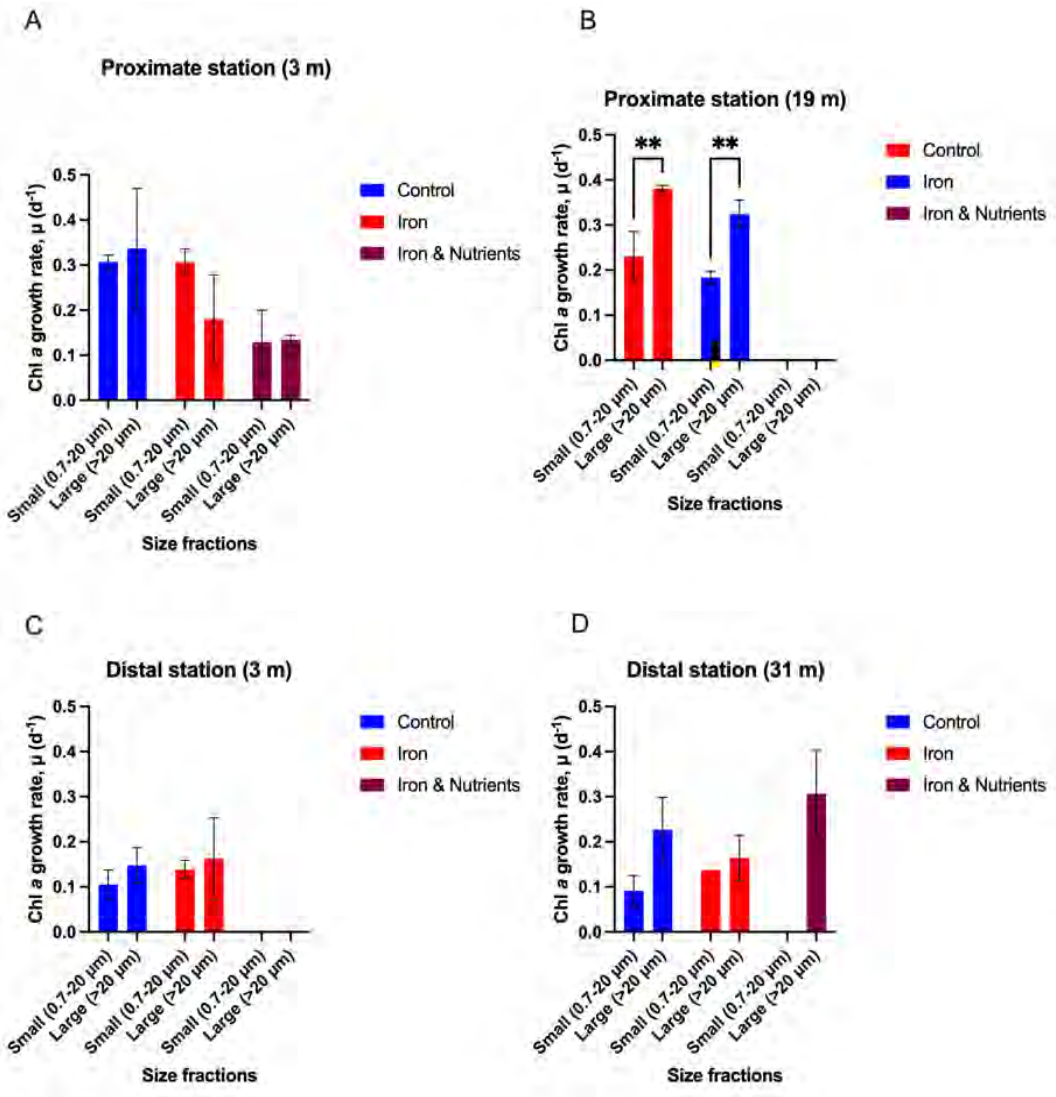

Figure 7. Average diurnal exponential growth rates of the small cells (0.7-20μm) and the large cells (20-200 μm) based on the chlorophyll *a* concentration for three different treatments (control in blue, iron addition in red, and combined iron and nutrient treatment in purple) and two different sampling sites and the corresponding depths. Error bars represent the standard deviation between the triplicates. No data indicate a negative growth rate. Error bars mark the standard deviation between the triplicated samples and the asterisks denote a significance level of 5% (*) and 1% (**) between the indicated growth rates, respectively.

The effect of the different treatments on the two size fractions has been statistically analyzed. For direct comparison, the two size fractions have been grouped by sampling station in Figure 7. Generally, the cells of the larger size fraction show a higher growth rate than smaller cells for all of the experiments in the samples from all the different sampling sites. The only exception is the sample taken from the surface column at the proximate station. Here, the larger size fraction had a smaller diurnal growth rate than the smaller ones. It has to be noted

that the standard deviation between the triplicates was large, indicating a similar growth rate in at least one of the triplicates. However, only in the sample taken from 19m at the proximate station was the growth rate of the larger cells was significantly higher than the growth rate of the small cells, indicated by a 1% significance level. At the distal site at both depths, the differences in growth rates between the size fraction was less pronounced and not statistically significant.

Comparing sampling stations, the discrepancy between growth rates of the two size fractions is higher in the shallow water samples than in the deep samples. This has, however, not been tested statistically.

6. Discussion

6.1 Iron Treatment

Contrary to expectations, the measurements from the iron addition experiments were similar to those in the control experiment for all four sampling sites. The chlorophyll *a* concentration of both size fractions in the iron experiments showed similar growth rates and rates of decline, often at similar times throughout the experiment, to the phytoplankton in the control samples of all sizes. As anticipated, an iron surplus is inferred proximate to the river mouth (in our proximal sites), where the water is enriched with washed-out iron-rich sediments from Disko Island basal rock dominated by Fe-rich igneous basalts. These findings are supported by the statistical analysis in Figure 6. Here, each treatment was compared against each other by size (large against large, small against small), within the same site. No significance was found in each of the four sites between iron treatments and control experiments, however significance was found between iron & nutrient and control as well as iron & nutrient and iron experiments. As such, the null hypothesis—that there was no effect on growth rates due to treatment type—could not be rejected for the iron treatment and control relationship. Hence, there is statistical confidence that the similar observations from the iron and control experiments was due to the iron treatment having no effect on growth rates.

The primary productivity at around 6km distance to the shore (distal sites) does not appear to be growth-limited by iron, however, the total iron concentration has not been measured at any of the sites. Therefore, no clear assertions about a possible iron surplus in the waters around Disko Island can be made. Iron concentration measurements for use in marine microbiology experiments are complicated by undissolved iron particles as well as by the important distinction between dissolved iron and bioavailable iron. It can, however, be assumed

that the concentration is high enough for the phytoplankton to survive even at this late point of time in the growing season. Even at the distal site, the phytoplankton are not iron-limited, as the control experiments at D3 and D31 did show lower growth rates than the iron experiments. It is also unclear if the iron discharged from the red river (largely in the form of a stable iron mineral, Hematite) is bioavailable, particularly when compared with studies of iron inputs such as dust-borne iron in the Southern Ocean (Raiswell et al., 2008). Despite this, our results show that the phytoplankton communities (small and large) in each of the water bodies studied are not iron-limited, otherwise a clearer growth signal would have been observed in the iron experiments where bioavailable iron was added.

Another explanation for the same growth and decline patterns in the two experiments could be a different limiting factor which has not been directly analyzed in the experiments. The supply of photosynthetically active radiation (via grow lights) was higher throughout the day than the amount that phytoplankton receives in nature. The ocean water at the proximate site was turbid due to increased washout of sediments as result of higher precipitation in the preceding days. At the distal site, the turbidity at 31m depth was higher than in the surface column. As a consequence of turbidity, larger suspended particles are unable to settle to the seafloor, and less light can penetrate the water column. At the fluorescence maximum, the PAR had a value of approximately 10 Em-2s-1 at the distal site, and a value of >5 Em-2s-1 at the proximate site caused by increased river discharge.

The photosynthetically available radiation in our experiment (82.555 Em-2s-1) was thereby up to 16 times higher than observed during late morning (a relative daily radiation peak) in nature. Even though it is a distinct measurement, and the value can fluctuate in nature, it can be concluded that the primary productivity might have been limited by light rather than iron or other nutrients. This is particularly important for the diatom community. Microscopy analysis of diatoms in the N2P19 sample, as well as from other groups researching the same water body at the Arctic Station, demonstrated that they were in different physiological state compared with other plankton communities. Rather than tending towards dormancy, they were in a more active state - this means that favorable light conditions could lead to faster rates of growth than for other communities. Although Diatoms only typically comprise around 30% of the biomass for this area and season (Lett et al., 2011), this could explain the relatively slow growth rates across the experiments. Ultimately, the chlorophyll *a* concentrations were perhaps only reflecting growth of just one taxon. It should be noted that our samples were collected on a particularly overcast day where the fluorescence maximum was higher in the water column

than on subsequent days in the field. This means that the light available to the phytoplankton was lower than usual for the time of day and season.

6.2 Iron & Nutrient Treatment

During this late state in the growing season, the waters are depleted in nutrients. Therefore, the nutrient treatment was expected to result in an increase in biomass indicated by a higher chlorophyll *a* concentration. Comparing the growth rates of the larger cells in the samples from the deep distal site to the one from the shallow proximate site, a significant influence (5% level of significance) of the nutrient treatment can be seen. This indicates a higher demand in nutrients distal to the coast of Disko Island. This is potentially due to a higher supply in nutrients from terrestrial sediments and nutrient-sufficient discharge of the Red River fertilizing phytoplankton at the proximate site. At further distance from the river mouth, the available nutrient concentrations could be lower, explaining the higher growth rates in the samples from the deep site at the distal sampling station.

This is further evidenced by statistical analysis in Figure 6, where each treatment was compared against each other by size (large against large, small against small), within the same site. The analysis shows 5% significance increase in chlorophyll *a* doubling in the large size fraction for the iron & nutrient experiment when comparing with the iron experiment in the deep, distal sample (D31). This means that, based on these samples, the null hypothesis—that the treatment type had no effect on growth rates—could be rejected and the alternative hypothesis accepted. As such, the growth rates were affected by the treatment.

The same can be seen when comparing the small size fraction in the shallow proximate sample. Here again, a 5% significance between the iron and the nutrient experiments indicates an influence of the treatments. However, contrary to expectations, the growth rates in the nutrient experiment were smaller than the growth rates in the iron experiments. This might, again, be explained by a higher nutrient concentration in coastal waters. Heavy rainfall previous sampling could have increased the nutrient supply, making additional nutrients less important to the phytoplankton. Furthermore, the uptake and processing of nutrients can be less efficient when low iron concentrations are present (Timmermanns et al., 1994; Milligan and Harrison, 2000; Schoffmann et al., 2015). Iron stress has tried to be prevented by adding both iron and nutrients to the samples. Nevertheless, it cannot completely be ruled out that the iron concentrations needed to be higher in the nutrient experiment in order to favor the nutrient uptake. Since the chlorophyll *a* concentrations declined in most of the samples after the nutrient

treatment, only tentative conclusions about a possible nutrient limitation can be made. If the biomass was generally limited by nutrients, a distinct positive growth rate would be expected in all the samples.

6.3 Community Composition and Size Fractions

Despite the generally lower concentration, the larger cells show a higher growth rate than the smaller cells in all the experiments from all the different sampling sites except for at the proximate 3m site. Generally, this would satisfy the expectation of larger cells outcompeting smaller cells under nutrient-sufficient conditions. Due to their larger surface area, their ability to take up nutrients is higher, and increased nutrient levels, thus, favor larger cells (Quigg et al., 2013; Marchetti et al., 2006). The lower growth rate of the larger cells compared to the smaller ones in the shallow, proximate water sample contradicts this statement. This effect could be explained by the predicted larger iron concentration in the surface water column compared to deeper waters. Based on this hypothesis, the growth rates of the larger cells were expected to be significantly higher in the samples taken from the deep, distal site. However, this could not be statistically proven.

From visual inspection, the discrepancy of growth rates between the two different size fractions has been said to be higher in the deep samples than in the samples taken from the surface column. Here, the iron addition is thought to have the largest influence as the start concentration in the deep below the thermocline are supposedly lower than in the mixing layer. This, further, supports the thesis of larger cells reacting faster and better to increased nutrient levels than smaller phytoplankton. It has, however, been noted that the growth rates in the control and the iron experiments were closely following each other. This, again, indicates the small influence of the iron addition compared to untreated water.

Due to the high number of samples, the influence of the different sampling sites and depth has not been tested statistically, and would be highly suggested for a potential repetition of this experiment.

6.4 Nutrient treatment error analysis and experiment optimization

The chlorophyll *a* concentration distinctly declined in five out of eight samples after the combined iron & nutrient treatment. This was contrary to the expectation that additional nutrients will stimulate primary productivity. As indicated by the small standard deviation (see

standard error in Figure 2 and 3), the triplicates show a measurement consistency and handling issues can be excluded. Regular mixing of the flasks ensured even nutrient distribution—preventing sinking of larger non-motile phytoplankton within the water of each experiment—maintaining the availability of the nutrients to all plankton in the flasks. This was especially important, as the net plankton fraction was dominated by chain-forming diatoms. Regular random re-arrangement of the flasks' spatial configuration ensured an even light distribution, ensuring the central experiments did not receive more light over the experiment's duration. Four chlorophyll *a* measurements showed larger standard errors, indicating a higher deviation between the triplicates. This was the case for both the small and the large cells in P19 towards the end of the control experiment (140 and 188 hours) and for the large cells in P3 and D3 in the beginning (42 hours) and the end (188 hours) of the nutrient and control experiment, respectively. Due to the non-uniformity both in treatment, concentration, and time of these deviations, no clear error source can be concluded. The random re-arrangement can, however, not exclude any uneven handling of the different samples throughout the experiment.

The air temperature was almost constant between 4.5°C and 5.0°C and therefore, the water temperature of the samples can be said to be comparable to the water temperature at the sampling sites (see Figure B1.A and B1.E). Furthermore, the pH was regularly controlled, and acidification prevented. One could argue the enhanced iron concentration may be inhibiting nutrient uptake by phytoplankton. However, the cells continued to grow after the iron treatment where no nutrients were added, therefore this explanation can likely be ruled out. The possibility of a handling or calculation error leading to toxic concentrations in our nutrient addition media can be ruled out, due to the growth seen in some nutrient experiments, particularly for large fraction organisms in the D31 site. Given all experiments received the same quantity of media, any toxic effects would have caused decline of phytoplankton in every experiment—an effect we did not observe.

Due to the advanced time in the growing season, some phytoplankton species can be hypothesized to be dormant and thus, not able to be stimulated by additional nutrients. In fact, some chain-forming diatoms like *Chaetoceros spp* and *Thalassiossira* showed a large amount of internal lipid droplets, indicating a productive growing season under the microscope. Many of the *Chaetoceros* species were observed to have formed resting spores, which is evidence for them entering a physiologically non-active period where they leave the surface column and sink towards deeper waters. Other diatoms like *Rhizosolenia hebetata f. hebetata* and *Leptocylindrus dancicus*, on the other hand, still seemed to be active during the sampling period. Nevertheless, the same water was used in all the different experiments and the cells

were therefore expected to show the same behavior regardless of the treatment. If the cells were dormant, no chlorophyll *a* increase would be visible in either of the samples, or at least the same growth rate were to expect, if the cells still were sensitive to light despite their dormancy period.

It has to be noted, however, that the chlorophyll *a* concentration of the larger cells has only been between 0.03µgl-1 and 0.29 µgl-1 in the sampled water. These considerably low start concentrations might hamper the experiment as any effect is less visible with fewer initial cells present in a sample. Additionally, a possible need for recovery during the experiment would be complicated when the cell concentration is low. The dilution at an early state in the experiment (after approximately 40 hours) further decreased the concentration. This can be supported by the sample taken from the distal site at 3m depth. Here, the start concentration of the smaller cells was the lowest of the four sampling sites, and likewise is the growth rate in all three experiments. Higher growth rates might be achieved by increasing the initial phytoplankton concentration in the samples, and is therefore a suggested procedure when reproducing this experiment.

Furthermore, a higher availability of nutrients might have favored larger grazing organisms feeding upon the phytoplankton. This effect has the potential to distinctly reduce the measured chlorophyll *a* concentrations in the samples with the combined nutrient and iron treatment. To rule out this possibility, one 20-micron filter was analyzed under the microscope for plankton composition. The sample N2P19 showed a distinctly low chlorophyll *a* concentration, with a large quantity of marine snow (characteristic of dead phytoplankton) but no grazers could be identified. The small fractions were not analyzed in such a way, so we cannot confirm the presence of smaller ciliate grazers. However, other research groups at the Arctic Station observed ciliates within this size fraction, confirming their presence within the same water body that we researched. Alveolates can engulf smaller flagellates - this could explain why some of the nutrient experiments had declining chlorophyll *a* measurements, as the ciliates could have proliferated, using the nutrients, and outcompeted phytoplankton. Our growth rates were not typical of experiment growth rates, more akin to natural marine rates. This could be due to our growth rates being based on a water body which contains grazers. However, this is only speculation as time constraints limited our ability to visually inspect each experiment, so it cannot be confirmed as a primary driver for declining chlorophyll *a* concentration in some of the nutrient experiments. Moreover, as ciliates are physiologically delicate, seawater has to be sampled in a very gentle manner to make sure they are preserved until reaching the laboratory—our experiment did not take this precaution.

The planktonic cells that were visible in this sample appeared damaged—explaining the low chlorophyll *a* concentration. Moreover, it was observed that the phytoplankton were in a resting spore formation, their physiology showing a non-active state, often with large lipid reserves within multi-layered cell walls. These accumulations are characteristic of phytoplanktonic resting stages, and play a central role in resilience of plankton to extreme conditions, such as those found in the Arctic (Ellegaard and Ribiero, 2017). This suggests that an explanatory factor for the low growth rates seen in many of the experiments could be due to a seasonal effect, where plankton growth rates had already peaked in late spring and early summer (Arteaga et al., 2020).

In order to completely eliminate this possibility, more samples would be analyzed for community compositions. This would likewise give the opportunity to draw conclusions about how different taxa react to the different treatments. Simultaneously, the cells could be quantified to give a more precise picture of the actual amount of phytoplankton. For the scope of this project, the chlorophyll *a* concentration is, however, considered a good proxy. The experiment could be further optimized by sampling earlier in the growing season where the possibility for dormancy is low and the demand of nutrients is high. This way, the stimulation by iron and nutrient additions can result in higher growth rates. Aside from that, the chlorophyll *a* concentrations could be controlled over a longer time period than 188 hours. Nutrient treatments can show a lag time due to adaptation of the new environment and processing of the enhanced nutrient supply. In fact, some of the samples showed an increase in the chlorophyll *a* concentration after reaching a minimum. Therefore, a long-term experiment is suggested.

7. Conclusion

Arctic marine ecosystems play an important role in mitigating climate change, however increasing temperatures in the Arctic have led to an increase in alterations to marine environments, particularly through the deposition of sediment-rich meltwater to near-shore marine ecosystems. The role of trace elements, particularly iron, in driving arctic marine ecosystem function is well understood, however its changing influence under climate change conditions is still relatively unknown. This study seeks to investigate the influence of laboratory iron additions and iron & nutrient addition on marine water samples taken in Disko Bay in late summer. Sites included the University of Copenhagen Department of Marine

Biology's permeant monitoring station and a site close to the mouth of the Red River, proximate to the influx of sediment-rich meltwater. The influence of proximity to the mouth of the river (a proxy for proximity to runoff), depth in the water column, and marine organism size fractionation were analyzed. This study concluded that organisms at two size fractionations do not seem to be growth limiting at either sampling station (close to the mouth of the Red River, 3km distance). Instead, the increased turbidity caused by the river discharge can be considered growth-limiting. In addition, the sediment discharge of the Red River dominates other factors such as vertical mixing of the water column and thereby the nutrient concentration and light in different depths at the same site. Despite generally lower concentrations, the growth rates were higher for the large size fraction. Larger cells, such as diatoms, do not appear to be dormant and thus benefit from the increased nutrient concentrations as well as light availability. However, the experiment should be repeated under optimal conditions in order to draw any final conclusions.

8. References

Armand, L., Cornet-Barthaux, V., Mosseri, J. and Quéguiner, B. (2008). Late summer diatom biomass and community structure on and around the naturally iron-fertilised Kerguelen Plateau in the Southern Ocean. Deep Sea Research Part II: Topical Studies in Oceanography, 55(5-7), pp.653-676.

Arteaga, L.A., Boss, E., Behrenfeld, M.J. *et al.* Seasonal modulation of phytoplankton biomass in the Southern Ocean. *Nat Commun* 11, 5364 (2020). https://doi.org/10.1038/s41467-020-19157-2

Bassi, D., Menossi, M. and Mattiello, L. (2018). 'Nitrogen supply influences photosynthesis establishment along the sugarcane leaf', Scientific Reports. Springer US, 8(1), pp. 1–13. doi: 10.1038/s41598-018-20653-1.

Basu, S., Mackey, K.R.M. (2018). Phytoplankton as key mediators of the biological carbon pump: their responses to changing climate. *Sustainability* 10(867):doi:10.3390/su10030869.

Bhatia, M.P., Kujawinski, E.B., Das, S.B., Breier, C.F. Henderson, P.B., et al. (2013). Greenland meltwater as a significant and potentially bioavailable source of iron to the ocean. *Nature Geoscience.* DOI: 10.1038/NGEO1746

Boscolo-Galazzo, F., Crichton, K.A., Barker, S., Pearson, P.N. (2018). Temperature dependency of metabolic rates in the upper ocean: a positive feedback to global climate change? *Global and Planetary Change* 170:201-212
https://doi.org/10.1016/j.gloplacha.2018.08.017

Boyd, P., Watson, A., Law, C. et al. (2000). A mesoscale phytoplankton bloom in the polar Southern Ocean stimulated by iron fertilization. Nature 407, 695–702 . https://doi.org/10.1038/35037500

Broecker, W.S. and Peng, T.H. (1982). Tracers in the Sea, Lamont-Doherty Earth Observatory. Palisades, New York.

Currie, H.A. and Perry, C.C. (2007). Silica in Plants: Biological, Biochemical and Chemical Studies. Annals of Botany 100, 1383–1389.. doi:10.1093/aob/mcm247

Doney, S. C. (2013) 'Marine ecosystems, biogeochemistry, and climate', in International Geophysics. Academic Press, pp. 817–842. doi: 10.1016/B978-0-12-391851-2.00031-3.

Doney, S. C., Bopp, L., Long, M. (2014). Historical and Future Trends in Ocean Climate and Biogeochemistry. Oceanography, 27(1), 108-119. Retrieved October 25, 2020, from http://www.jstor.org/stable/24862126

Ellegaard, M. and Ribeiro, S., 2017. The long-term persistence of phytoplankton resting stages in aquatic 'seed banks'. *Biological Reviews*, 93(1), pp.166-183.

Feely, R., Doney, S., Cooley, S. (2009). Ocean Acidification: Present Conditions and Future Changes in a High-CO_2 World. Oceanography, 22(4), 36-47. Retrieved October 25, 2020, from http://www.jstor.org/stable/24861022

Glibert, P. M., Wilkerson, F. P., Dugdale, R. C., Raven, J. A., Dupont, C. L., Leavitt, P. R., Parker, A. E., Burkholder, J. M. and Kana, T. M. (2016) 'Pluses and minuses of ammonium and nitrate uptake and assimilation by phytoplankton and implications for productivity and community composition, with emphasis on nitrogen-enriched conditions', Limnology and Oceanography, 61(1), pp. 165–197. doi: 10.1002/lno.10203.

Hawkings, J., Wadham, J., Tranter, M. *et al.* Ice sheets as a significant source of highly reactive nanoparticulate iron to the oceans. *Nat Commun* 5, 3929 (2014). https://doi.org/10.1038/ncomms4929

Hecky, R. E. and Kilham, P. (1988). 'Nutrient limitation of phytoplankton in freshwater and marine environments: A review of recent evidence on the effects of enrichment', Limnology and Oceanography, 33(4part2), pp. 796–822. doi: 10.4319/lo.1988.33.4part2.0796

Hopwood, M.J., Bacon, S., Arendt, K. *et al.* Glacial meltwater from Greenland is not likely to be an important source of Fe to the North Atlantic. *Biogeochemistry* 124, 1–11 (2015). https://doi.org/10.1007/s10533-015-0091-6

Hopewood, M.J., Carroll, D., Browning, T.J., Meire, L., Mortensen, J., et al. (2018). Non-linear response of summertime marine productivity to increased meltwater discharge around Greenland. *Nature Communications* 9:3256. https://doi.org/10.1038/s41467-018-05488-8

Lett, S., Paulsen, M., Larsen, S. and Daugbjerg, N. (2011). Marine eukaryote picophytoplankton in the waters around Disko Island (West Greenland): a first attempt to evaluate their relative contribution to total biomass and productivity.

Marchetti, A., M. T. Maldonado, E. S. Lane, and P. J. Harrison. 2006. Iron requirements of the pennate diatom *Pseudo-nitzschia*: Comparison of oceanic (high-nitrate, low-chlorophyll waters) and coastal species. *Limnol. Oceanogr.* 51: 2092–2101. doi:10.4319/lo.2006.51.5.2092.

Markussen, T. N., Elberling, B., Winter, C., Andersen, T. J. (2016). Flocculated meltwater particles control Arctic land-sea fluxes of labile iron. Sci Rep, 6, 24033. Street, J.H., Paytan, A. (2005). Iron, phytoplankton growth, and the carbon cycle. Met Ions Biol Syst.;43:153-93. doi: 10.1201/9780824751999.ch7. PMID: 16370118.

Martin, J. H. (1990), Glacial-interglacial CO2 change. The Iron Hypothesis, *Paleoceanography*, 5(1), 1– 13, doi:10.1029/PA005i001p00001.

Milligan, A. J., and Harrison, P. J. (2000). Effects of non-steady-state iron limitation on nitrogen assimilation in the marine diatom Thalassiosira weissflogii (Bacillariophyceae). J. Phycol. 36, 78–86. doi: 10.1046/j.1529-8817.2000. 99013.x

Moore, C. M., Mills, M. M., Arrigo, K. R., Berman-Frank, I., Bopp, L., Boyd, P. W., Galbraith, E. D., Geider, R. J., Guieu, C., Jaccard, S. L., Jickells, T. D., La Roche, J., Lenton, T. M., Mahowald, N. M., Marañón, E., Marinov, I., Moore, J. K., Nakatsuka, T., Oschlies, A., Saito, M. A., Thingstad, T. F., Tsuda, A. and Ulloa, O. (2013) 'Processes and patterns of oceanic nutrient limitation', Nature Geoscience. Nature Publishing Group, pp. 701–710. doi: 10.1038/ngeo1765.

Planquette H, Sherrell RM, Stammerjohn S, Field MP (2013) Particulate iron delivery to the water column of the Amundsen Sea, Antarctica. Mar Chem 153:15–30

Quigg, A., Finkel, Z., Irwin, A. *et al.* (2003). The evolutionary inheritance of elemental stoichiometry in marine phytoplankton. *Nature* 425, 291–294. https://doi.org/10.1038/nature01953

Raiswell, R., Benning, L.G., Tranter, M. *et al.* Bioavailable iron in the Southern Ocean: the significance of the iceberg conveyor belt. *Geochem Trans* 9, 7 (2008). https://doi.org/10.1186/1467-4866-9-7

Rout, G. R. and Sahoo, S. (2015). Role of Iron in Plant Growth and Metabolism', Reviews in Agricultural Science, 3(0), pp. 1–24. doi: 10.7831/ras.3.1.

Rue, E. L. and Bruland, K. W. (1995). Complexation of iron(III) by natural organic ligands in the Central North Pacific as determined by a new competitive ligand equilibration/adsorptive cathodic stripping voltammetric method', Marine Chemistry, 50(1–4), pp. 117–138. doi: 10.1016/0304-4203(95)00031-L.

Rychter, A. and Rao, I. (2005). 7 Role of Phosphorus in Photosynthetic Carbon Metabolism. Handbook of Photosynthesis.

Schoffman H, Lis H, Shaked Y and Keren N (2016) Iron–Nutrient Interactions within Phytoplankton. Front. Plant Sci. 7:1223. doi: 10.3389/fpls.2016.01223

Sharp, J. H. (2001). Marine and Aquatic Communities, Stress from Eutrophication,
Editor(s): Simon Asher Levin, Encyclopedia of Biodiversity. Elsevier. Pages 1-11. https://doi.org/10.1016/B0-12-226865-2/00185-1.

Sheng, H. and Chen, S. (2020). Plant silicon-cell wall complexes: Identification, model of covalent bond formation and biofunction. Plant Physiology and Biochemistry, 155, 13-19. https://doi.org/10.1016/j.plaphy.2020.07.020.

Smith, L. V., McMinn, A., Martin, A., Nicol, S., Bowie, A. R., Lannuzel, D. and Van der Merwe, P. (2013) 'Preliminary investigation into the stimulation of phytoplankton photophysiology and growth by whale faeces', Journal of Experimental Marine Biology and Ecology, 446(April), pp. 1–9. doi: 10.1016/j.jembe.2013.04.010.

Timmermans, K. R., Stolte, W., and Baar, H. J. W. (1994). Iron-mediated effects on nitrate reductase in marine phytoplankton. Mar. Biol. 121, 389–396. doi: 10.1007/BF00346749

Tréguer, P., Nelson, D., Van Bennekom, A., DeMaster, D., Leynaert, A. and Quéguiner, B., 1995. The Silica Balance in the World Ocean: A Reestimate. *Science*, 268(5209), pp.375-379.

Twining, B.S., Antipova, O., Chappell, P.D., Cohen, N.R., Jacquot, J.E., Mann, E.L., Marchetti, A., Ohnemus, D.C., Rauschenberg, S. and Tagliabue, A. (2021), Taxonomic and nutrient controls on phytoplankton iron quotas in the ocean. Limnol Oceanogr Lett, 6: 96-106. https://doi.org/10.1002/lol2.10179

http://envcoglobal.com/files/docs/trilogy-spec-sheet-2008.pdf

Wang, S., Bailey, D., Lindsay, K., Moore, J. and Holland, M. (2014). Impact of sea ice on the marine iron cycle and phytoplankton productivity. Biogeosciences, 11(17), pp.4713-4731.

Watson, A.J., Schuster, U., Shutler, J.D. *et al.* Revised estimates of ocean-atmosphere CO2 flux are consistent with ocean carbon inventory. *Nat Commun* 11, 4422 (2020). https://doi.org/10.1038/s41467-020-18203-3

Williamson, P., Wallace, D.W.R., Law, C.S., Boyd, P.W., Collos, Y., et al. (2012). Ocean fertilization for geoengineering: A review of effectiveness, environmental impacts and emerging governance. *Process Safety and Environmental Protection* 90(6):475-488.
https://doi.org/10.1016/j.psep.2012.10.007

Zhou, M., Shen, Z. and Yu, R., 2008. Responses of a coastal phytoplankton community to increased nutrient input from the Changjiang (Yangtze) River. Continental Shelf Research, 28(12), pp.1483-1489. https://doi.org/10.1016/j.csr.2007.02.009

Appendix A

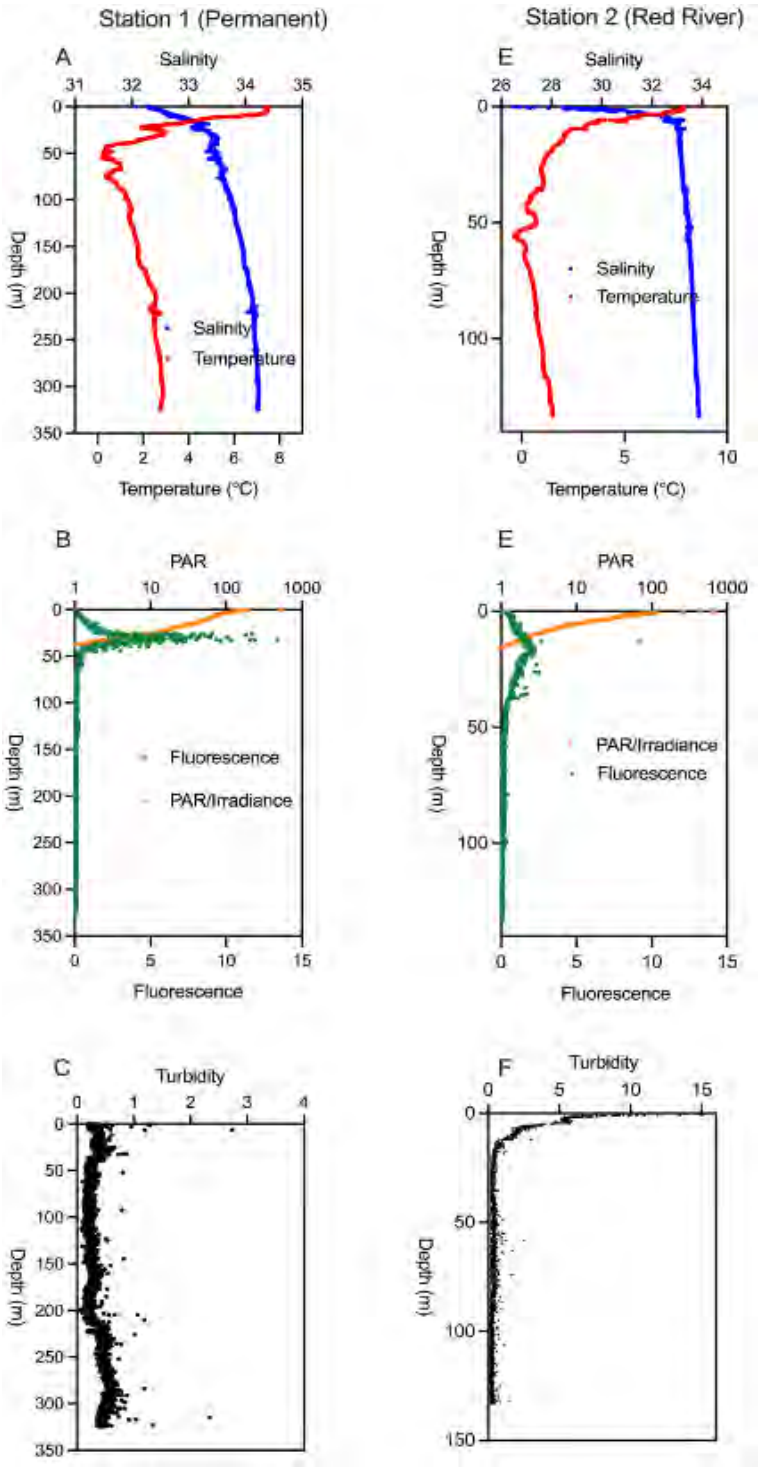

Figure A1. Measurements from the CTD taken at the distal site (Station 1) and the proximate site (Station 2) showing the temperature and salinity (A and D), the photosynthetically active radiation (PAR) and fluorescence (B and E) and the turbidity (C and F) as function of depth. Note the different scales of the salinity, temperature, turbidity and depth for Station 1 and Station 2, respectively.

Appendix B

Table B1. Standard errors of the averaged chlorophyll *a* concentrations of the triplicated samples for the two size fractions, four sampling sites, and three different treatments for each measurement. Key: P3 = Proximate Site, 3m depth; P19 = Proximate Site, 19m depth; D3 = Distal site, 3m depth; D31 = Distal site, 31m depth.

Treatment	Site	40 Hours		92 Hours	
		200µm - 20µm µG/L	20µm - 0.7µm uG/L	200µm - 20µm µG/L	20µm - 0.7µm uG/L
Control	P3	0.0033	0.0186	0.0042	0.0232
Control	P19	0.0233	0.0273	0.0292	0.0341
Control	D3	0.0000	0.0200	0.0000	0.0250
Control	D31	0.0133	0.0186	0.0167	0.0232
Iron	P3	0.0033	0.0208	0.0042	0.0260
Iron	P19	0.0291	0.0115	0.0363	0.0144
Iron	D3	0.0033	0.0186	0.0042	0.0232
Iron	D31	0.0120	0.0133	0.0150	0.0167
Nutrients	P3	0.0153	0.1729	0.0191	0.2161
Nutrients	P31	0.0100	0.0153	0.0125	0.0191
Nutrients	D3	0.0033	0.0067	0.0042	0.0083
Nutrients	D31	0.0058	0.0353	0.0072	0.0441
Treatment	Site	140 Hours		188 Hours	
		200µm - 20µm µG/L	20µm - 0.7µm uG/L	200µm - 20µm µG/L	20µm - 0.7µm uG/L
Control	P3	0.0167	0.0417	0.0250	0.0083
Control	P19	0.4918	0.9071	0.5544	1.1905
Control	D3	0.0000	0.0458	0.0115	0.1646
Control	D31	0.0260	0.3156	0.0614	0.1512
Iron	P3	0.0033	0.1706	0.0182	0.1543

Iron	P19	0.0253	0.1438	0.0505	0.1092
Iron	D3	0.0072	0.1296	0.0000	0.0688
Iron	D31	0.0583	0.3171	0.0708	0.1446
Nutrients	P3	0.0110	0.2852	0.0397	0.5855
Nutrients	P31	0.0167	0.0144	0.0110	0.0125
Nutrients	D3	0.0000	0.0042	N/A	N/A
Nutrients	D31	0.0417	0.0072	N/A	N/A

Appendix C

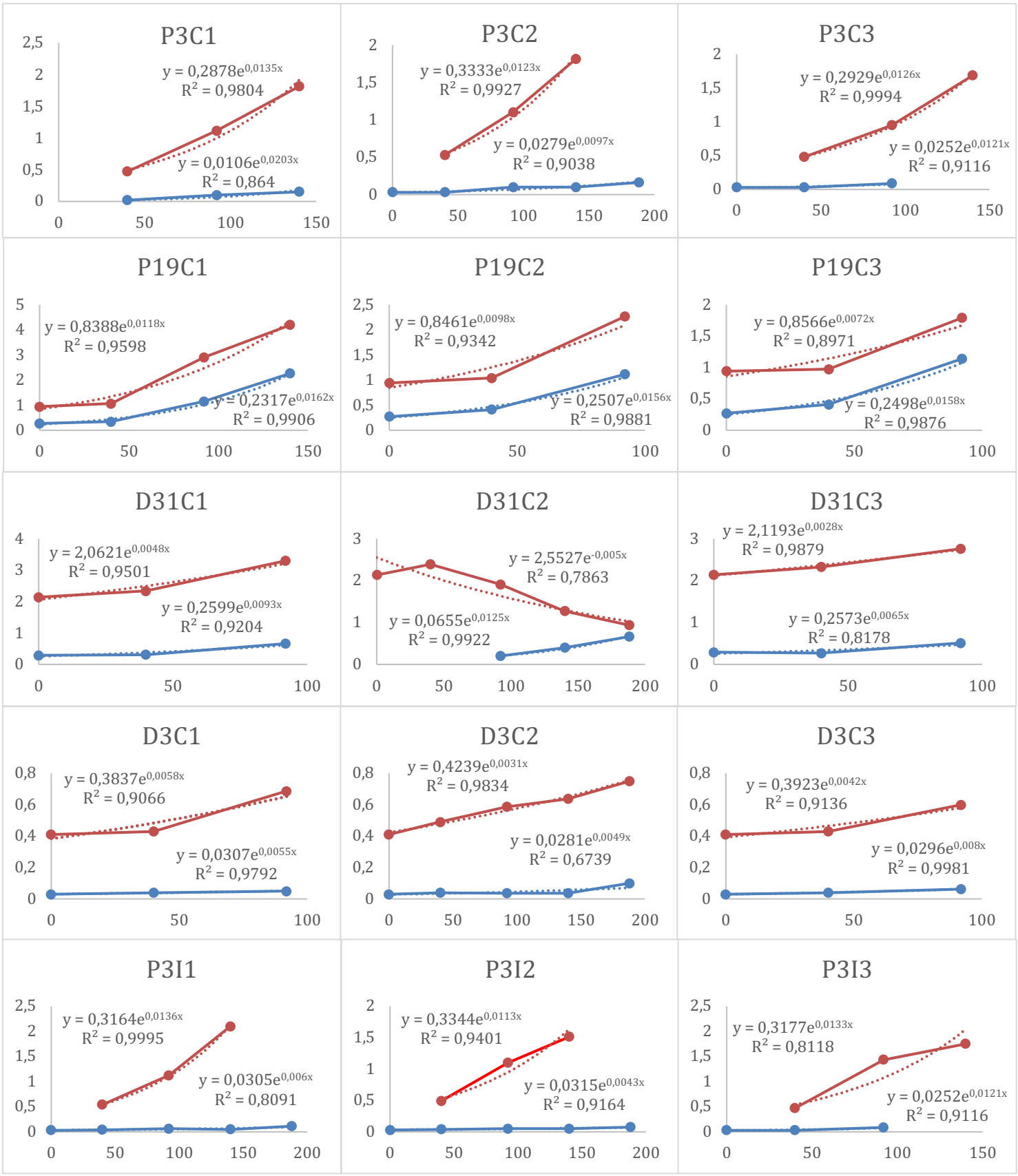
P3C1
y = 0,2878e^0,0135x
R² = 0,9804
y = 0,0106e^0,0203x
R² = 0,864
P3C2
y = 0,3333e^0,0123x
R² = 0,9927
y = 0,0279e^0,0097x
R² = 0,9038
P3C3
y = 0,2929e^0,0126x
R² = 0,9994
y = 0,0252e^0,0121x
R² = 0,9116
P19C1
y = 0,8388e^0,0118x
R² = 0,9598
y = 0,2317e^0,0162x
R² = 0,9906
P19C2
y = 0,8461e^0,0098x
R² = 0,9342
y = 0,2507e^0,0156x
R² = 0,9881
P19C3
y = 0,8566e^0,0072x
R² = 0,8971
y = 0,2498e^0,0158x
R² = 0,9876
D31C1
y = 2,0621e^0,0048x
R² = 0,9501
y = 0,2599e^0,0093x
R² = 0,9204
D31C2
y = 2,5527e^-0,005x
R² = 0,7863
y = 0,0655e^0,0125x
R² = 0,9922
D31C3
y = 2,1193e^0,0028x
R² = 0,9879
y = 0,2573e^0,0065x
R² = 0,8178
D3C1
y = 0,3837e^0,0058x
R² = 0,9066
y = 0,0307e^0,0055x
R² = 0,9792
D3C2
y = 0,4239e^0,0031x
R² = 0,9834
y = 0,0281e^0,0049x
R² = 0,6739
D3C3
y = 0,3923e^0,0042x
R² = 0,9136
y = 0,0296e^0,008x
R² = 0,9981
P3I1
y = 0,3164e^0,0136x
R² = 0,9995
y = 0,0305e^0,006x
R² = 0,8091
P3I2
y = 0,3344e^0,0113x
R² = 0,9401
y = 0,0315e^0,0043x
R² = 0,9164
P3I3
y = 0,3177e^0,0133x
R² = 0,8118
y = 0,0252e^0,0121x
R² = 0,9116

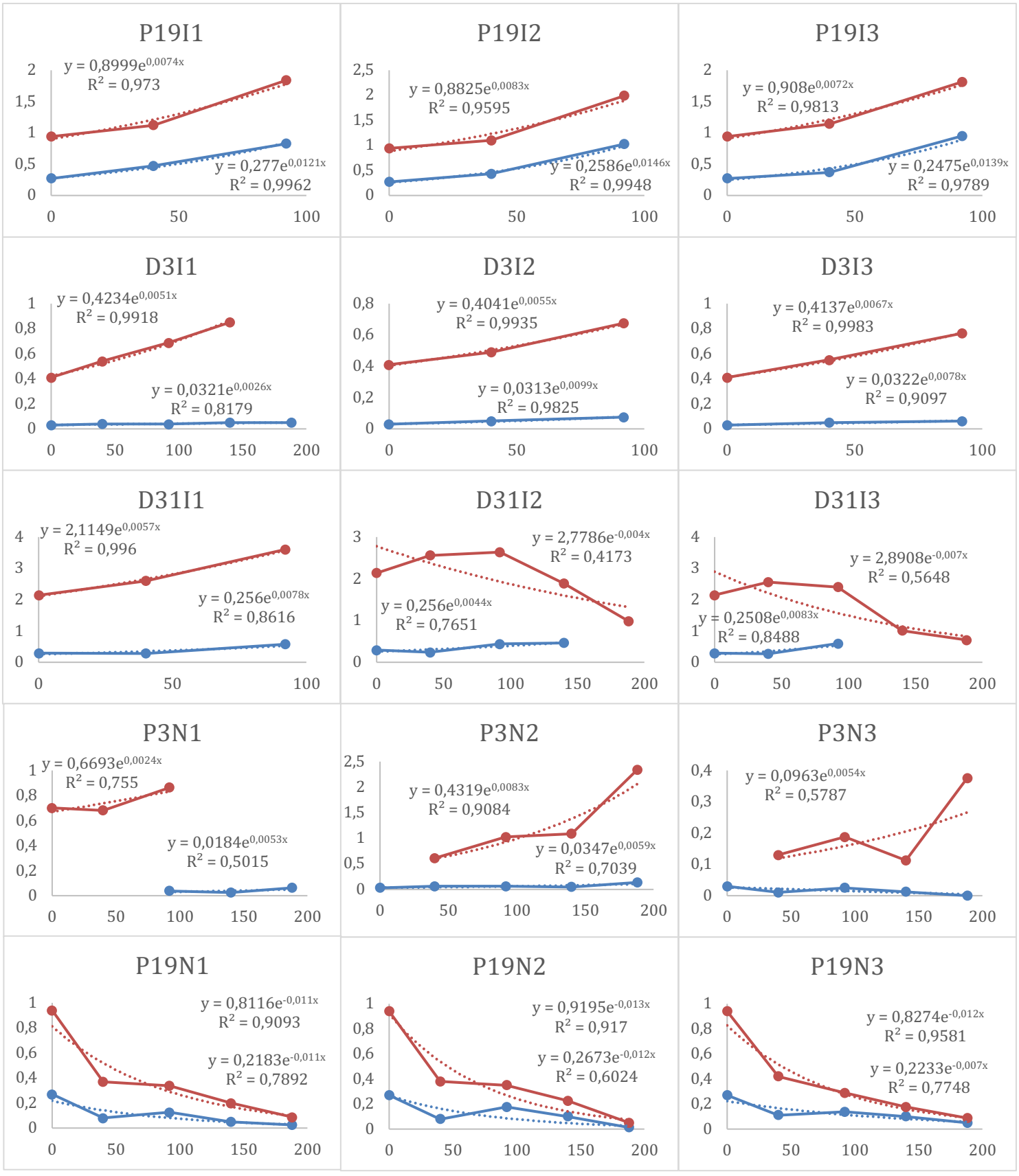
P19I1
y = 0,8999e0,0074x
R² = 0,973
y = 0,277e0,0121x
R² = 0,9962
P19I2
y = 0,8825e0,0083x
R² = 0,9595
y = 0,2586e0,0146x
R² = 0,9948
P19I3
y = 0,908e0,0072x
R² = 0,9813
y = 0,2475e0,0139x
R² = 0,9789
D3I1
y = 0,4234e0,0051x
R² = 0,9918
y = 0,0321e0,0026x
R² = 0,8179
D3I2
y = 0,4041e0,0055x
R² = 0,9935
y = 0,0313e0,0099x
R² = 0,9825
D3I3
y = 0,4137e0,0067x
R² = 0,9983
y = 0,0322e0,0078x
R² = 0,9097
D31I1
y = 2,1149e0,0057x
R² = 0,996
y = 0,256e0,0078x
R² = 0,8616
D31I2
y = 2,7786e-0,004x
R² = 0,4173
y = 0,256e0,0044x
R² = 0,7651
D31I3
y = 2,8908e-0,007x
R² = 0,5648
y = 0,2508e0,0083x
R² = 0,8488
P3N1
y = 0,6693e0,0024x
R² = 0,755
y = 0,0184e0,0053x
R² = 0,5015
P3N2
y = 0,4319e0,0083x
R² = 0,9084
y = 0,0347e0,0059x
R² = 0,7039
P3N3
y = 0,0963e0,0054x
R² = 0,5787
P19N1
y = 0,8116e-0,011x
R² = 0,9093
y = 0,2183e-0,011x
R² = 0,7892
P19N2
y = 0,9195e-0,013x
R² = 0,917
y = 0,2673e-0,012x
R² = 0,6024
P19N3
y = 0,8274e-0,012x
R² = 0,9581
y = 0,2233e-0,007x
R² = 0,7748

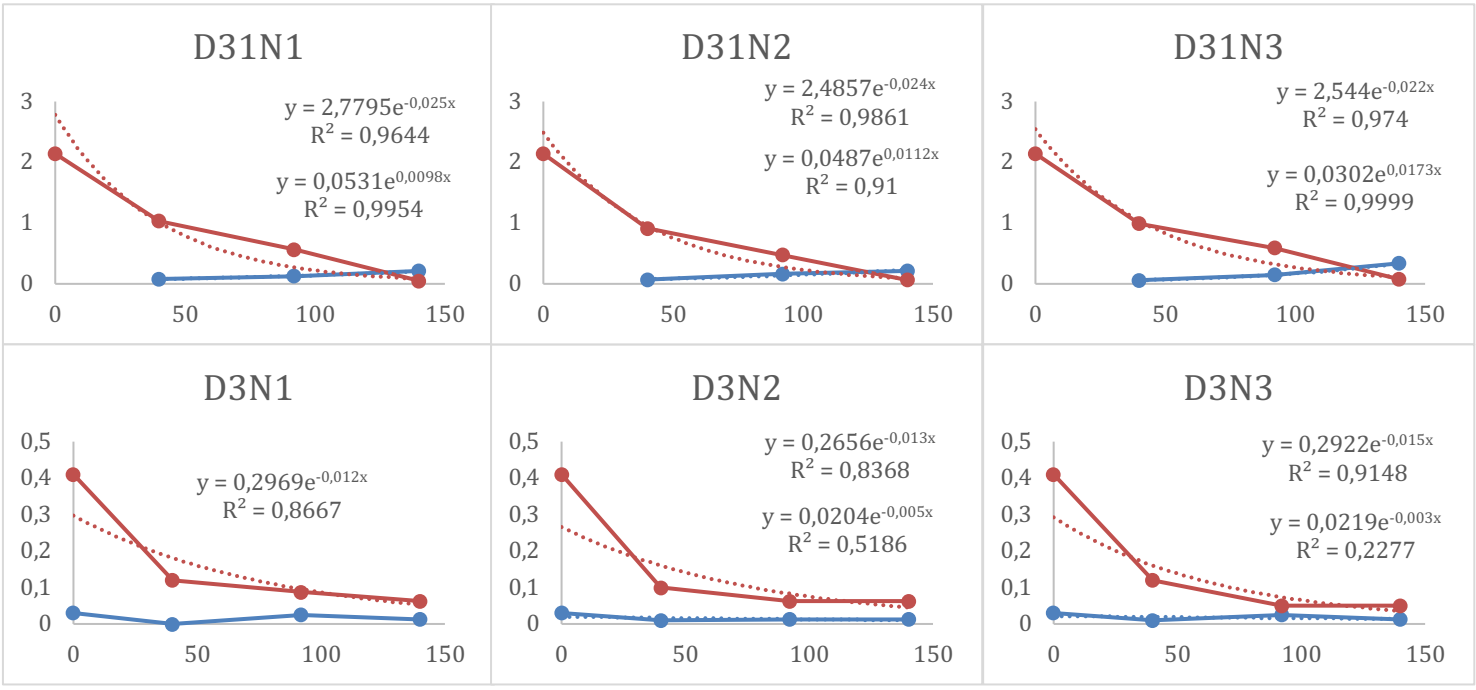

Figure C1. Chlorophyll *a* concentration (μgl^{-1}) as function of time (hours) for all the different samples from the four sampling sites and the three treatments. The small size fraction (0.7-20µm) is presented in red, and the large size fraction (20-200µm) in blue. Note, that only data points, which are exponentially fitted to are displayed. The function of the fit and the corresponding determination coefficient (R^2) are presented in the plots. Key: P3 = Proximate Site, 3m; P19 = Proximate Site, 19m; D3 = Distal Site, 3m; D31 = Distal Site, 31m; C1-3 = Control triplicates; I1-3 = Iron triplicates; N1-3 = Iron & Nutrient triplicates.

UNIVERSITY OF COPENHAGEN
FACULTY OR DEPARTMENT

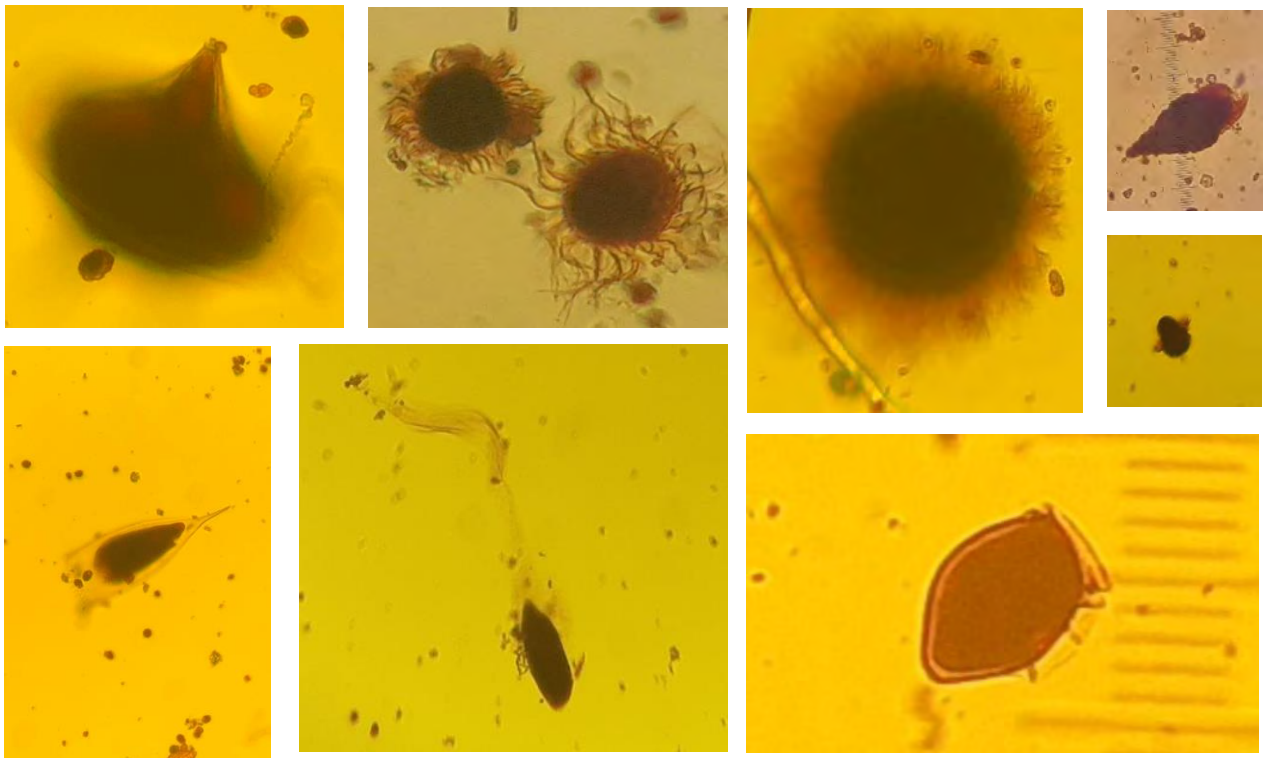

From top row, left to right: *Protoperidinum* spp., *Mesodinium major next to a Strobilidium* spp., another large *Mesodinium major.* Top right corner shows a *Laboea strobila* and below is a *Mesodinium spp* laying on its side. Bottom left row, left to right: Tintinnid ciliate, *Gyrodinium spirale*, *Dinophysis* spp. Pictures are from different microscopes and magnifications.

Protistan grazer responses to a nanoflagellate bloom in the Arctic

Alexander Scheel, Dan Johan Kristensen and Caroline Woergaard Gram

Supervisor: Per Juel Hansen

Submitted on: 15th of August 2022

Course:	Arctic Biology Field Course (NBIK18001U)
Author(s):	Alexander Scheel (txj263), Dan Johan Kristensen (wfd602) and Caroline Woergaard Gram (vxk693)
Department:	Department of Biology, Faculty of Science
Number of characters:	46180 (without spaces, frontpage and reference-list)

Abstract

Mixotrophs are important components in the plankton in the Arctic, often dominating during stratified waters in summer, and having a profound impact on the planktonic ecosystem including enhanced primary production and biomass transfer to higher trophic levels. Even though mixotrophy is considered fundamental to marine ecosystems, little is known about the dynamics of the planktonic ecosystem and how the availability of a specific type of prey influences the different functional protozoan groups of the plankton. We investigated the response of 12 selected mixotrophic and heterotrophic ciliates and dinoflagellates to the addition of different concentrations of the photosynthetic nanoflagellate, *Pyramimonas diskoicola* to a summer plankton community from Disko Bay, Northwest Greenland to explore which functional groups would be promoted by the addition of high and low algal concentrations. In this study, two treatments were set up with final concentrations of ~1000 cells mL^{-1} and high ~5000 cells mL^{-1} of *P. diskoicola* along with a control without the addition of prey. Nutrients were added to all treatments. Responses in total chl*a* concentrations as well as the cell concentrations of selected protistan grazers were then monitored for 6 days: *Dinophysis* spp., *Gyrodinium spirale, Gyrodinium/Gymnodinium* spp., *Laboea strobila, Lohmaniella oviformis, Mesodinium major, Mesodinium rubrum, Protoperidinium* spp. *Strobilidium* spp., *Strombidium conicum, Strombidium* spp., and tintinnid ciliates. Mixotrophic ciliates, *Strombidium* spp., dominated the initial plankton community, where they constituted 43% of the total cell count. Overall, cell concentrations declined as a function of incubation time with no observable effect of the added prey concentrations for any of the mixotrophic ciliates and dinoflagellates. Heterotrophic ciliates varied in their response to incubation, with prey concentrations having a significant effect on the cell numbers and growth rate of the heterotrophic ciliate *Lohmaniella oviformis* ($p<0.05$), which was the highest for all the ciliates. The heterotrophic dinoflagellate, *Protoperidinium* spp., had the highest cell concentration and growth rate at high prey concentration. No change in cell concentrations were observed for the heterotrophic dinoflagellates within the *Gyrodinium/Gymnodinium* genera. These results show that when changing the availability of a specific type of prey, the responses of mixotrophic and heterotrophic protozoans are complex and vary to a great extent. Our study highlights the difficulty and complexity in working with natural planktonic populations.

Table of Contents

1 Introduction

1.1 Mixotrophy and acquired phototrophy

Mixotrophy is an organisms' use of different nutritional strategies of nutrient acquisition including carbon, nitrogen, phosphorous and trace elements. Mixotrophic protists combine phototrophy and heterotrophy as a nutritional mode (Stoecker *et al.*, 2017) in a wide variety of nutritional strategies, resulting in mixotrophy being more of a gradient (Flynn *et al.*, 2013), thus, challenging the traditional dichotomy of "producers" and "consumers" and structure of planktonic food webs (Flynn *et al.*, 2013; Mitra *et al.*, 2016). How the specific species utilizes and combine the different strategies is dependent on a range of factors including niche, environmental conditions, species (Hansen and Tillmann, 2020) and evolutionary history (Stoecker *et al.*, 2009).

Mixotrophs can be divided into constitutive mixotrophs (CMs), which have chloroplasts of their own, and non-constitutive mixotrophs (NCMs), which acquire phototrophy trough the retention of chloroplasts from prey (Hansen *et al.*, 2013; Hansen and Tillmann, 2020). Some non-constitutive mixotrophs are specific in which prey they sequester chloroplasts from. These are termed *specialist non-constitutive mixotrophs* (SNCM), whereas the non-constitutive mixotrophs that can utilize chloroplasts from different prey species are termed *generalist non-constitutive mixotrophs* (GNCMs).

1.2 Dynamics between non-constitutive mixotrophs and their prey

The dynamics between non-constitutive mixotrophs and their prey are complex, and many aspects are still not understood. For example, Maselli *et al.,* 2020 found that some algal species sustained growth of the ciliate *Strombidium* spp. better than others, despite that *Strombidium* spp. can sequester chloroplasts from a wide range of taxonomically different algal prey, within a specific size range. This suggests that some factors other than prey algal group determines if a prey is suitable. GNCMs are not able to divide their stolen chloroplasts and therefore, they will get diluted out of the cells after prey depletion, even though their ability to photosynthesis can extend the survival of their heterotrophic counterparts (Hughes *et al.*, 2021). Contrary, many SNCMs have been shown to be able to sequester their prey's nuclei (Hughes *et al.*, 2021) and divide their stolen chloroplasts, which increase their survival to exceed the survival of GNCMs and heterotrophs when prey is depleted (Hansen *et al.*, 2012). Despite being SNCM *Mesodinium rubrum* was found to be able to exchange its symbiont *Teleaulax amphioxeia* with a different *Teleaulax* species over the course of 35 days (Hansen *et*

al., 2012), suggesting some flexibility in the prey they can utilize. Our knowledge on acquired phototrophy in ciliates and dinoflagellates is still limited, and there are still many open questions e.g., how are sequestered chloroplasts controlled, and how large are species and strains variations within the non-constitutive mixotrophs (Hansen *et al.*, 2012). The non-constitutive mixotrophs can also be key to understanding the evolution of oxygenic photosynthesis within the eukaryotic life (Stoecker *et al.*, 2009; Hansen *et al.*, 2012), as well as challenging how we understand symbiosis, planktonic food webs, evolutionary processes and how diverse microbial life is.

1.3 Planktonic ecosystems in the Arctic during summer

The Arctic is characterized by extreme seasonal variation in solar irradiance and primary productivity (Stoecker and Lavrentyev, 2018). The planktonic community in the Arctic follows a seasonal characteristic pattern in biomass, production and species composition following the highly variable levels of irradiance, salinity and nutrients (Levinsen *et al.*, 2000). Mixotrophs have been found to be widespread amongst the plankton and is believed to have an advantage in polar regions due to the seasonal variation. In the summer period, mixotrophs can utilize the irradiance for photosynthesis and either acquire nutrients directly from the water-masses (eutrophic conditions) or through phagotrophy (oligotrophic conditions). In the winter period where light is scarce, they can benefit from their phagotrophic mode (Stoecker and Lavrentyev, 2018). In summer, mixotrophic ciliates often dominate the chlorophyll biomass in the mixed layer in summer, taking advantage of the 24 hour sunlight, being an important food source for key Arctic copepod species and therefore an important trophic link, increasing energy transfer through the food web (Stoecker and Lavrentyev, 2018; Maselli *et al.*, 2020). Observations suggest that in the Arctic an alternative food web based on mixotrophy may dominate the planktonic pelagic food web (Stoecker and Lavrentyev, 2018), with mixotrophy increasing the retention of N, P, and Fe in the upper water column, and influencing the carbon fluxes with the improvement of the biological pump (Stoecker *et al.*, 2009, 2017).

Generally, for planktonic predators, the size ratios between prey and predator seem to be consistent within groups (incl. ciliates and dinoflagellates), meaning that these dinoflagellates and ciliates can only prey on organism in a specific size range. The timing of the bloom for these predatory species follows the bloom of their prey (Hansen *et al.*, 1994). However, climate is ultimately resulting in a decrease in sea-ice extent and duration. These changes will likely lead to earlier spring blooms of diatoms, prolonging the period where the primary production is dominated by the nano-flagellates. This will impact the entire plankton food web dynamics (Nghiem *et al.*, 2007; Ardyna and Arrigo, 2020).

1.4 Climate change and its impacts on Arctic planktonic ecosystems

Climate change is rapidly changing the physical/chemical environment, especially in the Arctic region. Species have evolved to fit the environmental conditions there for thousands of years and the native species might be challenged to keep up with the rapid changes. Therefore, there is an urgency in studying the effects of mixotrophy in the Arctic because the marine environment is undergoing rapid changes due to climate change. Changes includes the water masses in Disko Bay changing with warmer Atlantic water replacing the Northern Arctic Water. This shift accelerates the freshwater input from the glaciers, which can increase stratification, prevent mixing (nutrient input) to the upper water column (Hansen *et al.*, 2012). A stratified water column could potentially lead to a decrease in primary production (Stoecker and Lavrentyev, 2018) and favour smaller phytoplankton species ultimately leading to a decrease in the energy transfer to higher trophic levels (Stoecker *et al.*, 2017), underlying the importance in understanding the role of heterotrophs and mixotrophs and their influence in planktonic ecosystems.

1.5 Scope of study

In this study we examined the responses of heterotrophic and mixotrophic Arctic protozoan species to a chosen prey species, the green algae *Pyromominas diskoicola* collected at Disco Bay, mimicking a nano-flagellate bloom in the Arctic. The projected changes in the Arctic might potentially favour blooms of phototrophic nanoflagellates (Nghiem *et al.*, 2007; Ardyna and Arrigo, 2020). Little is known on how the different Arctic protistan grazers respond to a nanoflagellate bloom and what effects would a change in prey availability have on the population dynamics of the plankton. Hughes *et al.* 2021 argues that GNCMs will outperform heterotrophs at low prey concentrations since they can both utilize light and prey, giving them a competitive advantage. However, in high prey concentrations heterotrophs outperform GNCMs since it has a metabolic cost to be a mixotroph. Mixotrophs have both the photosystem and the system for phagotrophy to maintain, thus heterotrophs can achieve higher maximum growth rates (Fischer *et al.,* 2016). With this knowledge, we have formulated the two following hypothesis:

Generalist non-constitutive mixotrophs will have higher growth rates at low prey concentrations compared to heterotrophs.

Heterotrophs will have higher growth rates than mixotrophs at high prey concentrations.

Ciliates would be expected to have a faster response to a change in prey concentrations since ciliates have higher growth rates than dinoflagellates. There is a consistent relationship between cell volume and metabolic rate, with ciliates having a smaller cell volume and therefore having a 2-3

times higher metabolic rate (Hansen *et al.,* 1994;1997). Predator:prey size ratio determines which prey can be utilized by a protistan grazer (Hansen *et al.* 1994). The size of the prey is an important factor in how much energy is gained from ingestion, with a specific prey size optimum giving the maximum growth rate. Ciliates and dinoflagellates' prey size optimum differs with ciliates ingesting prey 8 times smaller than themselves, whereas dinoflagellates feeds on prey the same size as themselves (Hansen *et al.,* 1994). The predator:prey size ratio will therefore be expected to influence the response of the different protistan grazers in a nanoflagellate bloom with:
Ciliates in the size range of 30-50 µm, and dinoflagellates in the size range 6-25 µm being the main grazers on Pyramimonas diskoicola (Length: 8.3 +/- 2.6 Width: 5.1+/-0.8 µm). Furthermore, *Ciliates will have a higher growth rate than dinoflagellates.*

This study focuses on ciliates and dinoflagellates since ciliates with acquired phototrophy are commonly found around the world and can make up 30% of the ciliate biomass in the euphotic zone (Stoecker *et al.*, 2009; Maselli *et al.*, 2020). Contrary, despite their diverse range of plastids, there are only a few identified dinoflagellate species with acquired phototrophy (Stoecker *et al.*, 2009) but several genera of heterotrophic dinoflagellates are found during summer in the Arctic (Levinsen *et al.* 2000). In this study, we have chosen to focus on 12 species of different non-constitutive mixotrophs and heterotrophs to investigate if there is a difference in their response and utilization of the added prey species (*Pyramimonas diskoicola*). Species or genera representing both non-constitutive mixotrophs (GNCM) and specialist non-constitutive mixotrophs (SNCM) are included.

This study aims to get an understanding of population dynamics (change in size and structure) between nano-flagellate prey and mixotrophic and heterotrophic protistan grazers in the Arctic, contributing to the knowledge of non-constitutive mixotrophs and their role in planktonic food-webs. To answer the following question: which protistan grazers will be promoted and exhibit an increased growth rate by the addition of nano-flagellate prey, the following hypothesises were tested:

1. Ciliates in the size range of 30-50 µm, and dinoflagellates in the size range 6-25 µm are the main grazers on *Pyramimonas diskoicola* (Length: 8.3 +/- 2.6 Width: 5.1+/-0.8 µm).

2. Generalist non-constitutive mixotrophs have higher growth rates at low prey concentrations compared to heterotrophs.

3. Heterotrophs have higher growth rates than mixotrophs at high prey concentrations.

4. Ciliates have a higher growth rate than dinoflagellates.

2 Materials and Methods

2.1 Sampling

20 L of water were collected from the permanent marine sampling station in Disko Bay, West Greenland (69°11.333' N and 53°29.766 M) the 23rd of July 2022. A 10-L Niskin Water Sampler was used for collecting water at 6 metres depth which was carefully transferred to a 20-L container through a silicone tube. Large copepods were removed from the sample using a Pasteur pipette.

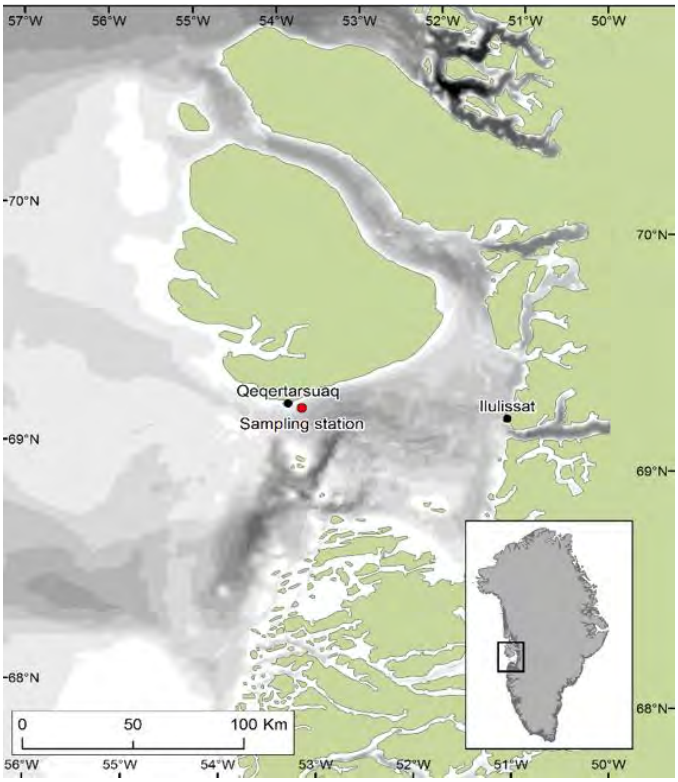

Figure 1; Map of the sampling station in Disko Bay, West Greenland. From Hansen *et al.,* 2012.

2.2 Physical, chemical, and biological parameters

Vertical depth profiles of light, salinity, temperature, Chlorophyll fluorescence were measured by a CTD at the sampling station.

2.3 Monoculture of *Pyramimonas diskoicola*

A monoculture of the prasinophyte green algae *Pyramimonas diskoicola* was used as prey for the selected ciliates and dinoflagellates in the collected water sample. *P. diskoicola* monoculture was provided by Niels Daugbjerg, University of Copenhagen (UCPH), a clone from the original culture, isolated from surface water collected at Baffin Bay and described by Harðardóttir *et al.*, 2014. The culture was acclimated to experimental temperature (4± 1° C) and light (90-115 µmol photons m^{-2} s^{-1}) for 24 h prior to the start of the experiment. Prior to the experimental start a subsample was enumerated. 3 ml of culture was fixed with Lugol's solution (final conc. 1%) and counted in a Sedgewick-counting chamber (S52) using a light microscope. transferred to a Sedgewick-Rafter chamber.

2.4 Media preparation

F/20 media was prepared by filtering water through a GF/F filter (Whatman) and stored in 1L blue-cap bottles at the experimental temperature (4± 1° C).

2.5 Species identification

Different mixotrophs and heterotrophs were identified to species or genera based on morphological traits using an inverted dissection microscope. Species of interest were selected based on their feeding strategy, morphology, and abundance in water samples (Table 2).

2.6 Experimental setup

Control experiments were set-up by transferring 4L of sampled water to a 10L mixing container. Triplicates were set-up by adding 1L from the mixing container to 3x1L bottles. The experimental bottles were made by transferring 3962 mL and 3993.4 mL of sampled water to two separate 10L mixing containers. Prey culture of *P. diskoicola* were added to the mixing containers, resulting in three different treatments with an initial start cell concentration of 0 (Control), 1000 cells mL^{-1} (P1000) and 5000 cells mL^{-1} (P5000), respectively. Prey culture was only added once during the whole experimental period. Triplicates were made similarly to the control bottles, resulting in 9x1L bottles. All experimental and control bottles were kept at 4± 1° C and at an irradiance of 90-115 µmol photons m^{-2} s^{-1} during the whole experimental period (6 days).

2.6.1 Cell concentrations and growth rate:

At 3 sampling days 0, 2 and 6, 110 mL from each replicate of experimental and control bottles were sampled (n=9) by fixating cells in Lugol (1%). Samples were stored in darkness until examination. Cells were quantified using the Uthermöhl sedimentation method (described in Lund, *et al.,* 1958).

50 ml of each sample was poured into a sedimentation chamber and left for min. 20 h before cells were quantified in an inverted microscope (Olympus CKX53, Olympus CK40 and Labovert F5, magnitude x20). Species of interest were counted and converted to cells mL^{-1}. Cell concentrations of *P. diskoicola* in control and experimental bottles were quantified using a Sedgewick chamber and a light microscope.

For all 9 bottles, the growth rate of the selected heterotrophic and mixotrophic species were calculated after 48 h until the termination of the experiment (day 2 – 6). Growth rates were not calculated for the first 48 hours of the experiment due to cells acclimatizing and therefore not growing exponentially.

Eq. 1 was applied for calculating growth rates, under the assumption of exponential growth:

$$Eq.1) \quad \mu = ln\left(\frac{N_2}{N_1}\right)/(t_2 - t_1)$$

Where N_1 is the initial cell concentration and N_2 the cell concentration after 4 days.

The cumulative cell concentrations for Day 2 – 6 are calculated using Eq. 2, assuming exponential growth:

$$Eq.2) \quad N_t = N_0 \cdot e^{\mu \cdot t}$$

Where N_t is the cumulated cell concentration for sample day, t. N_0 the cell concentration before dilution from N_{t-1}, μ is the growth rate from day N_t and t is the time between N_t and N_0.

Concentrations of *P. diskoicola* were calculated every 48 h (day 0, 2, 4 and 6) in the experimental and control bottles as:

$$Eq.3) \quad C_{prey} = \left(\frac{C_1}{N}\right) \cdot 1000 = cells\ mL^{-1}$$

Where C_1 is the prey concentration in the sample, N the number of squares counted in the chamber. A dilution factor of 0.59 was multiplied by the cell counts to correct for the volume of water removed from the experimental and control bottles during sampling.

2.6.2 Chl*a* measurements

Chl*a* concentrations (pg Chl*a* mL^{-1}) of the experimental and control bottles were determined by filtering 150 mL from each bottle on GF/F filters (Whatman) and adding 5 mL cold 96% ethanol to

the extraction for 24 hours. Samples were kept in darkness at 5 ° C. Chl*a* concentrations were measured on a fluorometer (Trilogy, Turner Designs CA, USA) equipped with a Chlorophyll non-acid insert, and values were converted to pg Chl*a* $cell^{-1}$.

2.6.3 Statistical analysis

Two models, one-way ANOVA, were used to test if different concentrations of *P.* diskoicola. had a significant effect on the selected ciliates' and dinoflagellates' growth rates and cell concentrations. In both models, the concentration of *P.* diskoicola was the explanatory independent variable (categorical variable, three levels) and the concentration and growth rates of the different functional groups of grassers are the dependent variable (discrete variable on a ratio scale). Data was tested for homoscedasticity. Mean growth rates followed a normal distribution, hence a linear normal model, one-way ANOVA, was applied to test for overall significant differences in mean growth rates across samples. A post-hoc Tukey's multiple comparison test at significance level 0.05 was used to identify the species and treatments which had a statistically different mean growth rate.

Cells counts of ciliates and dinoflagellates did not follow a normal distribution but reflected a skewed dataset with many low and zero-counts, making the Poisson distribution the most appropriate. The Poisson distribution is well-suited for low-frequency count variables with a positively skewed distribution (Nussbaum *et al.,* 2008). A generalized linear model, one-way ANOVA, was applied to test for overall significant differences in mean cell numbers at a significance level 0.05.

The statistical software SAS version 9.4 was used for statistical analysis and graphs were created using Microsoft Excel and GraphPad Prism ver. 9.4.1. Results are presented as means ± standard deviation in Table 3 and Table 4. Statistically significant differences are represented by *. Tendencies are defined as p-values between 0.05 - 0.1 and represented by #.

3 Results

3.1 *In situ* measurements of water column properties

A CTD profile the location where the water collection was collected revealed an increase in salinity from 1 meter-depth with 32.2 salinity to 33-meter depth with 33.3 salinity, at the same depth the temperature decreased from 7° C to 2° C. The light decreased steadily (exponentially) in the

water, and 1% of surface light radiation was reached at a depth of 29 m, which is the same depth where most of the fluorescence were accumulated (Figure 2).

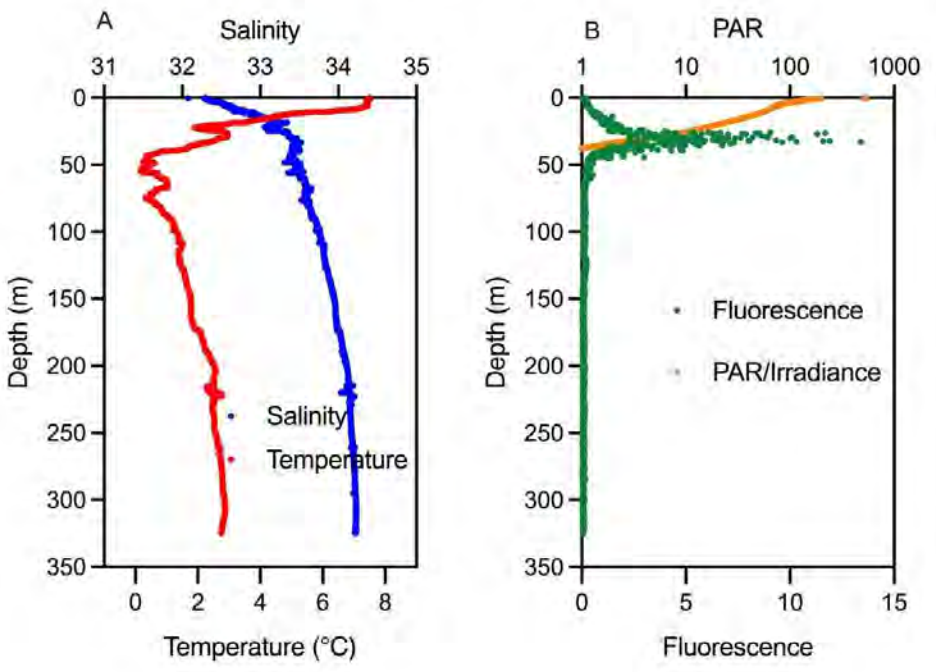

Figure 2; Vertical depth profile of salinity, temperature, photosynthetic active radiation (PAR) and chlorophyll fluorescence at the sampling station the 23rd of July 2022.

3.2 Prasinophytes grew in the treatments

It was not possible to distinguish the added *P. discoicola* from other prasinophytes and prey concentration are therefore based on prasinophytes concentrations. Prasinophytes increased slightly in control and P1000 experiments but quadrupled their cell numbers in P5000 treatment (day 0-6) (Figure 3). The chlorophyl-*a* concentration also followed a steady state for control and P1000 treatments but in P5000 treatments it had doubled in concentration (Figure 4).

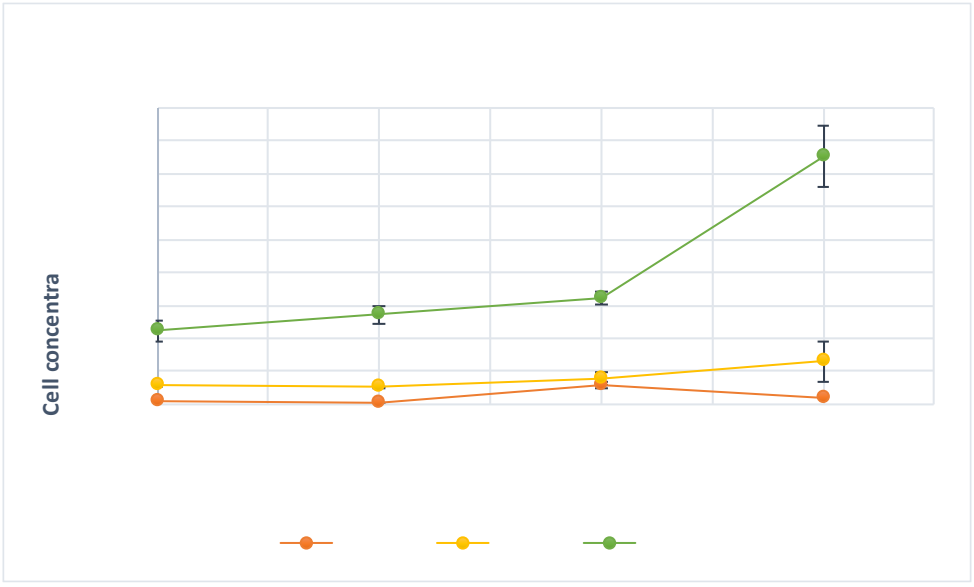

Figure 3 Changes in cell concentration of prey prasinophytes. (cells mL^{-1}) at three different start concentrations (0, 1000 and 5000 cells ml^{-1}). Numbers refer to means and error bars indicate standard deviation.

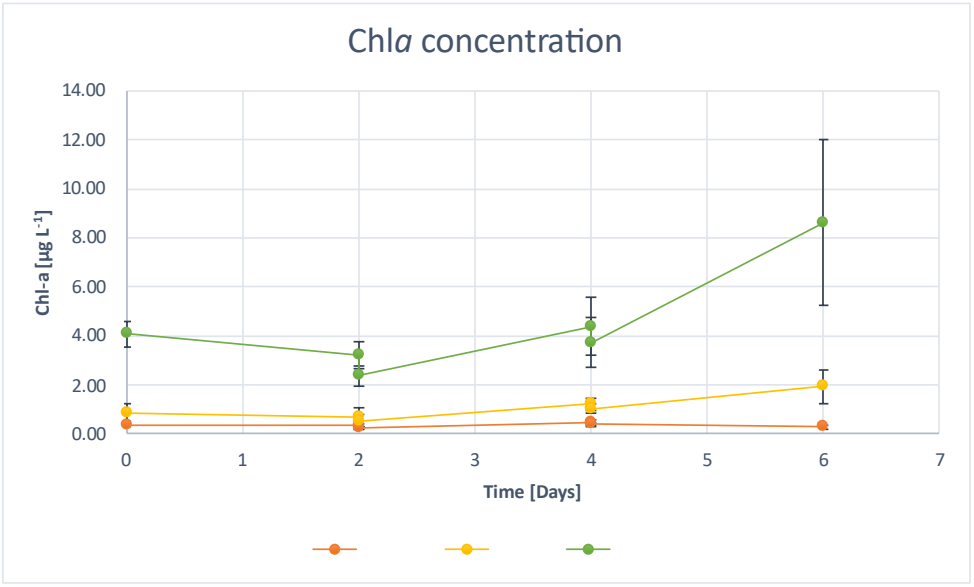

Figure 4; Chl*a* concentrations (µg L^{-1}) in experimental and control bottles at three different start concentrations of *Pyramimonas diskoicola* (0, 1000 and 5000 cells ml^{-1}). Numbers refer to means and error bars indicate standard deviation.

3.3 The species of heterotrophic and non-constitutive mixotrophic dinoflagellates and ciliates found in the plankton community at the Permanent station in Disko Bay, July 22, 2022.

In this study the chl*a* concentration at sampling Day 0 was low (0.37 ± 0.09, control) and the natural occurring concentration of prasinophytes were estimated to 220 cells ml^{-1} (Figure 3), illustrating post-spring bloom conditions, with the domination of smaller nanoflagellates and heterotrophic and mixotrophic protozoans. Species of interest were selected based on their feeding strategy, morphology, and abundance in water samples, resulting in representatives from each functional group (GNCMs, SNCMs and heterotrophs).

Table 1; Counted species' avg. cell concentrations (cells mL^{-1}) for Day 0 (sampling day) and respective % fraction of total cells counted.

Day 0 population structure		
Group	**avg. cells ml^{-1}**	**% of total**
Strombidium conicum	0.12	1.974
Dinophysis spp.	0.08	1.316
Gyro-/Gymnodinium spp.	0.35	5.757
Laboea strobila	0.07	1.151
Lohmaniella ovi-formis	0.17	2.796
Mesodinium Major	0.35	5.757
Protoperidinium spp.	0.23	3.783
Mesodinium rubrum	0.31	5.099
Gyrodinium spirale	0.78	12.829
Strobilidium spp.	0.93	15.296
Strombidium spp.	2.63	43.257
Tintinnid ciliates	0.06	0.987
SUM	6.08	100

At the sampling day the following species and genera of mixotrophic- and heterotrophic ciliates and dinoflagellates were most abundant prior to incubation (Table 1):

The GNCM *Strombidium* spp. (2.63 cells mL^{-1} and 43.256% fraction of total count) were the most abundant ciliate whereas other ciliate GNCMs (*S. conicum* and *L. strobila*) were estimated to be the second and third most dominant species for this group.

The SNCM ciliate *Mesodinium major* (0.35 cells mL^{-1} and 5.757%) was found to be the most abundant SNCM in this study. Within the different *Mesdonium* spp. *M. rubrum* was found to be slightly less abundant (0.31 cells mL^{-1} and 0.31%). The only mixotrophic dinoflagellate genus included is Dinophysis spp., which was found in low cell concentrations (0.08 cells mL^{-1} and 1.316%).

For the selected heterotrophic species, the ciliate *Strobilidium* spp. (0.93 cells mL^{-1} and 15.296%) and the dinoflagellate genera *G. spirale* (0.78 cells mL^{-1} and 12.828%) and *Gyrodinium/Gymnodinium* spp. (0.35 cells mL^{-1} and 5,756%) were the most abundant genera within the heterotrophs. Other less abundant heterotrophic species including *Protoperidinium* spp., *L. oviformis* and other tintinnid ciliates were observed and included into this study.

Table 2; is provided as an overview for trophic mode, estimated size and predator:prey size ratio for the selected mixotrophic and heterotrophic protistan grazers and the phototrophic prey species.

Table 2; The selected phototrophic prey species (in **bold**), mixotrophic and heterotrophic dinoflagellates and ciliates' size range (µm), trophic mode and relative predator:prey size ratio. Data from the literature, databases and observations during microscopy was used for size estimations. For predator:prey size (µm) ratio a general trend found by Hansen et al. 1994 was used.

Species	Trophic mode	Size (µm)	Predator:prey size ratio (µm)	References
Laboea strobila	GNCM	L: 60-130 W: 20-65	8:1	Nordicmicroalgae.com (Lohmann 1908) (Hansen *et al.,* 1994)
Strombidium conicum	GNCM	L: 71-106 W: 36-61	8:1	(Stocker *et al.,* 1988; Hansen *et al.,* 1994)
Strombidium spp.	GNCM	L/W: 30-40	8:1	(Stocker *et al.,* 1988; Masseli *et al.,* 2020)
Mesodinium rubrum	SNCM	L: 31 W: 21	8:1	(Garcia-Cuetos *et al.*, 2012) (Hansen *et al.,* 1994)
M. major	SNCM	L/W: 40-50	8:1	(Garcia-Cuetos *et al.*, 2012) (Hansen *et al.,* 1994)
Dinophysis spp.	SNCM	L: 22-105 W: 22-66	1:1-2	(Hansen *et al.,* 1994)
Tintinnid ciliates	Het	L: 20-50	8:1	Heinbokel and Wayne, 1985

Strobilidium spp.	Het	L/W: 30-55	8:1	(Hansen *et al.,* 1994)
Lohmaniella oviformis	Het	L/W: 15-20	8:1	(Hansen *et al.,* 1994)
Gyrodinium spirale	Het	L: 40-200 W: 20-45	1:1	Nordicmicroalgae.com (Kofoid & Swezy 1921) (Hansen,1992; Hansen et al. 1994)
Gyrodinium/ Gymnodinium spp.	Het	L/W: 20-50	1:1	(Hansen, 1992; Hansen *et al.,* 1994)
Protoperidinium spp.	Het	L: 20-110 W: 48-75	3-1:1	(Hansen, 1992)
Pyramimonas diskoicola	Phototrophic	L: 8.3 W: 5.1	-	(Harðardóttir *et al.*, 2014)

3.4 Effect of different prey concentrations on predator concentrations

Prey concentration was found to have a significant effect on cell concentrations of *Lohmaniella oviformis* ($p = 0.02$). Furthermore, statistical analysis showed a tendency between prey concentrations and concentrations of *Strobilidium* spp. ($p = 0.07$). The response of all other selected genera and species of predators was not found to be significant (Table 3) and more observations are needed for further analysis of the tintinnids. Cell counts exhibited large standard deviations, often higher than estimated mean.

Table 3; Concentration of the selected mixotrophic and heterotrophic ciliates and dinoflagellates genera at three different start concentrations of *P.* diskoicola (0, 1000 and 5000 cells ml^{-1}). Numbers refer to means±std and are calculated through-out the experimental period (Day 0 – 6). Result of one-way ANOVA p and F values together with degrees of freedom (DF) are also indicateted with a * for statistically significant growth rates. # Indicates a tendency. Table is colour coded, green = Mixotroph ciliate, blue = dinoflagellate, red = heterotroph ciliate.

Species	**Control (cells ml^{-1})**	**P1000 (cells ml^{-1})**	**P5000 (cells ml^{-1})**	**P-value**	**F-value**	**DF**
Laboea strobila	0.02±0.04	0.00±0.00	0.02±0.03	0.13	2.07	18
Strombidium conicum	0.07±0.04	0.04±0.04	0.05±0.04	0.30	1.17	18
Strombidium spp.	0.65±0.8	0.65±0.73	0.5±0.31	0.90	0.1	18
Mesodinium rubrum	0.14±0.11	0.13±0.13	0.08±0.06	0.56	0.58	18
Mesodinium major	0.17±0.09	0.22±0.17	0.18±0.06	0.71	0.34	18
Dinophysis spp.	0.04±0.03	0.05±0.03	0.06±0.05	0.66	0.42	18
Tinnitid ciliates*	0.02±0.03	0.00±0.00	0.00±0.00	0.02	3.9	18
Strobilidium spp. #	0.41±0.28	0.25±0.16	0.55±0.22	0.07	2.7	18
Lohmaniella oviformis *	0.40±0.37	0.17±0.12	0.68±0.51	0.02	3.88	18
Gyrodinium. spirale	0.45±0.14	0.51±0.29	0.61±0.12	0.37	0.98	18
Gyrodinium/Gymnodinium spp.	0.29±0.18	0.29±0.16	0.3±0.02	0.99	0.01	18
Protoperidinium spp.	0.36±0.28	0.33±0.27	0.53±0.40	0.43	0.84	18

3.5 Population dynamics of mixotrophic ciliates

Initially at the experiment (Day 0), *Strombidium* spp. constituted of 43% of the total predator cells counted. At Day 2, the *Strombidium* spp. population had decreased, reaching the same concentrations as the other selected species/genera of mixotrophic ciliates. *Strombidium* spp. was the only mixotrophic ciliate exhibiting any observable changes in cell concentrations. During the whole experimental period, no significant change was observed for the mixotrophic ciliates in any of the treatments (Figure 5).

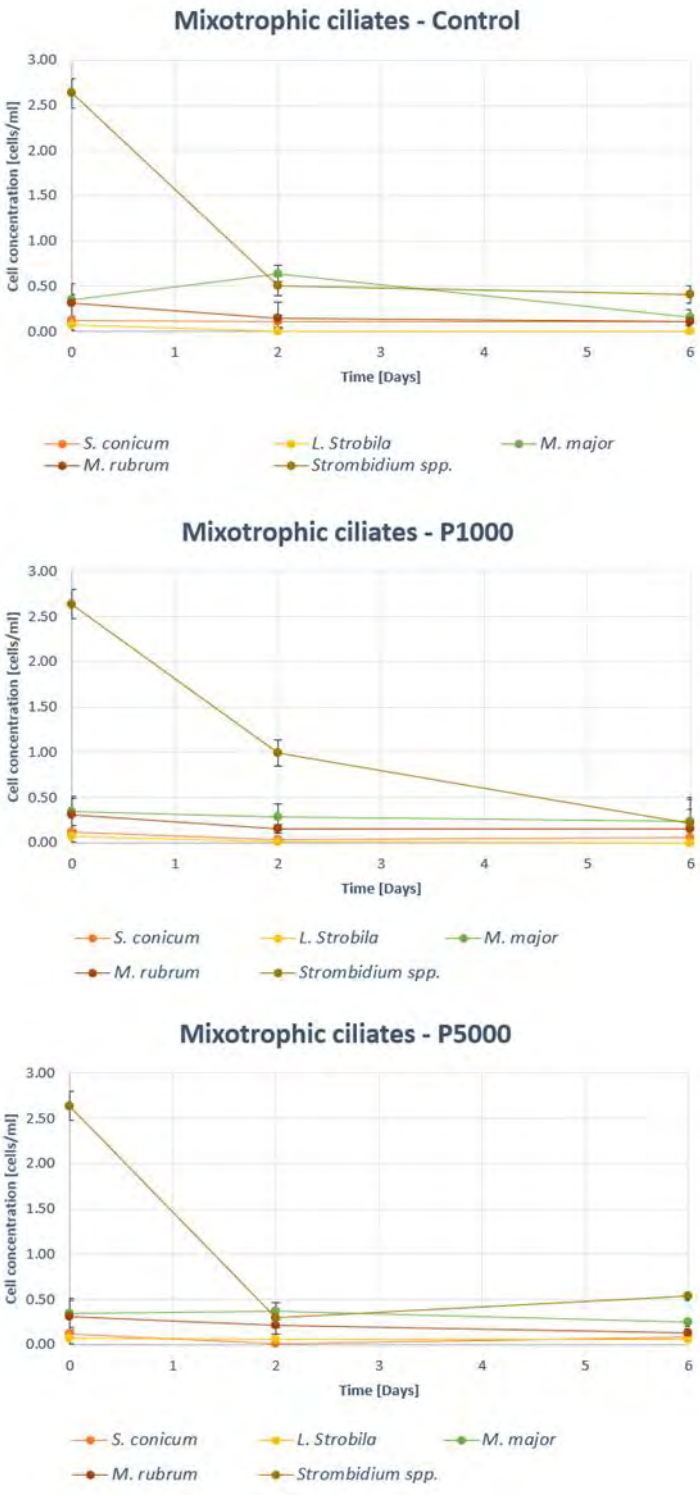

Figure 5; Cell concentrations of selected mixotrophic ciliate genera at three different start concentrations of *Pyramimonas diskoicola* (0, 1000 and 5000 cells ml^{-1}). Numbers refer to means error bars indicate standard deviation.

3.6 Population dynamics of heterotrophic ciliates

At Day 0, *Strobilidium* spp. were appx. 15% of the total amount of all cells counted, as well as constituting a large frac-tion of counted cells of heterotrophic cili-ates. The concentrations of tintinnids and *L. oviformis* were less than 0.2 cells mL^{-1}. At Day 2, the *Strobilidium* spp. population de-clined in all treatments and was in the same concentration range as the other two het-erotrophic ciliates in the Control and the P1000 treatments. In high prey concentra-tions (P5000) *Strobilidium* spp. had higher cell concentrations compared to other het-erotrophic ciliates, even though the cell concentration had declined after 48 h of in-cubation. At Day 6, both the cell concentra-tion of *Strobilidium* spp. and *L. oviformis* increased. However, tintinnids remained at a constant low concentration at approx. 0 cells mL^{-1} (Figure 6).

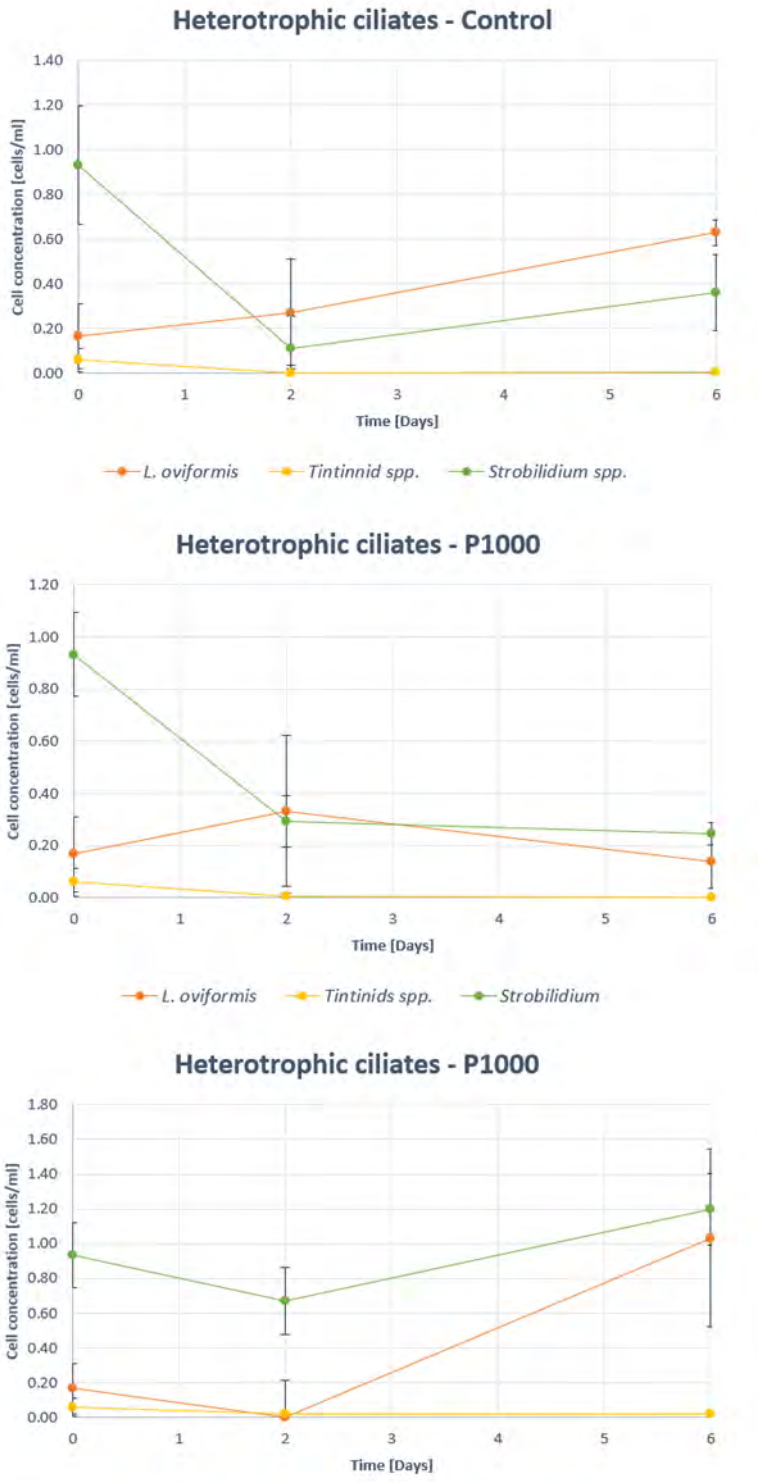

Figure 6; Cell concentrations of selected heterotrophic ciliate gen-era/species at the three different treatments (Control, P1000 and P5000). Numbers refer to means and error bars indicate standard deviation.

3.7 Population dynamics of dinoflagellates

During the whole experimental period, *Dinophysis* spp. remained at a constant low cell concentration for all treatments appx. 0.05 cells mL^{-1}. *Gyrodinium* spp. remained at a constant ~0.4 cells mL^{-1} during the experimental period across all treatments. At Day 0, the dinoflagellates were dominated by *G. spirale,* with the cell concentration of 0.8 cells mL^{-1}, which did not change significantly during the experiment period, however *Protoperidinium* spp. had increased to 1.2 cells mL^{-1} (Control) and 0.9 cells mL^{-1} (P5000) at Day 6, resulting in *Protoperidnium* spp. dominating the heterotrophic dinoflagellates in the and in high prey concentrations (P5000). While *Protoperidnium* spp. increased in P1000, cell concentrations did not exceed 0.5 cells mL^{-1} (Figure 7). However, the large standard deviations of *Protoperidnium* spp make the increase non-significant in relation to treatments (Table 3).

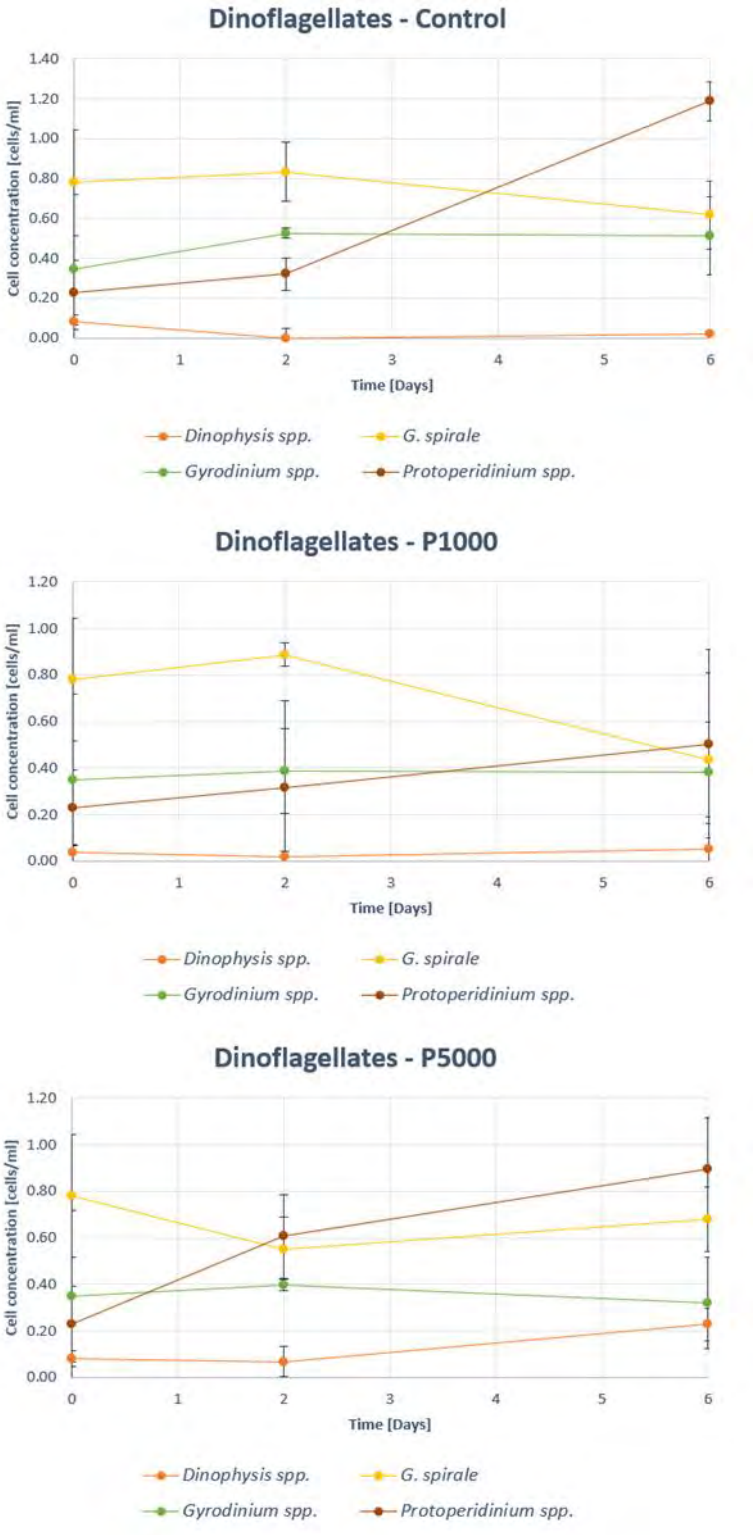

Figure 7; Cell concentrations of selected mixotrophic and heterotrophic dinoflagellate genera/species at the three different treatments (Control, P1000 and P5000). Numbers refer to means and error bars indicate standard deviation.

3.8 Effect of different prey concentrations on predator's growth rates

Prey concentration did not have a significant effect on growth rate (calculated from day 2 to day 6), for the selected predators, except for *L. oviformis*, which had a positive correlation with prey concentration between the low and high prey concentrations, where growth rates changed from -0.22 to +0.29 d^{-1} ($p = 0.043$), whereas the control had +0.21 d^{-1} (Table 4). Fastest growth rates were found for *Protoperidinium* spp. (0.39 d^{-1}) and *L. oviformis* (0.29 d^{-1}). The growth rates for *L. strobila* and most of the tintinnid ciliates could not be calculated due to too few cells counted (Figure 8).

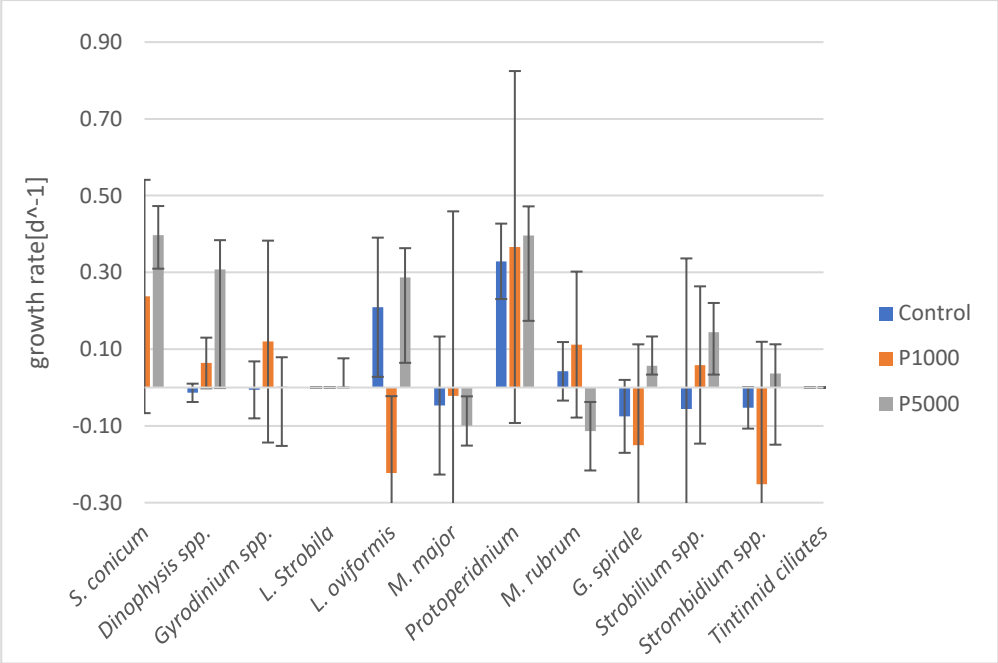

Figure 8; Growth rates (cell divisions pr. day) of selected mixotrophic and heterotrophic dinoflagellates and ciliates genera at three different start concentrations of *Pyromimonas diskoicola* (0, 1000 and 5000 cells ml^{-1}) during the period of exponential growth (Day 2 - 6). Numbers refer to means and error bars indicate standard deviation.

Table 4; Growth rates of selected mixotrophic and heterotrophic dinoflagellates and ciliates genera at three different start concentrations of *P diskoicola* (0, 1000 and 5000 cells ml^{-1}). Numbers refer to means±std and are calculated in the exponential growth phase (Day 2 – 6). *Indicates statistically significant cell numbers. Table is colour coded, green = Mixotroph ciliate, blue = dinoflagellate, red = heterotroph ciliate.

Species	Control (μ, d^{-1})	P1000 (μ, d^{-1})	P5000 (μ, d^{-1})	P-value	F-value	DF
Laboea strobila	0.00±0.00	0.00±0.00	0.00±0.00	-	-	-
Strombidium conicum	0.00±0.06	0.24±0.30	0.04±0.086	0.104	3.38	2
Strombidium spp.	-0.53±0.06	-0.25±0.37	0.03±0.18	0.390	1.11	2
Mesodinium rubrum	0.04±0.07	0.11±0.19	-0.11±0.10	0.187	2.25	2
Mesodinium major	-0.04±0.18	-0.02±0.48	-0.09±0.05	0.949	0.05	2
Dinophysis spp.	-0.01±0.02	0.06±0.07	0.31±0.31	0.158	2.55	2
Tinnitid ciliates	*0.00±0.00*	*0.00±0.00*	*0.43±0.08*	*0.422*	*1*	*2*
Strobilidium spp.	*-0.06±0.39*	*0.05±0.20*	*0.14±0.11*	*0.658*	*0.45*	*2*
Lohmaniella oviformis	*0.21±0.18*	*-0.22±0.2 **	*0.29±0.22 **	*0.043*	*5.54*	*2*
Gyrodinium. spirale	-0.07±0.09	-0.15±0.26	0.05±0.23	0.343	1.29	2
Gyrodinium/Gymnodinium spp.	0.00±0.07	0.12±0.26	0.00±0.15	0.650	0.46	2
Protoperidinium spp.	0.32±0.10	0.36±0.46	0.39±0.22	0.963	0.04	2

4. Discussion

4.1 Natural populations and environment

The water body at Disko Bay is affected by the highly variable sea-ice and glacier outflow (Dünweber *et al.,* 2010), with the freshwater input and solar heating forming a warmer less-dense surface water as found in other sampling e.g., (Levinsen *et al.,* 2000). A similar profile was found in this study (Figure 2). In Disko Bay, sea ice conditions are highly variable, which might have impacted the spring phytoplankton. In the present study the sea ice breakup was later than other years, however the vertical profile of the water column followed a similar pattern found in previous studies (Levinsen *et al.,* 2000). In previous years, Levinsen *et al.,* 2000 found nanoflagellates, such as *Pyramimonas* spp., to dominate the upper water column during summer with a sub-surface bloom of diatoms around the pycnocline. The vertical profile from this study found a peak in biomass at appx. 30 meters, suggesting a sub-surface bloom around the pycnocline and/or remaining phytoplankton biomass sinking out of the photic zone after the spring-bloom.

Previous studies of the phytoplankton dynamics at Disko Bay, showed that the chl*a* concentration reached 31.2 ± 1.0 µg l^{-1} around June 1, and declined to a level of 9 mg m^{-3} the following week (Frette *et al.,* 2010), exemplifying how dynamic the system is. Spring bloom is initiated by the increasing irradiance due to the increase in incoming radiation and increased day length, the withdrawal of sea ice, and high winter nutrient concentrations in the surface waters (Levinsen *et al.,* 2000). High chl*a* concentrations during the spring bloom are primarily due to blooms of chain forming centric- and pennate diatoms that uses up the inorganic nutrients. In the post-spring bloom phase, the phytoplankton community change towards nanoflagellates and by the start of August heterotrophic- and mixotrophic ciliates (*Strombilidium, Strobilidium, Lomaniella, Laboae and Tontonia* spp.) and dinoflagellates (*Gymnodinium* and *Gyrodinium* spp.) are the most abundant (Levinsen *et al.,* 2000).

4.2 Were ciliates in the size range of 30-50 µm and dinoflagellates in the size range 6-25 µm the main grazers on prasinophytes?

Our hypothesis was ciliates in the size range of 30-50 µm and dinoflagellates in the size range 6-25 µm the main grazers on prasinophytes. This hypothesis is rejected, generally oligotrich (e.g *Strombidium* spp.) and choreotrich (e.g., *Strobilidium* spp.) ciliates in the size range of 30-50 µm and heterotophic dinoflagellates in the size range 6-25 µm (n=6) were apparently not the main grazers on the added *P. diskoicola*. The statistical analysis showed that the small heterotrophic choreotrich ciliate *L. oviformis* (size 15-20 µm) was the only affected predator across treatments (p=0.043) The five other selected species (*Strobilidium* spp*, Strombidium* spp., *Mesodinium rubrum, Gyrodinium/Gynodinium* spp. and *Protoperidinium spp.*) showed no statistical changes in growth rates in response to the addition of prey across treatments. This hypothesis was based on the idea that the predator:prey size ratio determines what prey microorganism may be ingested (Hansen *et al.,* 1994). This suggests that prey selection have other variables than predator:size ratio, and parameters like biomolecular prey recognition for protozoans, prey swimming motility and inorganic nutrient ratio in prey have been suggested to play a role (Wotton *et al.* 2007, Yang *et al.*, 2015; Maselli *et al.*, 2022). Indeed, some of the selected predators that fit the size range of this hypothesis are known to feed on other organisms than what would have been expected from their size. Red *Mesodinium* spp are selective with its prey and have been shown to feed and thrive on cryptophytes, and not on prasinophyceae (Johnson *et al.,* 2016: Hansen *et al.* 2013) Curiously,

L. ovirformis is known as a bacterivore (Sime-Ngando *et al.,* 1999), but it responded to the treatments of prey addition. Since this is a natural plankton community, it is possible that *L. oviformis* have responded to an increase of picoplankton, which formed in the experiment by increasing in cell size during the experimental duration, (observation). In this experiment species and individuals within the genera *Strobilidium* and *Protoperidinium* vary considerably in size, with some species and individuals being having the predator:prey size ratio that makes them able to prey on *P. diskoicola.* Since we have not sorted the individuals within species by size this could potentially affect the interpretations of our results.

4.3 Did GNCM's have higher growth rates than heterotrophs in low prey concentrations (Control/P1000)?

Our hypothesis was that GNCM's have higher growth rates than heterotrophs in low prey concentrations (Control/P1000). We expected that GNCMs (*Laboea strobila*, *S. conicum* and *Strombidium* spp.) had an advantage over heterotrophs in low prey concentrations since they can utilize the light and the added prey (Hansen 1992, Maselli *et al*., 2020).

Table 5: Average growth rates (d^{-1}) for heterotrophic ciliates- and dinoflagellates (*n=6*) and GNCMs (*n=3*) for control and P1000 treatment. Calculations based on growth rates (d^{-1}) found in Table 4

Trophic mode	**Control (d^{-1})**	**P1000 (d^{-1})**
Heterotroph	0.0667	0.0267
GNCM	-0.176	-0.003

The heterotrophic ciliates- and dinoflagellates exhibited a higher average growth rate for both the Control and P1000 treatment compared to the GNCMs (Table 5), however these findings are not statistically significant.

L. strobila was only found in very small cell concentrations (0.01-0.07 cells mL^{-1}) across replicates at day 0 and were absent throughout the rest of the experiment (day 2-6). Stoecker *et al.,* 1988 found that *L. strobila* was difficult to have in culture due to its fragility and achieved irregular shape after 6 days in culture. S*trombidium* spp. was found to have the lowest growth rate in the control and P1000 treatment (-0.53 d^{-1} and –0.25 d^{-1}, respectively) whereas *S. conicum* exhibited the highest growth rate (0.24 d^{-1}) in the P1000 treatment (Table 4). *S. conicum* generally have a larger cell size (30x70 µm) than the other *Strombidium* species investigated here. This could mean

that *Strombidium* spp. could be predated on by a larger number of predators (e.g., *Gyro*/-*Gymnodinium* spp.) resulting in lower growth for *Strombidium* spp. It was observed that smaller size *Strombidium* spp. cells disappeared in our sample.

The higher growth rates achieved in P1000 (–0.25 d^{-1}) and P5000 (0.03 d^{-1}) (Table 4) treatments for *Strombidium* spp. is in accordance with Maselli *et al.,* 2020 and Stoecker *et al.,* 1988 who found that mixotrophic oligotrich ciliates have higher ingestion rates (50-100 preys cell h^{-1}) when prey is plentiful. However, these results are not statistically significant, and we cannot verify if *Strombidium* spp. and *S. conicum'* growth is supported by phagotrophy or phototrophy.

In the P1000 and P5000 treatments prasinophytes increased in cell numbers (Day 2-6, Figure 3) suggesting that the addition of approximately 1000+ cells mL^{-1} (*P. diskoicola*) and enriched media (F/20) were enough for the prasinophytes to out-grow the predation pressure from e.g., *Strombidium* spp. and *S. conicum*. In the control treatment prasinophytes did not increase in cell numbers (Day 2-6, Figure 3), even after addition of F/20 growth media, suggesting that predators' grazing pressure on prasinophyceae could 'control' the natural population. In addition, it was observed that chain-forming diatoms and small nanoflagellates became more abundant during the incubation (from Day 2-6), probably due to the addition of media (F/20), which some of the predators could be ingesting instead of *P. diskoicola*, ultimately increasing the growth of the prasinophyte. For P1000 treatment it was expected that the prey populations would have been controlled by the grazers.

4.4 Did heterotrophs have higher growth rates than mixotrophs at high prey concentration (P5000)?

Our hypothesis was that heterotrophs have higher growth rates than mixotrophs at high prey concentration (P5000). This study found growth rates of heterotrophs (avg = 0.22 d^{-1}) to be higher than the mixotrophic species (avg =0.036) in the P5000 treatment. The main contributors of the difference of growth rates are from the *L. oviformis* (0.29 d^{-1}), *Protoperidinium* spp. (0.39 d^{-1}) and tintinnid ciliates (0.43 d^{-1}), and the only mixotrophic species with a high growth rate was *Dinophysis* spp. (0.31 d^{-1}) (Table 4). The hypothesis that heterotrophs have higher growth rates than mixotrophs in high prey concentration is based on the theory that there is a tradeoff for being mixotroph rather than purely heterotroph. Mixotrophs have an advantage when resources are scarce, and heterotrophs will have an advantage when resources are plentiful. Mixotrophic species have both the photosystem and the system for phagotrophy to maintain, resulting in a higher metabolism

for mixotrophs, and heterotrophs are thus capable of higher maximum growth rates (Fischer et al., 2016). The P5000 treatment was supposed to imitate high light, nutrient and prey concentrations.

A challenge in this study is to verify which mixotrophs and heterotrophs were grazers on *P. diskoicola* (e.g., *L. ovirformis* as previous discussed). The dinoflagellates within the *Protoperidinium* genus were not affected by the prey concentrations and might have been feeding on other prey as well (Hansen *et al.,* 1997). Tintinnid ciliates typically ingest relatively large prey items, and only small species are believed to ingest prey in the size range of *P. diskoicola* (Hansen *et al.,* 1994), However, in this study they seem to respond to the P5000 treatment. Since it is a challenge to verify which prey the selected mixotrophic and heterotrophic species and genera have grazed on, it is difficult to correlate growth rates with prasinophytes concentrations.

The low growth rates for the mixotrophic species in the different treatments could be due to that the experiment uses a natural plankton community where our selected predators' prey on other species and/or each other. The larger dinoflagellates are known to feed on prey their own size and this may have increased the mortality rate of the ciliates in our experiments (Hansen *et al.,* 1994). Most of the chosen mixotrophic species in this study were ciliates, (except *Dinophysis* spp.), and if they had high mortality rates, their real growth rates would be underestimated. Nevertheless, our results show that the heterotrophs had higher growth rates than mixotrophs (GNCM + SNCM) in high prey concentrations.

4.5 Did ciliates have a higher growth rate than dinoflagellates?

Our hypothesis was that ciliates would have higher growth than dinoflagellates because there is a relationship between cell volume and metabolic rate, with ciliates having a smaller cell volume and therefore having a 2-3 times higher metabolic rate (Hansen *et al.,* 1994;1997).

Table 6; Average growth rates (d-1) for ciliates (*n=8*) and dinoflagellates (*n=4*) across the three different treatments (Control, P1000 and P5000). Calculations based on growth rates found in Table 4.

Genera	**Control (d^{-1})**	**P1000 (d^{-1})**	**P5000 (d^{-1})**
Ciliates	-0.0475	-0.01125	0.09125
Dinoflagellates	0.06	0.0975	0.1875

The average growth rates (Table 6) increased across the three treatments (Control, P1000 and P5000, respectively) both for ciliates and dinoflagellates, which might indicate that the addition of prey have influenced both the selected ciliates and dinoflagellates, however this is not statically significant. The highest average growth rate was achieved by the dinoflagellates in the P5000 treatment, primarily due to *Protoperidinium* spp. and *Dinophysis* spp. while *Gyro-*/*Gymnodinium* clade contributed to a lower average growth rate across treatments. This is contrary to what we expected.

Ciliates can generally undergo 1–2 divisions pr. day. This mean that they might be able to grow as fast (or faster) than their prey (e.g., nanoflagellates) (Chen *et al.,* 2020) However, in this study, ciliates exhibited low to moderate growth rates across treatments. *Strobilidium* spp. *Strombidium* spp. and *S. conicum* were the only ciliate species found in this study to have a higher growth rate for P1000 and P5000 treatment, compared to the Control (Table 6), however these results could not be statistically verified. *Strobilidium* spp. are a heterotrophic ciliate, that have been shown to be able to grow on the ingestion of *Pyramimonas* spp. (Maselli *et al.,* 2020). From other studies, it is known that the mixotrophic- *Strombidium* spp. and *S. conicum* both fits the predator:prey size ratio and should be able to utilize the chlorophyte's chloroplast, which ultimately could support their growth (Maselli *et al.,* 2020; Stoecker *et al.,* 1988).

The species with the overall highest growth rate (+0.39 d^{-1}) was achieved by the heterotrophic dinoflagellates *Protoperidinium* spp. in the P5000 treatment. *Protoperidinium* spp. support its growth by enveloping prey of similar or larger size than itself (e.g., ciliates) (Hansen, 1992). If *Protoperidinium* spp. is in-fact grazing on the investigated ciliates this would contribute to lower growth rates for ciliates. A general trend is that the growth rates found in this study is much lower than maximum growth rates for selected species found in literature, especially for the ciliates *Strombidium* spp. and *Strobilidium* spp. The dinoflagellates *Protoperidinium* spp. is an exception, because it exhibited higher growth rates compared to literature (Supplementary, Table 7).

4.6 Uncoupling of chl*a* concentration and prasinophycea cell concentrations

The measured chl*a* concentrations and cell concentrations of prasinophytes did not follow the same trend in all treatments. Based on the P5000 treatment, cell concentrations (quadrupled, day 0-6) and measured chl*a* concentration (doubled, day 0-6). It is likely that the prasinophytes counted experienced lowered their average chl*a* content pr. cell during the experiment, due to being placed

under higher irradiance (90-115 µmol photons m^{-2} s^{-1}), compared to its natural environment (~75 µmol photons m^{-2} s^{-1}, Figure 2). Also, *P. diskoicola* was transported in darkness and only kept in light for 24 h prior to experimental start. Phytoplankton cells will generally lower their chl*a* content when placed under high irradiance, compared to low irradiance (photoacclimation) (Hansen *et al.,* 2013), possibly explaining the un-coupling of cell concentrations and chl*a* concentrations. Also, it cannot be excluded that other phytoplankton species, which were not enumerated might have affected the chl*a* concentrations.

4.7 Limitations

The selected genera and species in this study vary to a great extent in feeding biology and physiology e.g. in relation to mortality rates. Maselli *et al.* 2020 and Hughes *et al.,* 2021 found that mortality increased for the GNCM *Strombidium* spp. with cells starting to die after 3 – 4 days without prey, whilst heterotrophic ciliates generally starts to die already after 1-2 days after prey depletion (Maselli *et al.*, 2020). The SNCM *M. rubrum* and *Dinophysis* spp. can survive for months in light without prey, and even multiply 3-4 times after prey depletion (Hansen *et al.* 2013). The difference in mortality rates, grazing rates, growth rates, size, and prey specificity amongst others (as reviewed in Table 2), makes it a challenge to determine an appropriate experimental design and duration which can capture the response of all functional groups and correlate the added prey concentrations to the responses in cell numbers and growth rates.

It was not possible to find an explanation to the overall low growth rates estimated in this study with most being half of the estimated growth rates in literature (Supplementary, Table 7.). Most likely, several factors influence the estimated cell concentrations including low prey concentrations, stress from manipulation and different species preying on each other e.g. *Dinophysis* spp. on *M. rubrum* (Hansen *et al.,* 2013).

F/20 media was added to all treatments to make sure that responses in prey concentrations and that growth response of mixotrophs were not a result of inorganic nutrient limitation. However, it was not evident what effect the addition of F/20 media had on the different functional groups. At the sampling time, inorganic nutrients are low in Disko Bay (Dünweber *et al.*, 2010), and the effect of a rapid change in inorganic nutrient concentrations might have been a significant factor in the response of the different functional groups. Possibly, the effect of media differed between species e.g., the addition of media and a high irradiance should have resulted in an increased growth of *M.*

rubrum and *M. major*, which function as mainly phototrophs (Hansen *et al.*, 2013), whereas Maselli *et al.,* 2022 found that *Strombidium* cf. *basimorphum* was unable to utilize dissolved inorganic nutrients, but instead was directly influenced by the carbon:nutrient stoichiometry of its ingested prey. To assess the effect of the addition of inorganic nutrients on growth rates, a similar experimental set-up without added inorganic nutrients could have provided some insights.

Previous studies such as that Yang *et al*., 2015, Maselli *et al.,* 2020; 2022 have found feeding behaviour of mixotrophic *Strombidium* spp. to be influenced by different factors incl. inorganic nutrient concentrations and swimming motility of prey. However, those studies focus on one species and one type of prey, which cannot be accounted for when working with several species and functional groups in a natural population e.g., we observed chain-forming diatoms were appearing over the course of the experiment, possibly affecting the nutrient concentrations and potentially prey:predator dynamics in the different treatments.

Furthermore, different species and genera differ in how they respond to laboratory conditions. Ciliates are generally sensitive to manipulation and incubation with cells disintegrating and disappearing, Hansen, 1992; Hansen *et al.,* 1994; Stoecker *et al.,* 1988 found that the growth of *Laboea strobila* to possibly be affected by incubating in culture. The "robustness" of the different selected species in this study have influenced the estimated cell concentrations and growth rates. Additionally, some species change morphology or disintegrate when fixated in Lugol solution, making it more difficult to distinguish them.

Generally, the results of this study show high variation between replicates, highlighting the difficulty of working with natural samples. Other factors, which might have influenced the variation in estimated cell concentrations include the variation in count numbers with three different persons counting samples. The overall low cell concentrations (0.04 – 0.68 cells mL^{-1}, Day 2–6), across treatments and replicates, have led to high standard deviations in estimated cell concentrations and growth rates. Furthermore, several mixotrophs and heterotrophs were not included in this study incl. *Alexandrium* spp., *Dinobryon* spp., several athecate dinoflagellates and a dinoflagellate which predates or parasites on tintinnid ciliates, as well as many small unidentified cells which probably influence the cell numbers and growth rates of the selected species in this study. Chen *et al.,* 2020 found that neglecting the presence of bacteria in algal culture medium affected the oligotrich ciliates' growth and grazing rates on nanoflagellates with *Strombidium* spp. selectively grazing on algae at different prey concentrations.

5. Conclusion

The aim of this study was to investigate the response of protist grazers belonging to different functional groups at different availability of a phototrophic nanoflagellate prey. Our findings show that the response differed between the selected protist functional groups. Only *L. oviformis* had a significant growth rate response to prey concentration. The average growth rates of heterotrophs were nine times higher than average growth rates of mixotrophs at the high prey concentration treatment. Contrary to what we had expected, GNCMs had lower average growth rates than heterotrophic species in low prey concentrations. The growth rate of dinoflagellates was either higher or identical to the growth rates of ciliates, this did not agree with previous studies of zooplankton functional growth, which might be due to "internal grazing" within the grazers and this challenges the interpretations of experiments. Overall, estimated growth rates were lower, except for *Protoperidinium* spp., which had higher growth rates than found in literature, when taking temperature into account.

This study underlines the challenges of working with natural populations. It was not possible to verify how mixotrophs acquire their growth and who ingests who, therefore the predator:prey size ratio could not solely explain the growth rates in this study, and there are more variables to consider for prey selection. This highlights the need for further studies, which combine various methods and frameworks are needed for understanding the complex and dynamic of mixotrophic plankton in the Arctic. We stipulate that fluorescence marking of species in natural samples combined with fluorescence microscopy could be interesting for observing what species are ingested by other species and could bring new contributions to the understanding of the interactions in complex food webs.

References

Ardyna, M. and Arrigo, K. R. (2020) 'Phytoplankton dynamics in a changing Arctic Ocean', *Nature Climate Change*, 10(10), pp. 892–903. doi: 10.1038/S41558-020-0905-Y.

Chen, W., Chiang, K. and Tsai, S. (2020) 'Neglect of presence of bacteria leads to inaccurate growth parameters of the oligotrich ciliate *Strombidium sp.* during grazing experiments on nano-flagellates'. *Frontiers of Marine Science,* 7:569309. doi: 10.3389/fmars.2020.569309.

Drumm, K. *et al.* (2021), 'Physiological responses of *Mesodinium major* to irradiance, prey concentration and prey Starvation. *Journal of eukaryotic microbiology,* 68(4). doi: 10.111/jeu.12854.

Dünweber, M. *et al.* (2010) "Succession and fate of the spring diatom bloom in Disko Bay, western Greenland," *Marine Ecology Progress Series*, 419(1), pp. 11–29. doi: 10.3354/meps08813.

Fischer, R., *et al.* (2016) 'Importance of mixotrophic bacterivory can be predicted by light and loss rates.', *Oikos,* 125(5), pp. 713 – 722. doi: 10.1111/oik.03539.

Flynn, K. J. *et al.* (2013) 'Misuse of the phytoplankton-zooplankton dichotomy: the need to assign organisms as mixotrophs within plankton functional types', *Journal of Plankton Research*, 35(1), pp. 3–11. doi: 10.1093/plankt/fbs062.

Franzè, G., and Lavrentyev, P. J. (2014) 'Microzooplankton growth rates examined across a temperature gradient in the Barents Sea.' *PLOS ONE,* 9(1), pp. 1- 14. doi:10.1371/journal.pone.0086429.

Frette, L., Winding, A. and Kroer, N. (2010) 'Genetic and metabolic diversity of arctic bacterioplankton during the post-spring phytoplankton bloom in Disko Bay, Western Greenland,' *Aquatic Microbial Ecology*, 60(1), pp. 29–41. doi: 10.3354/ame01410.

Garcia-Cuetos, L., Moestrup, O. and Hansen, P. J. (2012) 'Studies on the genus Mesodinium II. Ultrastructural and molecular investigations of five marine species help clarifying the taxonomy', *The Journal of eukaryotic microbiology*, 59(4), pp. 374–400. doi: 10.1111/J.1550-7408.2012.00630.X.

Hansen, B., Bjornsen, P. K. and Hansen, P. J. (1994) 'The size ratio between planktonic predators and their prey', *Limnology and Oceanography*, 39(2), pp. 395–403. doi: 10.4319/lo.1994.39.2.0395.

Hansen, B., Bjornsen, P. K. and Hansen, P. J. (1997) 'Zooplankton grazing and growth: Scaling within the 2 – 2.000 μm body size range', *Limnology and Oceanography*, 42(4), pp. 687–704.

Hansen, M. O. *et al.* (2012) 'Oceanographic regime shift during 1997 in Disko Bay, Western Greenland', *Limnology and Oceanography*, 57(2), pp. 634–644. doi: 10.4319/LO.2012.57.2.0634.

Hansen, P. J. (1992) 'Prey size selection, feeding rates and growth dynamics of heterotrophic dinoflagellates with special emphasis on *Gyrodinium spirale*', *Marine Biology,* 114(2), pp. 327–334. doi: 10.1007/BF00349535.

Hansen, P. J. *et al.* (2012) 'Direct evidence for symbiont sequestration in the marine red tide ciliate *Mesodinium rubrum*', *Aquatic Microbial Ecology*, 66(1), pp. 63–75. doi: 10.3354/AME01559.

Hansen, P. J. *et al.* (2013) 'Acquired phototrophy in *Mesodinium* and *Dinophysis* - A review of cellular organization, prey selectivity, nutrient uptake and bioenergetics', *Harmful Algae*. 28(1), pp. 126–139. doi: 10.1016/j.hal.2013.06.004.

Hansen, P.J and Tillmann, U. (2020) 'Mixotrophy in Dinoflagellates: Prey Selection, Physiology and Ecological Importance. Dinoflagellates: Classification, Evolution, Physiology and Ecological Significance', (eds.) in Durvasula, S. R. V. Nova Science Publishers, pp. 201-260.

Harðardóttir, S,, Lundholm, N., Moestrup, Ø. and Nielsen, T. G. (2014) 'Description of *Pyramimonas diskoicola* sp. nov. and the importance of the flagellate *Pyramimonas* (Prasinophyceae) in Greenland sea ice during winter-spring transition', *Polar biology,* 37(10), pp. 1479-1494. doi: 10.1007/s00300-014-1538-2.

Heinbokel, J. F. and Wayne, D. C. (1958) 'Ciliates and nanoplankton in Arthur Harbor, December 1984 – January 1985' *Antarctic Journal of the United States,* 19(1), pp. 135-136.

Hughes, E. A. *et al.* (2021) 'Metabolic Reliance on Photosynthesis Depends on Both Irradiance and Prey Availability in the Mixotrophic Ciliate, *Strombidium cf. basimorphum'*, *Frontiers in Microbiology*, 12(1). doi: 10.3389/fmicb.2021.642600.

Johnson, M. D. *et al.* (2016) 'The genetic diversity of *Mesodinium* and associated cryptophytes', *Frontiers in Microbiology,* 7(1). doi: 10.3389/fmicb.2016.02017.

Kofoid and Swezy, 1921 *'Gyrodinium spirale'* Available at: http://nordicmicroalgae.org/taxon/Gyrodinium%20spirale (Accessed: 11 August 2022).

Levinsen, H., Nielsen, T. G. and Hansen, B. W. (2000) 'Annual succession of marine pelagic protozoans in Disko Bay, West Greenland, with emphasis on winter dynamics', *Marine Ecology Progress Series*, 206, pp. 119–134. doi: 10.3354/meps206119.

Lohmann (1908) '*Laboea strobila'* Available at: http://nordicmicroalgae.org/taxon/Laboea%20strobila (Accessed: 11 August 2022).

Lund, J. W. G., Kipling, C., Le Cren, E. D. (1958) 'The inversted microscope method of estimating algal numbers and the statistical basis of estimations by counting', *Hydrobiologia*, 11, pp. 143 – 170.

Maselli, M. *et al.* (2020) 'Ecophysiological traits of mixotrophic *Strombidium* spp', *Journal of Plankton Research*, 42(5), pp. 485–496. doi: 10.1093/plankt/fbaa041.

Maselli, M., Van de Waal, D. B. and Hansen, P. J. (2022) 'Impacts of inorganic nutrients on the physiology of a mixoplanktonic ciliate and its cryptophyte prey', *Oecologia*. Springer Berlin Heidelberg, 199(1), pp. 41–52. doi: 10.1007/s00442-022-05162-3.

Mitra, A. *et al.* (2016) 'Defining planktonic protist functional groups on mechanisms for energy and nutrient acquisition: incorporation of diverse mixotrophic strategies', *Protist*, 167(2), pp. 106–120. doi: 10.1016/J.PROTIS.2016.01.003.

Nghiem, S. V. *et al.* (2007) 'Rapid reduction of Arctic perennial sea ice', *Geophysical Research Letters*, 34(19). doi: 10.1029/2007GL031138.

Nussbaum, M., Elsadat, S. and Khago, A. (2008) 'Best practices in analyzing count data: Poisson Regression', in *Best Practices in Quantiative Methods.* Sage, pp. 454-483.

Sime-Ngando, T., Demers, S. and Juniper, S. K. (1999) 'Protozoan bacterivory in the ice and the water column of a cold temperate lagoon', *Microbial ecology,* 37(2), pp. 95–106. doi: 10.1007/S002489900134.

Smith, M. and Hansen, P. J. (2007), 'Interaction between *Mesodinium rubrum* and its prey: importance of prey concentration, irradiance and pH', *Marine Ecology - Progress Series,* 338(1), pp. 61-70. doi: 10.3354/meps338061.

Stoecker, D. K. *et al.* (1988) 'Obligate mixotrophy in *Laboea strobila,* a ciliate which retains chloroplasts', *Marine Biology*, 99(1), pp. 415 - 423.

Stoecker, D. K. *et al.* (2009) 'Acquired phototrophy in aquatic protists', *Aquatic Microbial Ecology*, 57(3), pp. 279–310. doi: 10.3354/ame01340.

Stoecker, D. K. *et al.* (2017) 'Mixotrophy in the Marine Plankton', *Annual Review of Marine Science*, 9(1), pp. 311–335. doi: 10.1146/annurev-marine-010816-060617.

Stoecker, D. K. and Lavrentyev, P. J. (2018) ‘Mixotrophic plankton in the polar seas: A pan-Arctic review’, *Frontiers in Marine Science*, 5(AUG). doi: 10.3389/fmars.2018.00292.

Yang, J. *et al.* (2015) ‘Factors influencing the grazing response of the marine oligotrichous ciliate *Strombidium cf. sulcatum*’, *Aquatic Microbial Ecology*, 74(1), pp. 59–71. doi: 10.3354/ame01729.

Wotton, E.C. *et al.* (2007), ‘Biochemical prey recognition by planktonic protozoa’, *Environmental Microbiology*, 9(1), pp. 216-222. doi: 10.1111/j.1462-2920.2006.01130.

Supplementary

Supplementary Table 7; Maximum growth rates (d^{-1}) from this study adjusted to 15°C across treatments (Control, P1000 and P5000) and maximum growth rates (d^{-1}) from literature (monocultures at 15-20 °C) for relevant species (C= Ciliate, D= Dino-flagellate) to this study. Growth rates (d^{-1}) from this study were adjusted to 15°C for comparison by adding a Q10 factor of 2.8 to original achieved growth rates (Table 4).

Species	**Maximum growth rates adjusted to 15 °C**			**Maximum growth rates from literature (d^{-1})**
	Control (d^{-1})	**P1000 (d^{-1})**	**P5000 (d^{-1})**	
Gyrodinium spirale (D)	-0.196 ± 0.252	-0.42 ± 0.728	0.14 ± 0.14	0.528 (Hansen *et al.,* 1997)
Gyrodinium-/Gymnodinium spp. (D)	0 ± 0.196	0.336 ± 0.728	0 ± 0.42	0.84 (Hansen *et al.,* 1997)
Protoperidinium spp. (D)	0.896 ± 0.28	1.008 ± 1.288	1.092 ± 0.616	0.576 (Hansen *et al.,* 1997)
Strobilidium spp. (C)	-0.168 ± 1.092	0.14 ± 0.56	0.392 ± 0.308	1.44 (Hansen *et al.,* 1997)
Strombidium spp. (C)	-1.484 ± 0.168	-0.7 ± 1.036	0.084 ± 0.504	1.872 (Hansen *et al.,* 1997)
Strombidium conicum (C)	0 ± 0.168	0.672 ± 0.84	0.112 ± 0.2408	0.33 (Maselli *et al.,* 2020)
Laboea strobila (C)	0	0	0	? (Stoecker *et al.,* 1988)
Mesodinium rubrum (C)	0.112 ± 0.196	0.308 ± 0.532	-0.308 ± 0.28	0.49 (Smith and Hansen, 2007)
Mesodinium major (C)	-0.112 ± 0.504	-0.056 ± 1.344	-0.252 ± 0.14	0.39 (Drumm *et al.,* 2021)
Direct comparison of growth rates (4.5 °C)				
	Control (d^{-1})	**P1000 (d^{-1})**	**P5000 (d^{-1})**	**Maximum growth rates from literature**

Lohmaniella ovi-formis (C)	0.21 ± 0.18	-0.22 ± 0.2	0.29 ± 0.22	0.33-1.67 (Franzè and Lavrentyev, 2014)
Dinophysis spp. (D)	-0.01 ± 0.02	0.06 ± 0.07	0.31 ± 0.31	0.765 (Franzè and Lavrentyev, 2014)